OCS STUDY MMS 85-0098

INTERIM REPORT

DEVELOPMENT OF A COASTAL OIL SPILL SMEAR MODEL

Phase I: Analysis of Available and Proposed Models

Prepared For:

MINERALS MANAGEMENT SERVICE
ANCHORAGE, ALASKA 99510

Prepared By:

COASTAL SCIENCE & ENGINEERING, INC.
(Formerly RPI/Coastal Science, Inc.)
COLUMBIA, S.C. 29202

With

APPLIED SCIENCE ASSOCIATES, INC.
ATTELLE NEW ENGLAND RESEARCH LABORATORY

MARCH 1986

OCS STUDY MMS 85-0098

Interim Report

DEVELOPMENT OF A COASTAL OIL SPILL SMEAR MODEL PHASE I. ANALYSIS OF AVAILABLE AND PROPOSED MODELS

This study was funded by:

MINERALS MANAGEMENT SERVICE
U.S. DEPARTMENT OF INTERIOR
Anchorage, Alaska
(Contract 14-12-0001-30130)

SECTIONS AND AUTHORS:

1. Introduction
   (Erich R. Gundlach[1] and Mark Reed[2])
2. Evaluation of Surf-Zone Current and Sediment-Transport Models
   (S. Jonathan Siah and Timothy W. Kana[1])
3. Analysis of Oil-Spill Partitioning Models
   (Paul D. Boehm and Adolpho Requejo[3])
4. Analysis of Oil/Shoreline Interactions
   (Erich R. Gundlach[1])
5. Comparative Analysis of Possible SMEAR Model Components
   (Mark Reed and Malcolm Spaulding[2])
6. SMEAR Model Development Plan
   (Malcolm Spaulding and Mark Reed[2])

PROJECT DIRECTOR: Timothy W. Kana[1]

[CSE'85-86 R-08]

Coastal Science & Engineering, Inc.
P.O. Box 8056
Columbia, SC 29202

[2]Applied Science Associates, Inc.
529 Main Street
Wakefield, RI 02879

[3]Battelle New England Marine Research Laboratory
397 Washington Street
Duxbury, MA 02332

TABLE OF CONTENTS

EXECUTIVE SUMMARY

This report is a collaborative and multidisciplinary effort to determine the best combination of algorithms and models representing surf-zone currents and sediment transport, oil weathering, and oil/shoreline interactions for use in a unified, interactive coastal oil-spill (SMEAR) model. The purpose of the SMEAR model is to produce stochastic predictions of oil-spill composition, amount, and spatial distribution across and along a beach as a function of time. This report is divided into six sections, three of which include the evaluations of primary model components--surf-zone current and sediment-transport models (Section 2), oil partitioning models (Section 3), and oil/shoreline interactions (Section 4). Section 1 is a brief introduction outlining the contracted scope of work. Section 5 evaluates the most appropriate combination of oil-partitioning and surf-zone current/sediment-transport models. Section 6 presents the SMEAR model development plan which leads into Phase II of this two-part study.

Transport of oil in the surf zone is primarily dependent on surf-zone currents; however, as oil interacts with sediments, sediment transport also increases in importance as an oil-transporting mechanism. Current velocity is influenced by six principal force components: (1) wave force resulting from radiation stress, (2) tidal force, (3) friction force on the bottom, (4) lateral turbulent mixing force, (5) wind force, and (6) coriolis force.

Section 2 describes and develops a set of algorithms that represent each of these forces and discusses two principal model formulations that can be used to determine surf-zone currents. The first is a very complex set of algorithms, many of which have not been satisfactorily resolved, representing currents as a two-dimensional, vertically averaged flow driven by wind, tide and waves (Section 2, Equations 2.1 and 2.2). The second method is a simple, one-dimensional model representing an engineering approximation but with a wind-stress factor added (Section 2, Equation 2.33). Similarly, there are two major classes of sediment-transport models--the best being represented by a simple, empirically based formulation derived by Komar (1976) and a complex formula by Bijker (1972). Although all these models are based on application to sandy shorelines, with modification they are the best available for other environments. Based on the evaluation process described in Section 2, it is recommended that two model groupings be evaluated for incorporation into SMEAR: the simple, one-dimensional current model with Komar (1976); and the complex, two-dimensional current model with Bijker (1972).

Section 3 reviews oil-partitioning or oil-weathering models. Algorithms, where available, are discussed for (1) spreading, (2) evaporation, (3) dissolution, (4) dispersion, (5) emulsification, (6) adsorption/desorption, (7) photooxidation, and (8) biodegradation. Five currently available models incorporate the primary weathering components (items 1,2,4, and 5). These are SAI (Science Applications, Inc.), USC/API (University of Southern California/American Petroleum Institute), VKI (Danish Water Quality Institute), ASA (Applied Science Associates, Inc.), and UOT (University of Toronto) (Section 3, Table 3.4). The performance of each model component was evaluated according to adaptability to SMEAR, degree of verification, flexibility of interaction, data requirements and attainability, and compatibility with other SMEAR components. The SAI and ASA model formulations were found to be essentially equal, however, since many MMS and NOAA researchers are familiar with the SAI model, it is recommended that the SAI model be incorporated into SMEAR.

Section 4 describes the methodology for developing an oil/shoreline interaction component of SMEAR since none currently exists. Seven widely applicable shoreline types are described in terms of oil-spill interactions based on observations of several major spill incidents and the Canadian BIOS field-oiling study; these are exposed and sheltered rocky shores, sand beaches, gravel beaches, peat scarps, tidal flats, and marshes. For each, a removal rate coefficient is developed to describe the approximate longevity of oil on any particular shoreline type. At this time, removal rate coefficients are equal for all types but as data become available, rate differences can be added. For beaches, which are subdivided into beach-face and backshore compartments, removal is additionally based on tidal level and wave heights. For all seven shoreline types, a maximum oil-holding capacity is introduced to realistically predict the maximum amount of oil that can be deposited on that shoreline before being transported to the adjacent shoreline segment. Currently, the maximum holding capacity, consisting of surface oil and oil incorporated in the sediment, is presented as varying with three major viscosity groupings based on observational evidence. An algorithm will be developed to mathematically depict the relationship between the holding capacity, oil type and temperature, sedimentary characteristics and other factors. As information becomes available, the algorithm can be modified. In lieu of this, default values can be used in conjunction with the algorithm. For SMEAR, oil can accumulate onshore (under appropriate environmental conditions) in a time-step fashion until the holding capacity is reached. Preliminary comparison to BIOS and *Amoco Cadiz* data shows relatively good agreement with predicted results.

Section 5 evaluates the surf-zone current/sediment-transport models recommended in Section 2 for combination with the SAI weathering model to produce a unified SMEAR model. Either model formulation must also interact with the proposed oil/shoreline interaction component. It was found that the SAI model in conjunction with the simple, one-dimensional current and Komar sediment-transport models, were best suited for SMEAR. Although the complex two-dimensional current/Bijker formulation scored higher in applicability and compatibility with ongoing MMS and NOAA program efforts, these gains were insufficient to overcome its lower scoring in data requirements, potential for interactive use, and development costs.

Section 6 presents an overview of the operation of the SMEAR model as currently envisioned. A conceptual flow chart of SMEAR operations and requirements is presented in Figure 6.1. Input requirements include location of shoreline types and bottom slopes, and environmental data such as time series for wind, temperature, tidal currents, and air and water temperatures. The model will compute nearshore wave environment, currents, and sediment transport for each shoreline reach as a function of time. Advection, spreading, emulsification, evaporation, dispersion, and shoreline deposition/removal will be calculated at each time step for up to 90 days after the spill. Throughout the run, the dynamic mass balance of petroleum (by boiling point constituent) can be quantified for the sea surface, the water column, the sea floor, the atmosphere, and the beach. The sum of all individual components equals the total mass of oil introduced across the model boundaries up to that time. In addition, the oil mass will be spatially distributed into three compartments for each shoreline reach--beach, surf zone, and nearshore zone. A probablistic assessment of spill distribution, quantity, and composition for any given reach of shoreline will be determined by pooling the simulations of a specific spill event run under a number of varying environmental conditions and internal model parameters.

SYMBOLS USED IN THIS REPORT

Symbols used in Section 2 (nearshore currents and sediment transport)

A	mean amplitude of 18.6
C_f	bed friction coefficient
C_r	Chezy coefficient
C_ν	mixing coefficient constant
C_{90}	Chezy coefficient based on D_{90}
D	effective turbulent diffusion coefficient
D_{50}	particle diameter (50 percent by weight exceeded)
D_{90}	particle diameter (10 percent by weight exceeded)
E	wave energy
F	nodal factor, a slowly varying function of time
G	Greenwich phase or epoch at given position (λ,ϕ)
H	wave height
H_b	breaking wave height
I_l	total sediment load
I_{susp}	suspended load
I_r	Iribarren number (surf similarity parameter)
K	constant
K_1,K_2,K_3	constants, determined from field data
L	wave length
Q_{bed}	bedload
Q_{susp}	suspended load
Re	Reynolds number
S	rate of erosion or deposition (source/sink term)
S_{ij}	the radiation-stress tensor
S_{xx},S_{yy},S_{xy}	radiation stress components
T	wave period
$\vec{U}_b$	wave orbital velocity vector near the bottom
V^*_c	shear stress velocity due to current
V_l	longshore current velocity
$V_l^{1/2}$	mid-surf current velocity
W_i^{10}	wind velocity component at 10 m (33 ft) above sea level
W_c	critical wind speed
W_n	wind velocity component
c	depth-averaged sediment concentration or the average volume concentration of sand in suspension
d	water depth at mean sea level
d_b	breaking depth
f	Coriolis parameter

g	gravity acceleration
h	water depth
h_b	water depth at breaker line
k	bed roughness or wave number
l	a length scale
m	beach slope
n	wave energy flux configuration
t	time variable
t_o	arbitrary starting time
$\tilde{u}$	a reference velocity
$\overline{u_i}$	the depth-averaged and fluctuation time-averaged velocity component
u_m	maximum value of the horizontal rms wave orbital velocity in the surf zone
u_{max}	maximum value of wave orbital velocity near bottom
$\overline{u}, \overline{v}$	depth-averaged velocity components
α, α_b	wave angle inside the surf zone and at the breaker line, respectively
γ_b	breaking parameter
δ_{ij}	Kronecker delta
$\overline{\eta}$	mean water-surface deviation
κ	von Karman coefficient
λ	geographical longitude
μ	ripple factor
$\nu_x^L, \nu_{xy}^L, \nu_y^L$	turbulent viscosity coefficients
ξ	Bijker's parameter; the tidal water-surface profile
ρ	fluid density
ρ_s	mass density of bed material
$\overline{\tau}_i^B$	the fluctuation time-averaged bottom shear-stress component
$\overline{\tau}_i^S$	the fluctuation time-averaged wind-stress component
$\overline{\tau}_i^T$	the depth-averaged tidal-stress component
$\overline{\tau}_{ij}^L$	the effective lateral turbulent-mixing stress component
ϕ	geographical latitude
χ	astronomical argument
ω_o	tidal frequency
ω	sediment particle fall velocity; angular rotation rate of earth

Symbols used in Section 3 (chemistry) and Sections 4-6 (oil interactions and model formulation)

A	spill area
Ao	constant
Cg	wave group velocity
C_i	concentration
C_i^s	pure component solubility
C_i^w	bulk water phase concentration of i
C_o	initial concentration of a particular fraction
C_s	solubility coefficient
C_1	constant
C_2	constant
D_e	diffusive coefficient
D_i	diffusion value
E	evaporation flux
F	fraction of slick evaporated
H	wave height
H_b	wave height at breaking
H_o	wave height in deepwater
H_s	tide height
H_x	wave height
K_A	a constant
K_B	a constant with a value of approximately 133
K_d	rate constant for dissolution process
K_e	rate constant for evaporation process
K_f	oil removal rate constant
L_o	deep-water wavelength
M	molecular weight
M_i	mass of oil in beach segment i
M_{io}	mass of oil originally deposited on the beach
M_v	molar volume of oil component
N_i^d	dissolution flux
P	vapor pressure
P_d	pressure at depth below surface (decibars)
Q	mass weight
R	gas constant
S_i	specific gravity
So_i	solubility in parts per million
S_p	surface area of particle class
T	temperature
T_e	temperature at which C_2 is evaluated
T_o	oil temperature
T_{ps}	tide period
T_{px}	wave period
U	wind stress factor
U_w	wind speed
US	surface wind
V	longshore transport velocity in the surf zone
V_a	volume of asphaltenes
V_o	volume
V_p	volume of particle class
V_r	volume of residuum
V_T	total volume of oil in surface reservoir
W	wind speed
Wo	reference wind speed (85 m/sec)
W_w	fractional water content
X_b	width of the surf zone
X_i	mole fraction of oil component
Z	depth of water
Z_o	roughness at sea surface
a	constant
b	separation of rays
d	mean water depth over the fetch
e_6	vapor pressure at 6-m altitude
e_i	solubility enhancement factor
e_o	vapor pressure at sea surface
f	fetch length
g	gravity
h	water depth at point of interest in surf zone
h_b	water depth at breaking
h_o	ofshore depth
k_b	wave number at breaking
o	reference location
pH	alkalinity

pH_w	alkalinity value for water
t	time
x_i	oil phase mole fraction
α	constant
β	beach slope
β_{bs}	slope of back shore
β_{fs}	slope of the foreshore
δ	average slick thickness
$\eta_{setdown}$	wave setdown at the breaker location
μ_o	seawater viscosity
ρ	oil density
ρ_w	density of water

1.0 INTRODUCTION

This report is Phase I of a three-year project to develop and test a probabilistic coastal oil spill (SMEAR) model for use by the Minerals Management Service (MMS). Phase I encompasses an evaluation of component algorithms and models of nearshore currents, sediment transport, and oil weathering to determine the most appropriate combination for use in a unified SMEAR model. Since a model depicting oil distribution and persistence on beaches does not currently exist, this report also introduces the format for developing one. Phase II entails model development, verification, and testing. The SMEAR model will have the option running alone or in coordination with outputs from an offshore, oil-spill trajectory model and an oil/suspended particulate matter interaction model. The model components proposed in the report will constitute a time-stepping interactive model with stochastic environmental data inputs and will produce as results probabilistic predictions of oil composition, amount, and locations at specified times.

A schematic diagram of nearshore and beach compartments to be modelled by SMEAR is presented in Figure 1.1. Each transfer process indicated (advection, dispersion, sedimentation, evaporation, burial, resuspension, etc.) is represented by an algorithm. The critical process by which each appropriate algorithm was selected is presented in Sections 2, 3, 4, and 5 of this report. A descriptive summary of the proposed SMEAR model is presented in Section 6.

Based on our scientific judgment, component algorithms and models are evaluated using scaling factors to develop a point score based on criteria that vary slightly between model categories being reviewed (e.g., sediment transport versus chemical weathering models). All scores are relative to each other and reflect attributes or weaknesses with respect to the other components being analysed. Therefore, the exact score of a particular algorithm or model attribute is less important than its value relative to the other models being evaluated. Within each appropriate section of this report, explanations are presented supporting the value assigned.

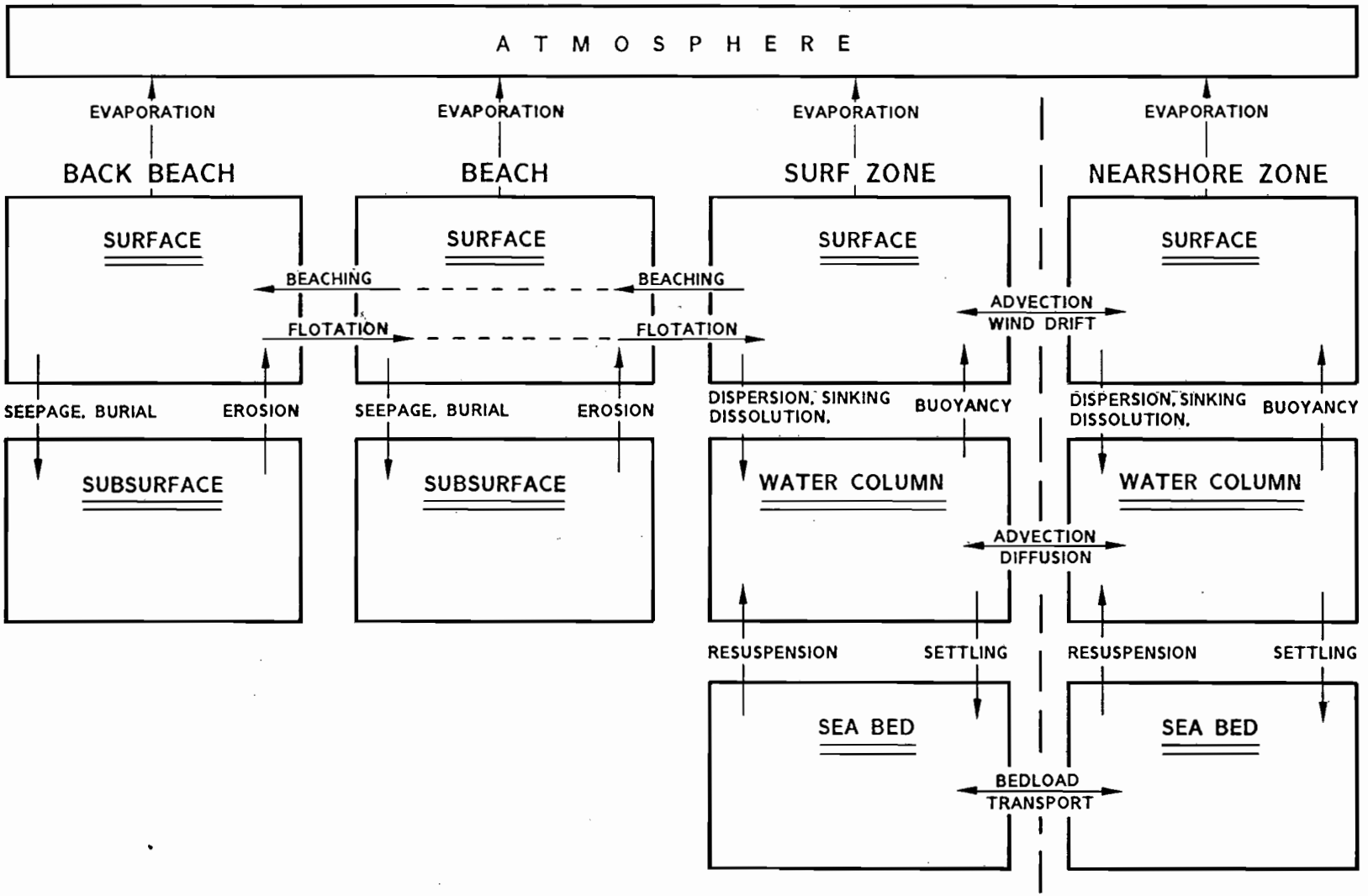

FIGURE 1.1. Onshore/offshore schematic compartments and dispersion processes for coastal oil-spill distribution model. The dashed line under the surface beach compartment indicates that beaching and flotation may occur directly from the backbeach to the surf zone and vice versa (depending on water levels). Processes associated with aggregation and agglomeration are indicated in "beaching." Oil in the surf-zone water column or on the seabed may beach after passing through the surface component.

1.1 Specific Scope of Work

Specifics of the project dictated the following tasks.

1) Evaluation of surf-zone sediment mass transport models (Section 2) based on:
   a) Cost-effectiveness of using energy-related parameters to drive the model (i.e., oil dispersion, transport, stranding, etc.).
   b) The degree to which existing models have been verified and applied in different localities and conditions.
   c) Adaptability of the reviewed models to the requirements of the project including use of interactive computer terminals.
   d) Development of alternative new model(s) including preliminary algorithms showing data requirements and outputs which would represent quantitative spatial and temporal sediment transport and distribution.
   e) Availability and attainability of data required for existing or conceptual new models.
   f) Estimates of programing, testing, sensitivity analyses and documentation of the proposed models.

2) Evaluation of oil-spill partitioning models (primarily Section 3) including:
   a) Analysis of the SAI oil partitioning model (Payne et al., 1984) (Section 3).
   b) Evaluation of alternate submodels (or model components) including a rank ordering of various alternatives and recommendations (Section 3).
   c) Adaptability of existing models or submodels to the requirements of the project (Section 3).
   d) Degree to which existing models have been verified and applied to different localities and conditions (Section 3).
   e) Flexibility of existing models with respect to problem solving using interactive computers (Section 3).
   f) Availability and attainability of data required for each model (Section 3).
   g) Degree to which existing models may be cost-effectively linked to a probabilistic surf-zone sediment mass-transport model (Section 6).

3) Evaluation and development of an oil-spill, surf-zone mass-transport (SMEAR) model including and/or based on:

a) Conceptual development of an interconnected sediment/surf-zone transport submodel, oil-partitioning submodel and oil/shoreline submodel (Section 6).

b) Compatibility of submodels and efficiency of linkages between submodels (Section 5).

c) Ability of model to be used for different localities (Section 5).

d) Ability of the model to function effectively with data which are readily and cost-effectively obtainable (Section 5).

e) Accuracy of model predictions of oil transport (estimated probable error) with respect to both the distribution in the surf-zone water column and beach materials and longshore transport (Section 6).

f) Flexibility of the model for interactive use in problem model application (Section 5).

g) Estimated costs of final programming, testing, sensitivity analysis, and documentation (Section 6).

h) Compatibility of the model with the outputs of the circulation and trajectory model developed for MMS by NOAA/OCSEAP, the oil weathering model developed by Payne et al. (1984), and an offshore particulate model now under development.

In addition to the above topics, a submodel is described in Section 4 to depict oil/shoreline interactions including:

1) Beach-face oiling,

2) Backbeach oiling and persistence (surface and buried oil),

3) Resuspension and subsequent transport, and

4) Changes with wave conditions and water levels.

2.0 EVALUATION OF SURF-ZONE CURRENT AND SEDIMENT-TRANSPORT MODELS

2.1 Introduction

Spilled oil in the surf zone can be transported as a surface slick, as particles within the water column, as oil adsorbed onto bottom or suspended sediments, or as oil mixed with sediment. This section presents the analytical process by which the most appropriate algorithms representing surf-zone currents and sediment transport are evaluated.

The format of this section is to first discuss both surf-zone and sediment-transport models in terms of theoretical algorithms and the practical solutions to those equations. Under surf-zone current models, a general model (depth-averaged, two-dimensional) is described in terms of each model component (e.g., radiation stress, tidal stress, etc.). Because the two-dimensional model is very complex and can be simplified under several circumstances, simplified one-dimensional models are also evaluated.

The second portion of this section evaluates the various algorithms developed to describe sediment transport in the surf zone. In addition, a depth-averaged, two-dimensional diffusion-dispersion equation is also described to more effectively model fine-grained sediment transport mechanisms.

The final portion of this section evaluates and ranks both surf-zone current models and sediment-transport models in terms of applicability to the SMEAR model.

2.2 Surf-Zone Current Model

As introduction, there are six principal force components determining the current velocity field in the surf zone. These components are:

1) Wave forces resulting from the radiation stress.
2) Tidal forces.
3) Friction forces on the bottom.
4) Lateral turbulent mixing forces.
5) Wind forces.
6) Coriolis forces.

Mathematically, these forces can be combined to form a general equation of momentum conservation. Basically, methods using conservation of momentum with the radiation stress principle have been thought to be the most reliable approach to the surf-zone current problem (Bijker, 1972: Basco, 1982).

The most sophisticated surf-zone current model currently available which incorporates the six principal force components is a depth-averaged two-dimensional model. It can be expressed by the following equations in tensor form:

Mass conservation:

$$\frac{\partial \bar{\eta}}{\partial t} + \frac{\partial}{\partial x_j}(h\bar{u}_j) = 0 \qquad j = 1, 2 \qquad (2.1)$$

Momentum conservation:

$$\frac{d\bar{u}_i}{dt} = f(1-\delta_{ij})\bar{u}_j + \frac{1}{\rho h}(\bar{\tau}_i^S - \bar{\tau}_i^B + \bar{\tau}_i^T) - \frac{1}{\rho h}\left[\frac{\partial S_{ij}}{\partial x_j} + \frac{\partial(h\bar{\tau}_{ij}^L)}{\partial x_j}\right] \qquad (2.2)$$

$$i,j = 1,2$$

where $h = d + \bar{\eta}$ = total local water depth.

d = water depth at mean sea level.

$\bar{\eta}$ = mean water-surface deviation.

$\bar{u}_i$ = the depth-averaged and time-averaged velocity component.

$f = 2\omega\sin\phi$ = Coriolis parameter.

$\bar{\tau}_i^S$ = the time-averaged wind-stress component.

$\bar{\tau}_i^B$ = the time-averaged bottom shear-stress component.

$\bar{\tau}_i^T$ = the depth-averaged tidal-stress component.

ρ = water density.

S_{ij} = the radiation-stress tensor.

$\bar{\tau}_{ij}^L$ = the effective lateral turbulent-mixing stress tensor.

δ_{ij} = Kronecker delta.

ω = angular rotation rate of earth.

The mass equation (2.1) neglects the small contribution of mass transport due to finite-amplitude wave orbital motion. The momentum equation (2.2) is similar to the equation used by Bowen (1969) with the exception that Coriolis force and tidal force have been included.

These equations (2.1 and 2.2) can be considered as the general governing equations for a two-dimensional surf-zone current model. Three unknowns, $\bar{u}$, $\bar{v}$, and

$\bar{\eta}$ can be solved simultaneously from (2.1) and (2.2) provided the boundary conditions are given and each force term on the right hand side of (2.2) can be properly expressed in an explicit mathematical form. In addition, a plane beach face from the high-tide water line down to the low-tide terrace is usually assumed in order to avoid a very difficult solution procedure relating the location of the breaker line to a varying tidal level and water line.

The following model components of Equation (2.2) are described in detail in the next sections: (a) radiation stress, (b) lateral turbulent mixing stress, (c) surf similarity parameter, (d) bottom shear stress, (e) tidal stress, and (f) local wind stress.

2.2.1 Radiation Stress

Radiation stress is defined as the excess momentum flux induced by the presence of wave motion (Longuet-Higgins and Stewart, 1964). Based on linear wave theory, these same authors derived the principal stress components which can be transformed into the expressions presented in Equations (2.3)-(2.8). Beach coordinates for each expression are indicated in Figure 2.1. In the past, these equations have been extensively used for surf-zone current modeling.

$$S_{xx} = E(\frac{3}{2} n - \frac{1}{2}) + E(\frac{n}{2}) \cos 2\alpha \tag{2.3}$$

$$S_{yy} = E(\frac{3}{2} n - \frac{1}{2}) - E(\frac{n}{2}) \cos 2\alpha \tag{2.4}$$

$$S_{xy} = En \sin\alpha\cos\alpha \tag{2.5}$$

where S_{xx}, S_{yy}, S_{xy} = Radiation stress components.

$E = \frac{1}{8} \rho g H^2$, wave energy.

$n = \frac{1}{2} (1 + \frac{2kh}{\sinh 2kh})$, wave energy flux configuration.

H = wave height.

$k = \frac{2\pi}{L}$, wave number.

L = wave length.

α = wave angle.

Longuet-Higgins and Stewart (1964) also provided expressions of radiation stresses for standing waves which, based on linear wave theory, are transformed into the following component expressions:

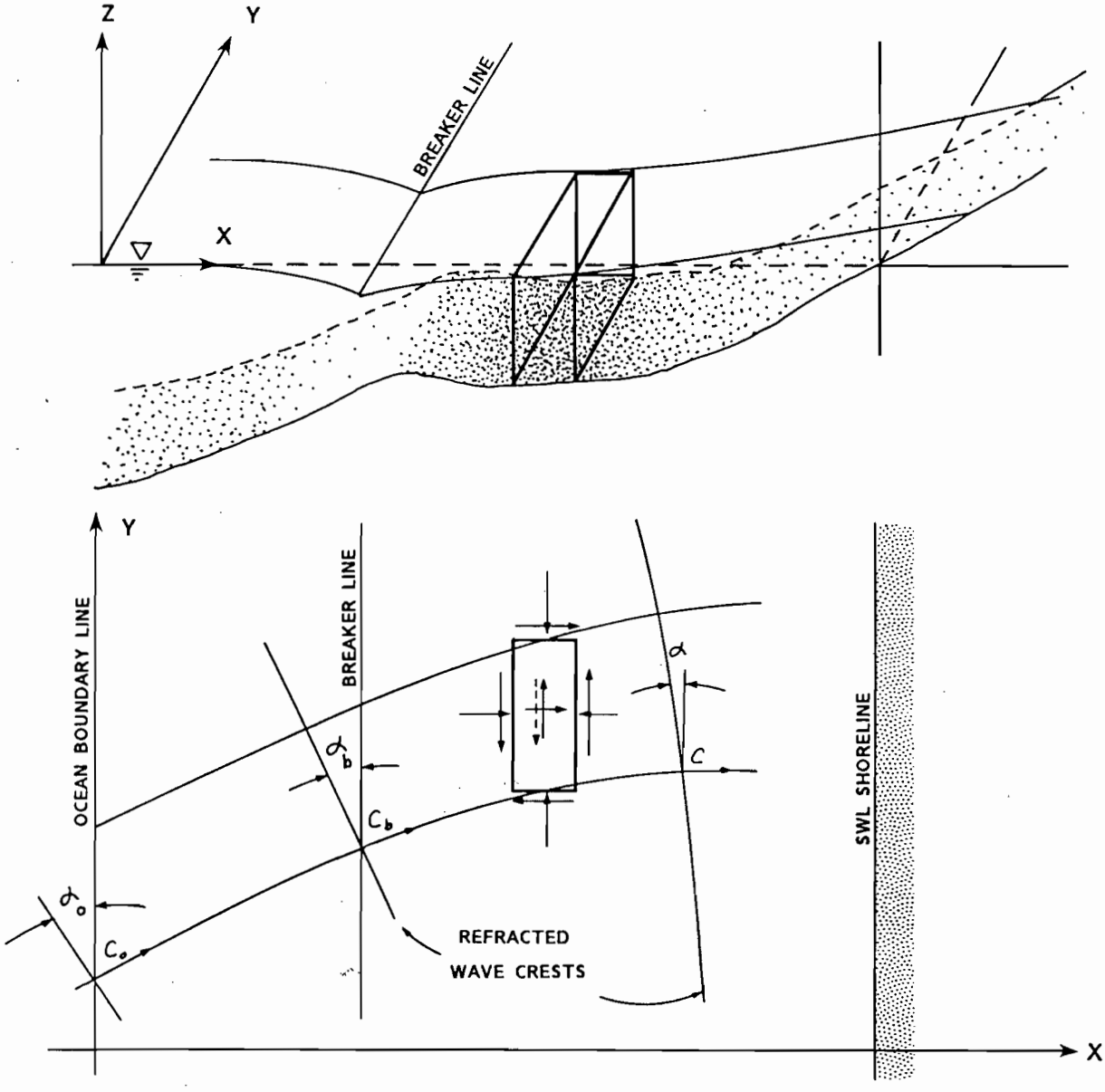

FIGURE 2.1. Surf-zone coordinate system. α = wave angle; c = wave celerity; o = refers to outside surf zone; b = refers to breaker line.

$$S_{xx} = E(3n - 1 + n \cos 2kx) + En(1 - \cos 2kx)\cos 2\alpha \quad (2.6)$$

$$S_{yy} = E(3n - 1 + n \cos 2kx) - En(1 - \cos 2kx)\cos 2\alpha \quad (2.7)$$

$$S_{xy} = En(1 - \cos 2kx)\sin 2\alpha \quad (2.8)$$

The crucial point in solving these equations is to properly quantify wave height, H. Outside the breaker line, wave heights can be modeled through shallow-water wave forecasting (CERC, 1984) by including wave transformation factors, such as water depth shoaling, damping refraction, diffraction, transmission, and even reflection if the bottom configuration suddenly changes. Since the theory of interaction of waves and currents is still not mature enough to be applied to practical engineering problems (Peregrine and Jonsson, 1983), inclusion of wave-current interaction factors is therefore not recommended.

In order to estimate the wave height distribution inside the surf zone, a breaking wave criterion must first be established after which a surf zone energy dissipation model must be developed. The empirical formula presented in Equation (2.9), derived by Weggel (CERC, 1984) incorporating the effects of changing bottom slope and wave steepness, is recommended for the breaking wave criterion.

$$\frac{H_b}{d_b} = b - (aH_b/gT^2) \quad (2.9)$$

where H_b = breaking wave height.

d_b = breaking depth.

$a = 43.75(1 - e^{-19\,m})$

$$b = \frac{1.56}{(1 + e^{-19.5\,m})}$$

m = beach slope.

T = wave period.

g = gravity acceleration.

For the surf-zone energy dissipation model, it is customarily assumed that the following Equation (2.10) is valid throughout the surf zone for the spilling breaker condition on a plane beach (Liu and Dalrymple, 1978):

$$H = \gamma \cdot (\bar{\eta} + d) \tag{2.10}$$

where γ is the wave-breaking parameter. In contrast, no suitable expressions are available for wave height inside the surf zone for beaches having relatively flat or bar-trough profiles (Basco, 1982). In this case, Equation (2.10) is still suggested.

Other assumptions, as follow, are also needed to express radiation stress inside the surf zone.

$$\cos\alpha \sim \cos\alpha_b \tag{2.11}$$

$$\sin\alpha = \left(\frac{h}{h_b}\right)^{1/2} \sin\alpha_b \tag{2.12}$$

where α, α_b = wave angle inside the surf zone and at the breaker line, respectively.

h, h_b = total local water depth inside the surf zone and at the breaker line, respectively.

2.2.2 Lateral Turbulent Mixing Stress

Due to weak understanding of surf zone turbulence, effective lateral stresses are usually described in terms of an eddy viscosity coefficient as shown below:

$$\bar{\tau}^{L}_{xx} = \bar{\nu}^{L}_{x}\left(\frac{\partial \bar{u}}{\partial x} - \frac{\partial \bar{v}}{\partial y}\right) \tag{2.13}$$

$$\bar{\tau}^{L}_{xy} = \bar{\nu}^{L}_{xy}\left(\frac{\partial \bar{u}}{\partial y} + \frac{\partial \bar{v}}{\partial x}\right) \tag{2.14}$$

$$\bar{\tau}^{L}_{yy} = \bar{\nu}^{L}_{y}\left(\frac{\partial \bar{v}}{\partial y} - \frac{\partial \bar{u}}{\partial x}\right) \tag{2.15}$$

These turbulent viscosity coefficients, ν^{L}_{x}, ν^{L}_{xy}, and ν^{L}_{y}, are directionally dependent. According to Prandtl's mixing length hypothesis, they can be expressed by Equation (2.16):

$$\bar{\nu}^{L} = \rho\overline{|\tilde{u}|}\ \bar{l} \tag{2.16}$$

where $\tilde{u}$ is a reference velocity and l is a length scale.

A reasonable reference velocity is the maximum bottom wave orbital velocity (Longuet-Higgins, 1970, 1972; Kraus and Sasaki, 1979). The maximum bottom wave orbital velocity has been expressed in Equation (2.17) for both the case outside the surf zone and the case inside the surf zone. The maximum bottom wave orbital velocity inside the surf zone, u_{max}, can be found from the note of Equation (2.23). Water depth, wave particle excursion, and surf zone width have been used as the scale for turbulent length. In order to simplify the solution procedure, a homogeneous mixing process is usually assumed (and is recommended for this project), that is:

$$\underline{\nu}^{L}_{x} = \underline{\nu}^{L}_{xy} = \underline{\nu}^{L}_{y} = \underline{\nu}^{L}$$

The suggested expression for ν^{L} is:

$$\underline{\nu}^{L} = \begin{cases} C_{\nu}\rho H(gh)^{1/2} & \text{outside surf zone} \\ C_{\nu}\rho\gamma h(gh)^{1/2} & \text{inside surf zone} \end{cases} \tag{2.17}$$

where $C_{\nu} = f(I_r)$ = mixing coefficient constant.

I_r = surf similarity parameter which is defined as

$$I_r = \frac{\text{beach slope}}{(\text{wave steepness})^{1/2}} \tag{2.18}$$

2.2.3 Surf Similarity Parameter

As defined by (2.18), the surf similarity parameter is the ratio of beach slope, m, and the square root of wave steepness. This parameter is also called the Iribarren Number which is useful to quantify several aspects of waves breaking on a plane beach, such as breaking criterion, breaker type, number of waves in the surf zone, wave runup and setup, beach type (dissipative versus reflective), reflection, etc. Overall parameters of the surf zone are listed in Table 2.1 (Sasaki and Horikawa, 1975; Sasaki et al., 1977; Wright et al., 1979; Basco, 1982).

TABLE 2.1 Overall parameters of surf zone versus Iribarren Number (I_r). [X_b = surf-zone width; n = offshore modal number of edge waves]

Iribarren Number (I_r)	0.1 (4 6 8)	2 4 6 8	1 2 4 6 8 10
Domain	Infragravity	Instability	Edge Wave
Microtopography	Longshore Bar	Crescentic Bar	Beach Cusp
Beach Slope	$<\frac{1}{50}$	$\frac{1}{20} \sim \frac{1}{40}$	$>\frac{1}{10}$
Wave Steepness	Large		Small
Surf Zone	Always Exists	Exist or Not Exist	Not Always Exist
Beach Type	Dissipative System		Reflective System
Wave Type	Progressive Waves		Standing Waves
Runup/Setup	Setup Predominant		Runup Predominant
Incident Wave Characteristics	Wind Wave	Swell Predominant	Incident Wave Predominant
Breaker Type	Spilling	Plunging	Collapsing/ Surging
Rip-Current Spacing	$157\ I_r^2 \cdot X_b$	$4 \cdot X_b$	$(\frac{2}{n+1})\pi \cdot X_b$, n = 1,2
Breaker Index	≃0.8	1.0 1.1	1.2
Number of Waves in Surf Zone	6~7	2~3 1~2	0~1 0~1
Reflection Coefficient	0.001	0.01 0.1	0.4 0.8
$I_r = \frac{m}{(H/L_o)^{1/2}}$	4 6 8 0.1	2 4 6 8 1	2 4 6 8 10

2.2.4 Bottom Shear Stress

The general expression for the bottom shear stress is:

$$\vec{\tau}^{B}(t,x,y) = C_f \rho |\vec{U}| \vec{U} \tag{2.19}$$

where C_f = $C_f(Re)$, combined friction coefficient from waves and current.

ρ = fluid density.

$\vec{U}$ = $\vec{U}_b + (\bar{u}, \bar{v})$.

$\vec{U}_b$ = wave orbital velocity near the bottom.

$(\bar{u}, \bar{v})$ = time-averaged current velocity.

Re = Reynolds number.

The velocity vector components in the surf zone are shown in Figure 2.2. The fluctuations of time-averaged mean bottom shear stress can be described by Equation (2.20):

$$\bar{\tau}_i^{B} = C_f \rho \langle |\vec{U}| \vec{U} \rangle_i \tag{2.20}$$

where $\langle\ \rangle = \frac{1}{T} \int_{t_o}^{t_o+T} (\quad) dt$

t_o = arbitrary starting time.

T = wave period.

t = time variable.

Based on Figure 2.2, the absolute value of the total velocity can be expressed as:

$$|\vec{U}| = [(U_b) + 2U_b(\bar{u}\cos\alpha + \bar{v}\sin\alpha) + (\bar{u}^2 + \bar{v}^2)]^{1/2} \tag{2.21}$$

where U_b = $|u_{max}|\cos(2\pi t/T)$.

u_{max} = maximum value of wave orbital velocity near bottom.

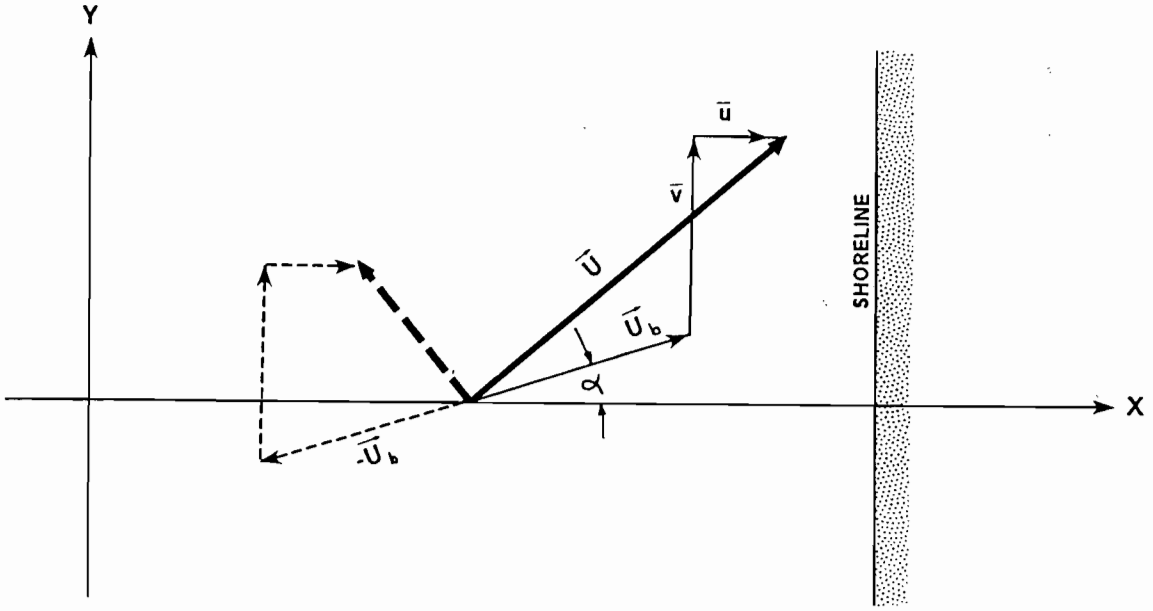

FIGURE 2.2. Surf-zone velocity vector components.

There are two extreme cases where Equation (2.20) can be greatly simplified. The first case is for a weak current flow (i.e., $|(\bar{u}.\bar{v})|<<|U_b|$). In this case, the mean stress components can be expressed by Equations (2.22) and (2.23):

$$<|\vec{U}|\vec{U}>_x \simeq <|U_b|>[\bar{u} + \cos\alpha(\bar{u}\cos\alpha + \bar{v}\sin\alpha)] \tag{2.22}$$

$$<|\vec{U}|\vec{U}>_y \simeq <|U_b|>[\bar{v} + \sin\alpha(\bar{u}\cos\alpha + \bar{v}\sin\alpha)] \tag{2.23}$$

where $<|U_b|> = (2/\pi)|u_{max}|$

$u_{max} = (1/2)\gamma(gh)^{1/2}$

$h = \bar{\eta} + d$

The other extreme case is for a strong current flow (i.e., $|(\bar{u}, \bar{v})|>>|U_b|$). Different expressions can be obtained for this case, as shown by Equations (2.24) and (2.25):

$$<|\vec{U}|\vec{U}>_x \simeq \bar{u}|(\bar{u}, \bar{v})| + \frac{|u_{max}|^2}{4|(\bar{u}, \bar{v})|}[\bar{u} + 2\cos\alpha(\bar{u}\cos\alpha + \bar{v}\sin\alpha)] \tag{2.24}$$

$$<|\vec{U}|\vec{U}>_y \simeq \bar{v}|(\bar{u}, \bar{v})| + \frac{|u_{max}|^2}{4|(\bar{u}, \bar{v})|}[\bar{v} + 2\sin\alpha(\bar{u}\cos\alpha + \bar{v}\sin\alpha)] \tag{2.25}$$

2.2.5 Tidal Stress

Based on the theory of long waves associated with tides, the tidal stress is:

$$\bar{\tau}_i^T = -\rho gh\frac{\partial \xi}{\partial x_i} \tag{2.26}$$

where ξ is the tidal water-surface profile. According to Schureman (1941):

$$\xi = A_o + \Sigma\, \xi_j \tag{2.27}$$

where $\xi_j = F_j(t)A_j(\lambda,\phi)\cos[\omega_{oj}t + \chi_j - G_j(\lambda,\phi)]$.

A = mean amplitude over 18.6 years.

λ = geographical longitude.

ϕ = geographical latitude.

G = Greenwich phase or epoch at given position (λ,ϕ).

ω_o = tidal frequency.

χ = astronomical argument.

F = nodal factor, a slowly varying function of time

2.2.6 Local Wind Stress

Nummedal and Finley (1978) suggest that local wind stress can be a very significant factor in generating surf zone currents (based on their research results at Debidue Island, South Carolina). To date, the knowledge of how wind stress affects the surf-zone current is poorly understood and remains largely unknown. Bodine (1971) and CERC (1984) proposed Equation (2.28) for expressing wind stress in storm surge calculations. This formula, as follows, is recommended for the present study:

$$\bar{\tau}_i^s = K\rho|W^{10}|W_i^{10} \tag{2.28}$$

where $K = \begin{cases} K_1 & W<W_c \\ K_1 + K_2 (1 - \frac{W_c}{W})^2 & W>W_c \end{cases}$

$K_1 = 1.1 \times 10^{-6}$

$K_2 = 2.5 \times 10^{-6}$

ρ = water density.

W_i^{10} = wind velocity component at 33 ft above sea level, based on 10-minute average.

W_c = critical wind speed (14 knots or 16 mph).

2.2.7 Surf-Zone Current Along Straight Shorelines

A fairly straight uniform beach without tidal inlets experiences almost unidirectional longshore currents in the surf zone, thereby enabling a simple solution to the general depth-averaged, two-dimensional model described previously. In this case, Coriolis force is not significant and tidal force is small relative to the other remaining forces (Bijker, 1972). Therefore, the important forces that have the greatest influence

are wave force, bottom friction force, lateral turbulent force, and wind force (if the local wind is relatively strong).

In the case of a fully developed, longshore current, as is fairly typical, the previously described, four major forces determine a state of dynamic equilibrium with the current velocity being constant. Therefore, a governing equation, deduced from Equation (2.2), is as follows:

$$\bar{\tau}_{sy} - \bar{\tau}_{by} - \frac{dS_{xy}}{dx} + \frac{d(h\bar{\tau}_{Lxy})}{dx} = 0 \qquad (2.29)$$

An analytic solution of this equation has not yet been developed, so a numerical scheme is needed. Several analytic solutions have been formulated in the following general form for a fully developed flow on a plane beach by omitting different stress terms (Bowen, 1969; Longuet-Higgins, 1970; Thornton, 1970; Bijker, 1972; Komar, 1975; Liu and Dalrymple, 1978; Kraus and Sasaki, 1979):

$$V_l = K \cdot F(I_r, m, C_f, H_b, h, g)\sin\alpha_b \cos\alpha_b \qquad (2.30)$$

where V_l = longshore current velocity.
K = constant.
I_r = Iribarren number.
m = beach slope.
C_f = bed friction coefficient.
H_b = breaker height.
h = local water depth in the surf zone.
g = acceleration of gravity.
α_b = breaker angle.

These formulae generally give the velocity distribution as a function of distance from the coast, but consistently omit the influence of wind stress.

Komar (1976) proposed the following empirical equation to describe mid-surf current velocity based on his research results from both field data and laboratory data:

$$V_l = 2.7\, u_m \sin\alpha_b \cos\alpha_b \qquad (2.31)$$

where u_m = maximum value of the horizontal rms wave orbital velocity in the surf zone.

V_l = mid-surf current velocity.

This empirical formula (2.31) is strongly supported by the analytical solution proposed by Kraus and Sasaki (1979), which is thought to be the best available analytical model of a steady state longshore current flow for a wide range of beach slope, bottom materials and breaking wave angles (Basco, 1982). CERC (1984), based on Longuet-Higgins' equation and field data, proposed the empirical equation (2.32) to compute mean longshore current velocity of fully developed flows.

$$V_l = 20.7\ m\ (gH_b)^{1/2} \sin 2\alpha_b \qquad (2.32)$$

where m = beach slope.

g = acceleration of gravity.

H_b = breaker height.

α_b = breaker angle.

The main difference between these two empirical formulae is the appearance of beach slope in (2.32). Komar (1976) argued that the ratio of beach slope to bed friction coefficient was approximately constant so that m did not appear in his formula. Kraus and Sasaki's study supported Komar's theory.

Komar (1975) argued that part of the wave-induced longshore current can be generated by longshore variations in wave breaker height. Based on radiation stress theory, this contribution can be incorporated into the governing equation in terms of longshore breaker height gradient. The gradient of longshore breaker height is a ratio of wave-height difference over the distance between two locations. In more complicated situations, a two-dimensional model could be used, and this effect will be automatically included in the radiation stress component. However, since it is considered to be a localized phenomenon and difficult to quantify, and the breaker height distribution along a straight plane beach is usually fairly uniform, we believe it can be neglected.

For practical reasons, we conclude the following empirical formula (2.33) should be considered for the SMEAR model in calculating mean surf zone longshore current

velocity (one-dimensional case); note that the local wind effect has also been incorporated:

$$V_l = K_1(gH_b)^{1/2} \sin 2\alpha_b + K_2 W_n + K_3 \tag{2.33}$$

where K_1, K_2, K_3 = constants, determined from field data.
W_n = wind velocity component.

Practical reasons for recommendation of Equation (2.33) include:

1) The existing solutions do not account for wind stress.
2) The parameters involved in the existing solutions are too many to be correctly measured in the field and the calculated solution accuracy is still a question.
3) Parameters in Equation (2.33) are only four and can be easily and correctly measured, and it includes local wind effects.
4) Computation of Equation (2.33) is very easy and time saving.
5) Equation (2.33) can correctly compute current velocity in the surf zone.

2.3 Surf-Zone Sediment Transport Model

The CERC (1984) longshore sediment transport formula has been widely applied to coastal engineering problems; however, this formula is applicable only to a straight plane beach where wave energy is a dominant factor. Komar and Inman (1970) proposed a formula with more general application to a simple straight beach. Similar formulae have been proposed by Dean (1973), Galvin (1972), and others.

In more complicated cases, the formulae mentioned above can not be used. In Europe, most of the sediment transport formulae used in coastal engineering have been derived from study of sediment transport in rivers. The major difference is that the effects of waves are properly included in the coastal studies. According to the evaluation by Graaff and Overeem (1979), primary formulations used in Europe are the Bijker formula (1971), the Swanby method, and adapted Engelund-Hansen and adapted Ackers-White formulae. All these formulae are suitable to more complicated cases. Graaff and Overeem (1979) also conclude that Bijker's formula is the best among the group.

2.3.1 The Bijker Formula

Bijker modified Friglink's formula by incorporating the increased wave-induced effect into the bottom friction stress to describe the bed load function. He also used Einstein's concept for predicting the suspended load (Bijker, 1972). Bijker's formula has the advantage of calculating the suspended load and bed load, separately. His formula for computing sediment-transport rate in the littoral zone is:

$$Q_{bed} = 5\ D_{50}\ \frac{v}{C_r}\ g^{1/2}\ \mathrm{Exp}\ \left\{ \frac{-0.27\ \Delta\ D_{50}\ \rho g}{\mu \tau_c [1 + \frac{1}{2}\ (\xi\ \frac{u_{max}}{v})^2]} \right\} \qquad (2.34)$$

where D_{50} = particle diameter (50 percent by weight exceeded).

C_r = Chezy coefficient.

Δ = $(\rho_s - \rho)/\rho$.

ρ_s = mass density of bed material.

μ = $(C_r/C_{90})^{1.5}$, ripple factor.

C_{90} = Chezy coefficient based on D_{50}.

τ_c = $\rho g(v^2/C_r^2)$.

ξ = Bijker's parameter, $f(k,C_r)$.

u_{max} = maximum wave orbital velocity near bottom.

Q_{bed} = bedload (m^3/m^2, including pores).

$$Q_{susp} = 1.83\ Q_{bed}\ [I_1\ \ln(33h/k) + I_2] \qquad (2.35)$$

where $$I_1 = \frac{.216(\frac{k}{h})^{(z-1)}}{(1-\frac{k}{h})^z} \int_{(\frac{k}{h})}^{1} (\frac{1-y}{y})^z\ dy$$

where $$I_2 = \frac{.216(\frac{k}{h})^{(z-1)}}{(1-\frac{k}{h})^z} \int_{(\frac{k}{h})}^{1} (\frac{1-y}{y})^z\ \ln y\ dy$$

$$Z = \frac{\omega}{K\ V^*_{wc}}$$

ω = sediment particle fall velocity.

K = von Karman coefficient.
$V^*_{wc} = V^*_c[1 + 1/2(\xi\ u_{max})^2]^{1/2}$
V^*_c = shear stress velocity due to current.
h = local water depth.
k = bed roughness.
Q_{susp} = suspended load (m^3/m^2).

The total sediment transport yields:

$$Q_{total} = Q_{bed} + Q_{susp} \tag{2.36}$$

2.3.2 The Komar Formula

Komar and Inman (1970) proposed the following empirical formula for estimating longshore sediment transport:

$$I_l = 0.28(ECn)_b \cos\alpha_b\ (v_l^{1/2}/u_m) \tag{2.37}$$

where $(ECn)_b \cos\alpha_b$ is wave energy flux evaluated at the breaker zone. This formula provides a more general consideration for the case where the surf zone current is generated by both wave force and local wind force. Komar (1976) also proposed the formula, Equation (2.38), to estimate suspended sediment transport in terms of total sediment transport, I_l:

$$I_{susp} = 7.0(\rho_s/\rho - 1)(c/\gamma_b m) \cdot I_l \tag{2.38}$$

where m = beach slope.
c = the average volume concentration of sand in suspension.
γ_b = breaking parameter.
I_l = total sediment load (dyne/sec).
I_{susp} = suspended load (dyne/sec).

Komar's formula also has the advantage of calculating I_{susp} and I_l, separately.

2.4 Fine-Sediment Transport Model

Whereas the Bijker and Komar equations are suitable for longshore transport, offshore waters and sheltered lagoons may be dominated by fine-grained suspended sediments requiring different modeling parameters. A diffusion/dispersion sediment transport model (depth-averaged, two-dimensional) is generally required in this case. Many similar models have been developed using different numerical schemes. The governing, mass-conservation equation for this model is as follows:

$$\frac{\partial c}{\partial t} + \bar{u}\left(\frac{\partial c}{\partial x}\right) + \bar{v}\left(\frac{\partial c}{\partial y}\right) = \frac{\partial}{\partial x}\left(D_x \frac{\partial c}{\partial x}\right) + \frac{\partial}{\partial y}\left(D_y \frac{\partial c}{\partial y}\right) + S \qquad (2.39)$$

where c = depth averaged sediment concentration.

D = effective turbulent diffusion coefficient.

$\bar{u}$, $\bar{v}$ = depth averaged velocity component.

S = rate of erosion or deposition (source/sink term).

The finite element scheme using the Galerkin method has been widely used recently to solve this governing equation (Ariathurai et al., 1977; Hayter and Mehta, 1982; Onishi and Trent, 1982; Siah, 1985). These references provide detailed discussion of this solution approach, therefore it is not given here. In case of fact, the actual fine-sediment transport rate is relatively small compared to the longshore transport rate under normal weather conditions.

2.5 Model Evaluation and Recommendation

2.5.1 Evaluation Criterion

The previously discussed surf-zone current and sediment models were evaluated for each type of shoreline based on a set of standard criteria. Each criterion has a maximum value which describes the perfect case for that item. The maximum sum of all criteria is 100. The criteria used were:

1) Model/formula reliability (50 points) based on theoretical formulation and verification from field data or laboratory data. This was considered to be the most important of all the criteria in order to formulate an effective SMEAR model. Ranking in terms of theoretical formulation was based on inclusion of the four primary forces--radiation stress, bottom stress, turbulent mixing, and wind stress. In addition,

the amount of uncertainty in the coefficients utilized in the model or equation was estimated. The extent of verification or, in the case of new models, the likelihood of verification was the last factor included under this criterion.

2) Availability and attainability of field data required for each model (15 points). This factor includes the ease by which input field data can be obtained from readily available sources. Lowest values were given to models requiring extensive field surveys before being able to run the model. Highest values represent models requiring the simple and rapid collection of field data with only a limited number of measurements.
3) Adaptability of the model to the requirements of the project including use on interactive computer terminals (15 points). This criterion includes evaluation based on two primary aspects--linkage with the SMEAR and offshore models, and use on a user-friendly microcomputer. If the model or equation being evaluated required extensive computer space and linkage appeared to be difficult, then the model was given a low score.
4) Relative cost-effectiveness of using the model (10 points). This factor includes such factors as model complexity in terms of requiring extensive CPU time, the costs of data collection, and the number and complexity of model inputs requiring user time. The highest scores reflect fewer and more simplistic input parameters resulting in more rapid data input and less CPU time.
5) Easiness of programming, testing, sensitivity analyses and documentation of the proposed models (10 points). This criterion included evaluation of the time required for model testing, debugging, analysis of model stability using various input parameters, and an analysis of model sensitivity to small changes in individual components.

2.5.2 Model Evaluation for Application to Sandy Beaches

Based on the discussions presented in Sections 2.1 to 2.4, a depth-averaged two-dimensional model and five longshore current models were selected for evaluation specifically for application to sandy beaches. As shown in Table 2.2, the suggested model described by Equation (2.33) received the highest scores and is therefore

recommended for computing current velocity inside the surf zone along sandy beaches. Several other models were very close in overall score. The two-dimensional nearshore current model received very high scores for its theoretical background (formula reliability) and adaptability, but was considered very poor in terms of data availability, cost effectiveness and programming ease, because of the overall model complexity and data requirements. All the other models have a slightly more limited theoretical basis but score much higher in terms of the same three factors that were rated poor in the more sophisticated, two-dimensional model. The suggested model, Equation (2.33), ranks slightly ahead of both the Komar and CERC formulations because of its inclusion of a wind stress component.

For longshore sediment transport, the formulae of CERC (1984), Bijker (1971), and Komar (1976) were selected for evaluation. As shown in Table 2.3, Komar's (1976) formula turns out to be the one with the highest scores and is therefore recommended. The CERC formula was considered weak in its theoretical basis while Bijker's formula received the lowest scores based on higher costs associated with obtaining input data, programming, and running the model.

TABLE 2.2 Evaluation of surf-zone current models for application to straight sandy beaches.

Model Criteria	2-D Nearshore Current Model	1-D Steady Longshore Current Model				
		Equation (2.29)	Komar Eq.(2.31)	CERC Eq.(2.32)	Kraus and Sasaki (1979)	Equation (2.33)
Formula Reliability (50 points)	45	43	35	35	40	42
Data Availability and Attainability (15 points)	5	10	15	15	10	12
Adaptability (15 points)	12	12	10	10	12	10
Cost-effectiveness (10 points)	1	5	10	10	6	10
Ease of Programming (etc.) (10 points)	1	5	10	9	6	10
Total Score	**64**	**75**	**80**	**79**	**74**	**84**

TABLE 2.3 Evaluation of surf-zone sediment transport models for application to straight sandy shorelines.

Model Criteria	CERC (1984)	Bijker (1971)	Komar (1976)
Formula Reliability (50 points)	30	40	35
Data Availability and Attainability (15 points)	14	12	14
Adaptability (15 points)	10	10	12
Cost-effectiveness (10 points)	10	5	10
Ease of Programming (etc.) (10 points)	9	5	10
Total Score	**73**	**72**	**81**

2.5.3 Model Evaluation for Application to Tidal Flats, Gravel Beaches and Rocky Shorelines

Since no good theories exist for developing surf-zone current models for application to these types of shoreline, the empirical current model accepted previously for sandy beaches is suggested for use in this project.

Sediment transport along rocky shoreline or gravel beach can, in most cases, be neglected because of the lack of sediment sources. As far as sediment transport in tidal flats is concerned, Bijker's (1971) formula is the most reliable.

2.5.4 Model Evaluation For Tidal Inlet/Marsh Systems

Marsh areas may be linked to offshore waters by either a tidal inlet or wide bay. In the marsh area, wave action is generally small compared to tidal actions under normal conditions so that a two-dimensional circulation model is usually needed to compute the velocity field. Fine-grained rather than coarse-grained sediments predominate so a two-dimensional diffusion-dispersion model with the governing Equation (2.39) should be used, although this is admittedly a relatively minor process compared to longshore transport.

Within a tidal inlet or waterway, the flow pattern and sediment-transport phenomena are very complicated. Both wave forces and tidal forces are important

factors. No one-dimensional steady current model can correctly predict the flow field. The proposed two-dimensional model [i.e., Equations (2.1) and (2.2)] should be considered. Bijker's formula is the only reliable sediment transport model that should be applied in this case. Modeling of transport into and out of coastal lagoons and embayments, in terms of the practical considerations of SMEAR are discussed in Section 6.4.

2.6 Summary Of Recommended Models

Based on the previous evaluations, we recommend that two combinations of current and sediment-transport models be considered for incorporation into the SMEAR model. The first utilizes a simple, one-dimensional current model together with a simple, semiempirical, sediment-transport model. As indicated in Tables 2.2 and 2.3, Equation (2.33) and the equation developed by Komar (1976) have received the highest scoring for this category.

The second combination recommended for incorporation into SMEAR links the complex, two-dimensional nearshore current model [Equations (2.1) and (2.2)] with the sophisticated Bijker (1971) formulation. As indicated in Tables 2.2 and 2.3, faults inherent in this combination are primarily related to programming difficulties and computer memory requirements but, perhaps, model outputs from other SMEAR components would compensate for these shortcomings. The analysis of both combinations, specifically with respect to the complete SMEAR model, is presented in Section 5.

3.0 ANALYSIS OF OIL SPILL PARTITIONING MODELS

3.1 An Overview

This section contains a discussion of the various, oil-spill partitioning components followed by an evaluation of the primary models developed to mathematically represent each process. Based on this critical evaluation, the best model for inclusion in SMEAR is designated. The final equations for each partitioning component are discussed under the SMEAR model development plan (Section 6.0).

Oil partitioning can be viewed as a series of interrelated equilibrium or pseudo-equilibrium processes involving partitioning of the oil between the gaseous (i.e., atmosphere), aqueous (seawater in this case) and solid (suspended particles or sediments) phases. The dynamic exchange of oil among these various compartments can be considered a function of eight basic processes:

1) Spreading
2) Evaporation
3) Dissolution
4) Dispersion
5) Emulsification/deemulsification
6) Adsorption/desorption
7) Photooxidation
8) Biodegradation

Mathematical modeling of these processes has been attempted through application of basic physical/chemical equilibrium relationships to the mass transfer of petroleum components between the various phases. The following are brief descriptions of each process and the general approaches toward their modeling.

3.1.1 Spreading

Spreading determines the areal extent of spilled oil and affects the various weathering processes influenced by surface area, including evaporation, dissolution, dispersion and photooxidation. Spreading is controlled by the driving forces of gravity and surface tension and the retarding forces of inertia and viscosity. In the surf zone and onshore, accumulation (or "inverse spreading") may result due to wave transport and/or onshore wind (oil accumulation processes in terms of the unified SMEAR model are discussed in Section 6.0). Various researchers have investigated the spreading process, and several methods are available for use in its modeling; however, none of these methods are able to completely describe the complex mechanisms involved. Fay's (1971) three-regime spreading theory is the most widely used (Huang and Monastero, 1982). Other methods include variations of Fay's (1971) spreading theory incorporating diffusion/dispersion, Murray's turbulent diffusion theory, random Fickian

diffusion, empirical regression, and Mackay's empirical thick and thin slick approach (Mackay et al., 1980b), which is derived directly from Fay's second (gravity-viscous) equation.

3.1.2 Evaporation

Evaporation, which typically accounts for 20-40 percent of spilled oil (Gundlach and Boehm, 1981), is strongly influenced by oil composition as reflected by spill area, slick thickness, oil-vapor pressure, and the mass-transfer coefficient. Oil composition is also important since the more volatile fractions evaporate most rapidly. Models which address evaporation do not usually account for all four of these physical parameters. Spill area is determined by spreading, while both vapor pressure and the mass-transfer coefficient are dependent on wind speed. Oil-vapor pressure changes as hydrocarbon fractions are lost into the atmosphere.

The methods currently in use to computationally characterize evaporation rate are the pseudocomponent approach and an analytical approach. In the pseudocomponent approach, oil is characterized by a set of hydrocarbon components grouped by their boiling points (Payne et al., 1984) or by a "synthetic" mixture of representative hydrocarbon components (Mackay et al., 1980b). The pseudocomponent approach of Payne et al. (1984) considers up to 20 groupings of hydrocarbons representing boiling-point ranges or distillate fractions of crude oil. The UOT (Mackay et al., 1980b) approach considers a number of selected hydrocarbons, each representative of a group of hydrocarbons of similar properties. For example, in the UOT pseudocomponent approach, n-decane would represent C_9-C_{11} alkanes; phenanthrene would represent the polynuclear aromatic hydrocarbons and "inert" hydrocarbons represent asphaltenes. Weathering models, including the Payne et al. (1984) approach, generally do not differentiate between physical properties of saturated and aromatic hydrocarbons as their pseudocomponent approach addresses evaporation and not dissolution. This method allows different fractions of the oil to evaporate at different rates and the density of the slick to change as a function of time. Both pseudocomponent approaches permit calculation of both the remaining oil mass and its chemical composition and physical properties as a function of evaporation. The analytical approach describes vapor pressure as a function of temperature and amount evaporated (Mackay et al., 1980a). Both approaches use a similar mass-transfer concept, expressing the mass-transfer coefficient as a function of wind speed, vapor pressure, spill size (both area and volume), and temperature.

Table 3.1 (Huang and Monastero, 1982) presents the modeling equations used by a number of models to express the rate of evaporation. While all the models include mass transfer coefficients, oil-vapor pressures, and spill areas (Table 3.2), only the SLIKFORCAST (VKI) and UOT models consider slick thickness.

TABLE 3.1 Evaporation models (modified from Huang and Monastero, 1982).

1) SEADOCK Model (Williams et al., 1975)

$$\frac{d\,C_i}{dt} = -K_{ei}C_i$$

2) UOD (University of Delaware) Model (Wang et al., 1976)

$$\frac{d\,C_i}{dt} = -D_e C_i$$

$$D_e = K_e(P_i - P_{i\infty}) \,/\, (RT) \simeq K_e P_i/RT$$

$$K_e = \alpha A^{\alpha}\, e^{\beta U} \;;\; \alpha,\alpha,\beta = \text{empirical coefficients}$$

3) USC/API Model (Kolpack et al., 1977)

$$\frac{d\,E_i}{dt}\ (m^3/_{hr}) = \frac{5.21388 \times 10^{-6}\, M_i\, U_6\, (e_6 - e_{oi})}{(M_i + 28.966)P_i(\ln 6/Z_o)^2}$$

4) ASA Model (Spaulding et al., 1982b) Same as the UOD model, but uses different solution scheme.

5) SLIKFORCAST Model (Audunson et al., 1980)

$$\frac{d\,Q_i}{dt} = -K_{ei}Q_i$$

$$K_{ei}(sec^{-1}) = (7.4 \times 10^{-3} + 1.87 \times 10^{-3}U)\, P_i M_i \,/\, (RT\delta\rho)$$

6) UOT Model (Mackay et al., 1980a)

$$\frac{dE}{dt} = \frac{K_e\, A\, M_v}{RTV_o/(1-F)}$$

$$\Delta F = (\Delta E)P = (\Delta E)P_o e^{-C_1 F}$$

$$T = T_o + C_2\, T_e\, F/10.6$$

$$F(t+1) = F(t) - \Delta F$$

$$K_e \simeq 0.0025U^{0.78}$$

TABLE 3.1 Evaporation models (continued).

7) Blokker (1964)

$$\frac{dV_i}{dt} = -K_{ei}\, U^{\alpha} b l^{1-\beta} P_i M_i \qquad \text{Rectangular Slick}$$

$$\frac{dV_i}{dt} = \frac{\pi}{4} K_{ei} U^{\alpha} D^{2-\beta} P_i M_i \qquad \text{Circular Slick}$$

$\alpha = (2-\eta)/(2+\eta)$: $\beta = \eta/(2+\eta)$

η = turbulence parameter

= 0.25 for a "neutral" atmosphere

8) Fallah and Stark (1976)

$$V_t = \gamma_1\, \gamma_2\, \ldots . \gamma_n V_o$$

$\gamma_i = V_i/V_{i-1}$ = random variable

9) Mackay and Leinonen (1977) (used in SAI model)

$$E_i = K_e\, X_i P_i / RT$$

$$K_e \simeq 0.0025\, U^{0.78}$$

Subscript i = i^{th} component in oil

C_i, E, Q, V_o = concentration, evaporation flux, mass weight, and volume

K_e = mass transfer coefficient or evaporative coefficient

D_e, A, U = diffusive coefficient, spill area, and wind speed, respectively

R, P, T, M = gas constant, vapor pressure, temperature, and molecular weight, respectively

e_6, e_o = vapor pressures at 6-m altitude and at sea surface, respectively

Z_o = roughness at sea surface (cm)

δ, ρ = average slick thickness and oil density

M_v, X_i = molar volume and mole fraction of oil component, respectively

F = fraction of slick evaporated

a, α, β, C_1, C_2 = constants

T_o, T = boiling point temperatures initially and after some time, respectively

T_e = temperature at which C_2 is evaluated

t = time

TABLE 3.2 Physical parameters considered in various evaporation models. [*Pseudocomponents method or analytical method]

Models	Spill Area	Mass Transfer Coefficient	Slick Thickness	Oil Vapor Pressure*
SEADOCK	No	Yes	No	Pseudo
UOD	Yes	Yes	No	Pseudo
USC/API	No	Yes	No	Pseudo
ASA	Yes	Yes	No	Pseudo
SLICKFORCAST	Yes	Yes	Yes	Pseudo
UOT	Yes	Yes	Yes	Analytical
Blokker	Yes	Yes	No	Pseudo
Fallah and Stark	Yes	Yes	No	Pseudo
Mackay and Leinonen (used in SAI model)	No	Yes	No	Pseudo

3.1.3 Dissolution

Dissolution is the process by which hydrocarbons dissolve in the water. This process is more active shortly after a spill and affects the same hydrocarbon fractions as evaporation. However, dissolution is generally two or more orders of magnitude smaller than evaporation in mass balance computations (McAuliffe, 1976; Harrison et al., 1975) and is highly dependent on the surface area in contact with water (and thus on dispersion processes which can create oil droplets of different sizes in water). Exact measurements are difficult to obtain.

Evaporation will tend to deplete volatile hydrocarbons in an oil slick much more rapidly than will dissolution, thus leaving relatively little hydrocarbon material for dissolution. The rates (i.e., mass transfer coefficients) of evaporation are much larger than those for dissolution (Table 3.3).

Another modeling technique used involves the approach of combining dissolution with evaporation to express the rate of oil-mass loss as a first-order kinetic process (Williams et al., 1975). A different approach essentially ignores dissolution as a separate process and instead considers the total amount of oil which enters into the water column as a dispersion process (Blaikley et al., 1977; Reed et al., 1980; Spaulding et al., 1982a). Such an approach is adopted because of the difficulty in distinguishing between dissolution and dispersion in the field and is justified by the probability that the bulk of any dissolution occurs after oil has been dispersed rather

than when it is in a slick. Dissolved and dispersed oil may be operationally distinguished by means of filtration, although the use of this technique may actually permit the passage of colloidal oil droplets through the filter and hence may be subject to the formation of artifacts if the filter becomes overwhelmed by oil (Boehm and Quinn, 1973; 1974). Together, the two processes of dissolution and dispersion are estimated to account for 1-10 percent of the mass of an oil spill (Mackay et al., 1980b; Huang and Monastero, 1982; Spaulding et al., 1982; Gundlach et al., 1983), depending on wave energy, with one percent or less being attributed to dissolution. [Note: The larger the light fraction of the oil, the greater will be the dissolution. Dispersion, on the other hand, is physically influenced and relatively independent of oil composition until the higher viscosities.]

Dissolution is not modeled separately, although Payne et al. (1984) describe a separate code to calculate the amount of dissolved oil on a component-specific basis rather than on a "pseudocomponent" basis (see next section). The rate of loss of oil mass (or concentration) through evaporation and dissolution is expressed as a first-order kinetic process via:

$$\frac{dc}{dt} = -(K_e + K_d)\, C \tag{3.1}$$

where C is the concentration of a particular hydrocarbon fraction and K_e and K_d are rate constants for evaporation and dissolution processes, respectively. Solving the previous equation, the concentration C at time t after the spill is:

$$C = C_o \exp(-K_e - K_d)t. \tag{3.2}$$

Here, C_o is the initial concentration of a particular fraction. With rate constants obtained from Moore et al. (1973) as given in Table 3.3, loss of oil mass through evaporation and dissolution can be calculated.

Kolpack et al. (1977) proposed the following complex formulation for the dissolution rate:

$$\frac{ds}{dt} = \frac{6.25\times10^{-7}\, C_s D_i T_o [7.0 + 3.5\,(pH_w - 7.01)]\, s_p}{P_d \ln(\delta/Z_o)^2\, V^p} \tag{3.3}$$

TABLE 3.3 First-order mass transfer coefficients for eight oil fractions [from Williams et al. (1975) based on data supplied by Moore et al. (1973)].

Fraction	Description	Evaporation[b] $(K_e)^e$	Dissolution $(K_d)^e$	Ratio (Diss/Evap)
1	Paraffin C_6-C_{12}	$0.8e^{0.2W}$	0.1	1/60
2	Paraffin C_{13}-C_{22}	0.002	0	0
3	Cycloparaffin C_6-C_{12}	$0.8e^{0.2W}$	0.5	1/12
4	Cycloparaffin C_{13}-C_{23}	0.002	0[c]	0
5	Aromatic (monocyclic and dicyclic) C_6-C_{11}	$0.8e^{0.2W}$	1.0	1/6
6	Aromatic (polycyclic) C_{12}-C_{18}	0.02	0.001	1/20
7	Naphthenoaromatic C_9-C_{25}	0.02	0.001[d]	1/20
8	Residual	0	0	0

a = These values are approximate and are probably all dependent upon temperature and oil film thickness.
b = W is the wind speed in knots.
c = Estimated from fraction 2.
d = Estimated from fraction 6.
e = K_e and K_d are mass-transfer coefficients (rate constants) for evaporation and dissolution processes, respectively.

where $\frac{ds}{dt}$ = volume of oil lost (m^3/sec).

C_s = solubility coefficient.

D_i = diffusion value.

pH_w = alkalinity value for water.

S_p = surface area of particle class (m^2).

P_d = pressure at depth below surface (decibars).

δ = boundary layer thickness of particle (mm).

V_p = volume of particle class (m^3).

T_o = oil temperature (°K).

Z_o = apparent roughness = 0.0001.

Aside from the difficulty of measuring the dissolution rate, a number of parameters considered in this equation, such as D_i, S_p, δ, and V_p, are either difficult to measure or imprecise, making the application of this equation in the oil-spill simulation model highly speculative.

Mackay and Leinonen (1977) propose a mass-transfer coefficient (MTC) model that is simpler than the diffusion equation proposed by Kolpack et al. (1977). The MTC model assumes a well-mixed water layer with most of the resistence to mass transfer lying in a hypothetical stagnant region close to the oil. The dissolution flux rate is expressed as:

$$N_i^d = K_d(e_i x_i C_i^s - C_i^w) \tag{3.4}$$

where N_i^d = dissolution flux (mol/cm^2/sec).

K_d = dissolution MTC (cm/sec).

e_i = solubility enhancement factor.

x_i = oil phase mole fraction.

C_i^s = pure component solubility (mol/cm^3)

C_i^w = bulk water phase concentration of i.

The solubility enhancement factor varies with different hydrocarbon classes; values used by Mackay and Leinonen (1977) are:

Hydrocarbon	e_i
Alkanes	1.4
Cycloalkanes	1.4
Aromatics	2.2
Olefins	1.8

3.1.4 Dispersion

Many expressions for modeling dispersion have been developed. Dispersion is governed primarily by wave breaking, so that variability due to oil composition is only significant at relatively high viscosities. The simplest approach uses tabulations of dispersion as a function of sea state and time after the spill (Blaikley et al., 1977). Audunson (1979) suggested an empirical form based on the square of the wind speed, reflecting the amount of energy available for driving oil droplets into the water column. Spaulding et al. (1982a) use a variation of Audunson's approach, including an exponential decay function to account for weathering and water-in-oil emulsion or "mousse" formation. In their formulation:

$$\text{Entrainment Rate} = Ao\ (W^2/Wo^2)e^{-t/2} \tag{3.5}$$

where Ao = constant.
W = wind speed.
Wo = reference wind speed (8.5 m/sec).

According to this formulation, 99 percent of dissolution and dispersion are complete the first few days after release of oil onto the sea surface. Mackay et al. (1980a) developed a complex set of dispersion equations (see Huang and Monastero, 1982; pp. 4.6-7 to 4.6-12) which uses empirical constants. These equations treat dispersion from thin and thick slicks separately. Spaulding et al. (1982c) have developed an oil-entrainment and dissolution model which gives particle-size distribution as a function of breaking wave turbulent energy and the dissolution of this oil by hydrocarbon fractions in the water column.

Spaulding et al. (1982c) have derived an overall entrainment rate correlation for any given oil slick if one knows (1) the average particle diameter entrained from the slick, (2) the significant wave height and period, and (3) the number of breaking wave events (N) per unit area and time (Fig. 3.1). Payne et al. (1984) have modeled dispersion as a function of wind speed, slick thickness, viscosity, and surface tension.

Let C_i be the oil constituent concentration (expressed as a fraction) in the slick; let S_i be its specific gravity; and let So_i be it solubility in parts per million (ppm). If the slick has area A in m^2, the total dissolution rate M_i of this constituent, in kg/s, is given by:

$$M_i = \frac{(2.04\times10^{-11})\ A\ C_i\ \mu_o\ S_i g\ H\ \delta\ (1+2H)\ So_i^{1.6}}{T^{0.5}\ D^{2.2}\ (1.025 - S_i)^{0.5}} \tag{3.6}$$

where $g = 9.81\ m/s^2$ and μ_o is the seawater viscosity. The average rate of dissolution can be correlated with wave height for different oil constituents, according to the expression:

$$M = (1+2H)(1-S)^{-1/2}\ T^{-1.5}\ D^{-0.2}\ S_c^{-1.6} \text{ (Fig. 3.1).} \tag{3.7}$$

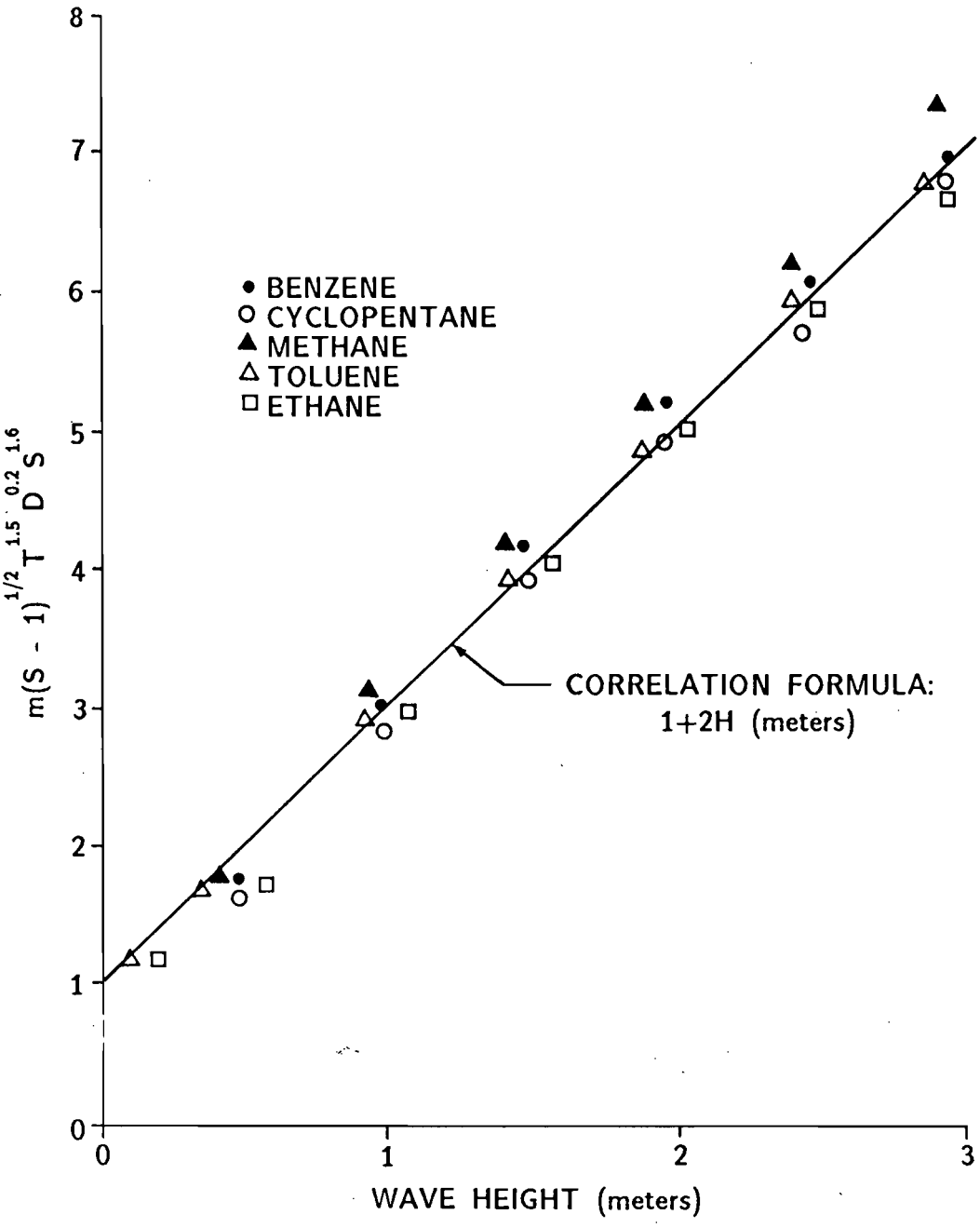

FIGURE 3.1. General correlation of component diffusion rates (Spaulding et al., 1982c).

3.1.5 Emulsification

Emulsification is the process of water droplets being dispersed into the oil, forming a "mousse" of increased viscosity and volume. The mechanism by which this process occurs is not well understood although it has been determined that turbulence, oil composition and temperature are important. A minimum turbulence level necessary for emulsification and a maximum water content of emulsified oil have been suggested (Wang and Huang, 1979), but have not been experimentally established. Simple, first-order expressions have been developed which can characterize most water uptake situations (Mackay et al., 1980a). A more complex mathematical formulation has been developed by Kolpack et al. (1977) to determine emulsification rate, but difficult-to-obtain input data is required and hence the formulation has not been verified (discussed later in more detail). Payne et al. (1984) predict water-in-oil emulsification by use of the oil/water mixture and a series of constants.

Exposures for the emulsification rate relate to the rate of uptake of water by oil. The first-order expression for this process is (Huang and Monastero, 1982):

$$\frac{\Delta w}{\Delta t} = k_3(1 - w/0.8) \tag{3.8}$$

where w is the fractional water content by volume and k_3 is a rate constant for water uptake. Kolpack et al. (1977) derived a complex mathematical formulation for the emulsification rate:

$$\frac{dV_{em}}{dt} = 9.34\text{x}10^{-9} \frac{\Delta V}{T} (10.5\text{-pH}) \rho_w g \pi \left(\frac{H_x}{T_{px}} e^{\frac{2\pi Z}{L^2}} + \frac{H_s}{T_{ps}} e^{\frac{2\pi Z}{L_s^2}} \right)^{1.92} \tag{3.9}$$

where $\Delta V = \frac{V_a V_r}{V_t^2}$

$\frac{dV_{em}}{dt}$ = emulsification rate (m^3/sec).

pH = alkalinity.

V_a = volume of asphaltenes (m^3).

V_r = volume of residuum (m^3).

V_T = total volume of oil in surface reservoir (m^3).

H_x = wave height (m).

T_{px} = wave period (sec).

H_s = tide height (m).

T_{ps} = tide period (sec).

ρ_w = density of water (gm/cm^3).

g = gravity acceleration (m/sec^2).

Z = depth of water (m).

Mackay et al. (1980b) suggest that the process of emulsion formation can be described as follows:

$$\Delta W_w = K_A(U_w+1)^2(1-K_B W)\Delta t \qquad (3.10)$$

where W_w = fractional water content.

K_A = a constant.

K_B = a constant with a value of approximately 1.33

U_w = the wind speed.

Δt = time.

3.1.6 Adsorption/Desorption

Numerous studies have been performed on the adsorption/desorption of oil to/from suspended particulate matter (SPM). Still, it remains difficult to adequately express the detailed dynamics of these processes in a quantitative manner. Variability in bulk oil characteristics is one confounding factor, but the key controlling variable appears to be percent of clay-sized particles, including glacially derived material, in the SPM population and the organic content of the particle surface (Meyers and Quinn, 1973; Bassin and Ichiye, 1977; Meyers and Oas, 1978; Winters, 1978; Zurcher and Thuer, 1978; Payne et al., 1981). These investigators generally agree that, at equilibrium, between 120 mg and 300 mg of hydrocarbons can be incorporated into each kilogram of the clay-size fraction of suspended sediment. This represents a key parameter needed for modeling the problem. In summary, factors affecting the significance and magnitude of oil-SPM interactions are:

1) SPM size-distribution profile. Fine-grained material has a greater surface area and thus presents more potential sites for interaction and

also has a longer residence time (slower settling rate) once resuspended in the water column. Potential contact time is therefore greater and available adsorption sites can be more thoroughly saturated.

2) Organic content of SPM. The presence of organic material on the surface of SPM greatly inhibits oil/SPM interactions, perhaps because oil and marine "humic" material (i.e., the complex high molecular weight of natural organic matter in seawater) compete for the same sites on the particles (Meyers and Quinn, 1973).
3) SPM concentration. As the SPM concentration increases, the effective viscosity of the fluid also goes up, thus reducing settling rates. The presence of oil is expected to contribute to this effect through flocculation in the surf zone.
4) Level of turbulence. Increased agitation allows SPM adsorption sites to become saturated by hydrocarbons.
5) Salinity. Sedimentation of oil by SPM is significantly lower in seawater than in fresh water (Hartung and Klinger, 1968; Bassin and Ichiye, 1977). This may be an important consideration in the Alaska coastal zone.

3.1.7 Photooxidation

Photooxidation is the process by which (with energy from sunlight) oil undergoes oxidation; and polar, water-soluble, oxygenated products are generated (reviewed by Payne and Phillips, 1985). This process is relatively unimportant over the first few days of a spill but may become significant after a week or more. Kolpack et al. (1977) use a conceptual expression for the rate of photooxidation based on the extrapolation of laboratory results to open-ocean slicks (discussed later in more detail).

3.1.8 Biodegradation

Biodegradation may continue for years after a spill occurs, and is affected by a variety of organisms. No general mathematical models have been developed to describe the rate of crude-oil biodegradation in the marine environment, although many studies have been undertaken on the characteristics and distribution of petroleum-degrading microorganisms (Bozell, 1973; Horowitz and Atlas, 1977; Passman et al.,

1979; URI, 1980; Atlas, 1981; Payne et al., 1981). Because of the complexity of the process, most studies of microbe/hydrocarbon interaction are conducted under controlled laboratory conditions, and the results may not be applicable to the marine environment (Atlas and Bartha, 1972; Solig and Bens, 1972; URI, 1980).

3.2 Algorithms Selected For Evaluation

Five existing oil spill models were selected for evaluation on the basis of their relevance and applicability to modeling partitioning processes considered in the SMEAR model. The models selected are:

1) The SAI model (Kirstein et al., 1983; Payne et al., 1984).
2) The USC/API model (Kolpack et al., 1977).
3) The VKI model, recently presented at the 1985 Oil Spill Conference (Rasmussen, 1985).
4) The ASA model (Spaulding et al., 1982a-d; 1983; 1985); also known in parts as the URI model.
5) The University of Toronto (UOT) model (Mackay and Leinonen, 1977; Mackay et al., 1980a,b).

The partitioning processes considered by each model are summarized in Table 3.4. Briefly, all five models contain algorithms describing the processes of spreading, evaporation, emulsification, and dispersion. None of the selected models at this time contains an expression which describes the process of adsorption/desorption of oil or oil buoyancy, although the USC/API model does consider the process of oil sedimentation, and the VKI model considers the upwelling of dispersed oil to the surface. The dissolution process is treated directly only in the USC/API and UOT models, although several of the models address this process in the form of chemical dispersion. Payne et al. (1984) have developed a separate code to calculate the amount of oil which will dissolve in seawater. However, this code is not included in the SAI model itself. Only the USC/API model considers biodegradation and photooxidation processes. The inherent components and mathematical algorithms employed by the five models are briefly summarized below. It will become apparent in the following discussion that the approaches employed by several of the models to describe a single process are either the same or differ only slightly, which greatly simplifies the evaluation and recommendation process.

3.2.1 SAI Model

This computerized partitioning model integrates the processes of evaporation, dispersion, emulsification, and spreading to predict the mass balance and composition of oil remaining in a slick as a function of time and environmental parameters. Spreading is modeled according to the thick/thin approach (Mackay et al., 1980a), which is derived from Fay's (1971) gravity/viscous regime. The evaporation process is treated through the pseudocomponent approach, whereby the oil is characterized as a series of hydrocarbon fractions which are grouped approximately by their boiling points and evaporate at different rates, thus changing the density of the slick over time. Both the emulsification and dispersion processes are treated empirically, through first-order expressions based on experimental studies (Mackay et al. 1980a). In addition, the SAI model computes in situ viscosity of spilled oil which may be a useful parameter in regard to considering spill cleanup options.

TABLE 3.4 Summary of models and associated components to be evaluated for incorporation into the SMEAR model.

	Model				
	(1) SAI	(2) USC/API	(3) VKI	(4) ASA	(5) UOT
Spreading	x	x	x	x	x
Evaporation	x	x	x	x	x
Emulsification/ Deemulsification	x	x	x	x	x
Dispersion	x	x	x	x	x
Dissolution		x			x
Adsorption/Desorption					
Biodegradation		x			

(1) Kirstein et al. (1983); Payne et al. (1984)
(2) Kolpack (1977); Kolpack et al. (1977); University of Southern California (1977)
(3) Rasmussen (1985)
(4) Spaulding et al. (1982a-d)
(5) Mackay and Leinonen (1977); Mackay et al. (1980a)

3.2.2 USC/API Model

This is a complex theoretical model which incorporates algorithms for nine processes [advection, spreading, evaporation, dispersion, dissolution, emulsification, biodegradation, sedimentation and photo(auto)oxidation] and contains both trajectory and partitioning elements. Spreading is modeled as a time-dependent change of slick

radius based on the spreading model of Cochran and Scott (1971), which considers only the inertial and surface tension phases and neglects other components of Fay's three-phase spreading. The evaporation component is expressed from theoretical considerations as a function of sea surface turbulence, wind speed, and the molecular weight and vapor pressure of the oil fractions. Rates of dispersion, dissolution, and emulsification are also formulated as a function of chemical and physical properties of the oil, along with sea-turbulence characteristics. The USC/API model is one of the few which includes explicit algorithms for biodegradation (modeled as a function of the growth and decay of microbial populations) and photooxidation (modeled conceptually as a function of sun angle, oil thickness, and cloud cover).

3.2.3 VKI/Danish Water Quality Institute Model

This is a computerized weathering model, which was recently presented at the 1985 Oil Spill Conference (Rasmussen, 1985). It consists of three interactive "modules;" one describing mass-transport processes, another describing heat-transport processes, and a third describing the physical and chemical properties of the oil. The mass-transport module takes into account the processes of spreading, dispersion (horizontal and vertical, including the buoyancy of dispersed oil droplets), evaporation, and emulsification. The spreading algorithm is based on Fay's three-regime theory and incorporates a term to account for spreading resulting from dispersion. Evaporation is modeled using an analytical approach, in which loss rate is a function of a diffusion coefficient which is, in turn, a function of a mass-transfer coefficient and the oil pressure (Mackay et al., 1980a). Both dispersion and emulsification processes are also modeled in a manner analogous to the SAI model. A modified pseudo-component approach is employed in the physical/chemical properties module, whereby inherent properties of the oil such as vapor pressure are incorporated by dividing the oil into six fractions defined according to their distillation properties and functionality.

3.2.4 ASA Model

The ASA Model is computerized and has been structured modularly, thus allowing for easy model updating as methodological improvements are developed. It contains both spill-trajectory and oil-partitioning elements. Processes considered within the latter category include spreading, evaporation, dispersion, and emulsification. Spreading is modeled according to Fay's three-phase regime, but there are also provi-

sions for specifying only the second-regime spreading algorithm (i.e., thick/thin approach of Mackay et al., 1980a). The pseudocomponent approach to modeling evaporation described for the SAI model is also used in the ASA model. Dispersion is expressed as a function of wind speed and "age" of the spill according to the empirical formulation of Audunson (1979) and Audunson et al. (1980), with slight modifications (Spaulding et al., 1982). The user can, as an alternate, also select the empirical dispersion algorithms of Mackay et al. (1980a). Emulsification is also modeled empirically as per Mackay et al. (1980a).

3.2.5 University of Toronto (UOT) Model

The UOT model has been included in our evaluation primarily for the sake of thoroughness, as all components of this model are incorporated in one form or another in the four previously described models. It is a computerized model, which describes the partitioning of oil according to the processes of spreading, evaporation, dispersion, dissolution, and emulsification. Details on the algorithms used in modeling these processes are contained in Mackay et al. (1980a).

3.3 Comparative Partitioning Model Analysis and Evaluation

3.3.1 Evaluation Criteria and Approach

The five models selected have been critically analyzed using a quantitative approach, whereby a set of evaluation criteria, each possessing a numerical weighting factor, have been applied to each model and a total score tabulated. Rather than evaluating models as discrete entities, our analysis has focused on individual processes and how they are addressed by each model; thus, all algorithms employed in modeling (for example, evaporation) have been considered together. This approach greatly simplifies components best suited for incorporation into the SMEAR model. The general criteria applied and the weighting factors assigned to each are described below.

Criterion 1: Adaptability of existing models to the requirements of this project [i.e., applicability to the surf zone and beach face (40 points)]

The features pertaining to adaptability which have been considered are:

1) Mathematical algorithm used in estimating the magnitude of each process.
2) Adaptability to surf-zone characteristics, particularly agglomeration of oil, interaction with particles, transfer to beach sediments, etc.
3) Compatibility with other OCS transport and weathering models.

Criterion 2: Degree to which existing models have been verified (10 points)

The degree to which each model algorithm has been applied under different laboratory or field conditions has been considered. Special consideration has been given to models successfully applied in estuarine or nearshore environments and models that have been verified under different climatic conditions (i.e., temperature) (see section 3.3.2).

Criterion 3: Flexibility of existing models with regard to problem-solving with interactive terminals (10 points)

The following features have been considered:

1) For existing computer models, how user-friendly is the program? How accessible is it from remote terminals? How flexible is it with regard to application in specific conditions (i.e., how many different modeling parameters can be adjusted to adapt to different environmental site conditions?
2) For mathematical algorithms, how difficult are they to computerize and at what cost?

Criterion 4: Availability and attainability of data required for each model (10 points)

The types of data inputs required by individual-process algorithms will influence their ultimate utility. We have identified the different data input types for each model and have evaluated them according to ease of attainability.

Criterion 5: Degree to which existing models can be linked to a surf-zone sediment mass-transport model (30 points)

This analysis consisted of two components:

1) The requirements of the surf-zone sediment, mass-transport model to produce a SMEAR model (i.e., the manner in which the mass-transport and oil-partitioning models can be effectively integrated.
2) The output of all oil-partitioning algorithms. For each partitioning expression analyzed, the potential output and format have been evaluated with respect to their compatibility with mass-transport and proposed SMEAR models.

3.3.1.6 Summary

A numerical score out of the maximum number of total points has been assigned to each of the five criteria for each of the model algorithms evaluated. Five of the eight processes considered (spreading, evaporation, dissolution, dispersion, and emulsification) have been evaluated in this manner. The individual and total scores (sum of scores for the five criteria) for each of these five partitioning processes considered are summarized in Tables 3.5 through 3.9. None of the models selected adequately addresses the processes of photooxidation, biodegradation, and adsorption/desorption. Instead of using evaluation tables, we recommend alternate approaches to modeling these processes and discuss these approaches in the text. Provided below are brief process-specific summaries of the rationale and justification for the scoring. The top-ranked algorithms for each process will be further evaluated as potential components of the final SMEAR model system.

TABLE 3.5 MODEL PROCESS: SPREADING. Evaluation of oil-spill partitioning model components. Numbers in parentheses are maximum number of points allowed for each criteria.

Model Approach	Adaptability to SMEAR (40)	Degree of Verification (10)	Flexibility of Interaction (10)	Data Requirements and Attainability (10)	Compatibility with SMEAR (30)	Total Score (100)
1) SAI Thick layer (Fay, 1971; Mackay et al., 1980a)	35	10	10	10	30	95
2) USC/API Radial spreading (Cochran and Scott, 1971)	25	4	7	5	25	66
3) VKI Fay's three-phase spreading (Fay, 1971)	30	10	7	10	25	82
4) ASA Fay's spreading or thick layer	35	10	10	10	30	95
5) UOT Thin and thick layer	35	10	10	10	30	95

TABLE 3.6 MODEL PROCESS: EVAPORATION. Evaluation of oil-spill partitioning model components. Numbers in parentheses are maximum number of points allowed for each criteria.

Model Approach	Adaptability to SMEAR (40)	Degree of Verification (10)	Flexibility of Interaction (10)	Data Requirements and Attainability (10)	Compatibility with SMEAR (30)	Total Score (100)
1) SAI Pseudocomponent (Kirstein et al., 1983)	40	7	10	9	30	96
2) USC/API Theoretical/pseudocomponent (Kolpack et al., 1977)	25	4	7	7	25	68
3) VKI Pseudocomponent	35	5	10	7	30	87
4) ASA Pseudocomponent	40	7	10	9	30	96
5) UOT Analytical	30	10	7	10	25	82

TABLE 3.7 MODEL PROCESS: DISSOLUTION. Evaluation of oil-spill partitioning model components. Numbers in parentheses are maximum number of points allowed for each criteria.

Model Approach	Adaptability to SMEAR (40)	Degree of Verification (10)	Flexibility of Interaction (10)	Data Requirements and Attainability (10)	Compatibility with SMEAR (30)	Total Score (100)
1) SAI Not considered	---	---	---	---	---	---
2) USC/API Theoretical (Kolpack et al., 1977)	20	4	6	3	20	53
3) VKI Not considered	---	---	---	---	---	---
4) ASA Not considered	---	---	---	---	---	---
5) UOT Mass transfer coefficient (Mackay and Leinonen, 1977)	30	6	8	10	25	79

TABLE 3.8 MODEL PROCESS: DISPERSION. Evaluation of oil-spill partitioning model components. Numbers in parentheses are maximum number of points allowed for each criteria.

Model Approach	Adaptability to SMEAR (40)	Degree of Verification (10)	Flexibility of Interaction (10)	Data Requirements and Attainability (10)	Compatibility with SMEAR (30)	Total Score (100)
1) SAI Mathematical (Mackay et al., 1980a)	35	9	10	7	30	91
2) USC/API Theoretical (Kolpack et al., 1977)	25	4	8	7	28	72
3) VKI Empirical (Rasmussen, 1985)	30	6	8	7	28	79
4) ASA Empirical (Audunson et al., 1980) or Mathematical	35	9	10	7	30	91
5) UOT Mathematical	35	9	10	7	30	91

TABLE 3.9 MODEL PROCESS: EMULSIFICATION. Evaluation of oil-spill partitioning model components. Numbers in parentheses are maximum number of points allowed for each criteria.

Model Approach	Adaptability to SMEAR (40)	Degree of Verification (10)	Flexibility of Interaction (10)	Data Requirements and Attainability (10)	Compatibility with SMEAR (30)	Total Score (100)
1) SAI Empirical (Mackay et al., 1980a)	35	8	10	9	30	92
2) USC/API Theoretical/mathematical (Kolpack et al., 1977)	25	4	8	5	25	67
3) VKI Empirical	35	8	10	9	30	92
4) ASA Empirical	35	8	10	9	30	92
5) UOT Empirical	35	8	10	9	30	92

3.3.2 Model Verification

One of the criteria applied to evaluate the various models available for use in the SMEAR model is the degree to which the mathematical expressions comprising the models have been verified by direct laboratory experimentation or through utilization of data acquired in the field during actual oil spills to verify mathematical constants and predictions in general. The initial laboratory experimental work conducted to derive constants or expressions is not considered to be verification runs.

The UOT model has been verified to a greater extent than any others through both laboratory and field data comparisons. Examples of the degree of verification of the UOT model expressions are:

1) Spreading algorithms were verified in detail by comparison with field data from JBF (1976) during experimental spills of crude oil (see Mackay et al., 1980b).
2) Evaporation algorithms were verified in the laboratory using "pan" evaporation data (Mackay et al., 1980b) under different climatic conditions (i.e., temperature).
3) The output of the UOT model was compared to experimental results obtained by McAuliffe et al. (1980) in which experimental releases of crude oil were used to verify the predicted model outputs, and to data by Boehm et al. (1982) where detailed surface and subsurface oil concentrations and compositions from the *Ixtoc I* blowout were available.

The algorithms which comprise the SAI model have been tested in extensive laboratory experiments at different temperatures and other conditions. The SAI model has not been subject to hindcasting field verification.

The USC/API model contains detailed mathematical expressions derived from laboratory data but not verified to any great degree using field or laboratory experimental data and minimal hindcast applications to field data in the case of spreading algorithms have been inconclusive (Huang and Monastero, 1982).

The ASA model has been verified in two real spills--the *Argo Merchant* (Spaulding et al., 1982) and after the *Ixtoc I* spill (Anderson, 1983).

The VKI model has been tested on an experimental spill of 300 m^3 of *Ekofisk* crude oil in the North Sea. The mass balance of oil and losses due to evaporation and dispersion were well-predicted by the model.

3.3.3 Spreading

Three different approaches to modeling oil slick spreading are employed by the selected models: Fay's three-phase regime (VKI and ASA models), Mackay's thick and thin layer approach (SAI, UOT, and ASA models), and Cochran and Scott's spreading (USC/API model). Fay's three-phase regime spreading is the most widely applied in oil-spill simulation models. In fact, Mackay's model is based on Fay's gravity-viscous equation, with the volume term simply being replaced by the product of surface area multiplied by thickness. The first (gravity-inertial) regime in the Fay formulation applies only a few minutes after an oil spill and can therefore be safely discarded for long-term simulations. Mackay's adaptation of Fay's gravity-viscous equation allows for a smooth transition to a terminal spreading thickness. Otherwise, the Mackay and Fay formulations are equivalent (Mackay et al., 1980a). The terminal spreading behavior of the Mackay formulation makes it more attractive for inclusion in the SMEAR model; we have therefore awarded a higher score in this category to the latter, which is employed in both the SAI and UOT models. The ASA model contains provisions for specifying either Fay's or Mackay's approach. ASA's variation has been expanded in relation to SAI's by allowing multiple spillets to exist, thus allowing the simultaneous evaporation of old (weathered) and new (fresh) oil. On the basis of this feature, this model has been awarded the highest score for adaptability to SMEAR. In our evaluation of spreading algorithms, the lower scores for adaptability for use in the SMEAR model, degree of verification, and data requirements were awarded to the USC/API model, which employs a highly theoretical and relatively unvalidated equation based on Cochran and Scott's dual-phase spreading.

3.3.4 Evaporation

The selected models employ two basic approaches toward modeling evaporation. Four models (SAI, USC/API, VKI and ASA) use variations of the pseudo-component approach described by Kirstein et al. (1983), which simulates evaporation of the oil through a multicomponent mixture having a range of volatilities, which when combined in the correct proportions have vapor-pressure properties similar to the parent oil. The UOT evaporation model is based on the analytical approach of Mackay et al. (1980a), in which vapor pressure is expressed as a function of both temperature and fraction evaporated. The pseudocomponent approach is preferable for incorporation into the SMEAR model as it yields a more realistic expression for the evaporation rate.

However, the variation employed in the USC/API model is complex, requires parameters not easily obtainable, and is independent of any slick spreading; this algorithm therefore received low scores in our evaluation for adaptability and data requirements. The VKI variation employs only six pseudocomponent fractions, while those of SAI and ASA are both similar and more flexible, employing several additional pseudocomponent characteristics. The latter two therefore received our highest scores for adaptability to SMEAR.

3.3.5 Dissolution

Dissolution is frequently neglected in fate models because it accounts for removal of only a small fraction of spilled oil. Only two of the models selected directly address the process of dissolution. The USC/API model employs a very complex formulation for the dissolution process which has proven difficult to verify. The UOT model employs a simpler, mass-transfer coefficient equation, but is highly empirical and is based on scant observational data. Of the two, the UOT approach is preferable for incorporation into the SMEAR model on the basis of its adaptability, simpler data requirements, and degree of verification.

3.3.6 Dispersion

Several different approaches are employed for modeling oil-in-water dispersion. The most common, employed in three of the models (SAI, ASA and UOT), consists of variations of the mathematical formulation of Mackay et al. (1980a), in which the mass fraction of oil removed from a slick is related to the fraction of sea surface covered by breaking waves. The USC/API model employs a theoretical equation which considers dispersion only in the horizontal plane and lacks physical characterization of vertical dispersion mechanisms. This approach represents a severe limitation in the present application, and the USC/API effort was therefore awarded our lowest score with regard to adaptability to SMEAR. The VKI model uses an empirical approach in which dispersion is a function of wind speed and age of the spill. The ASA model, in additon to the Mackay formulation, also contains provisions for specifying an empirical approach similar to the VKI model, which is based on the empirical formulation of Audunson et al. (1980). With exception of the USC/API model, all of the above dispersion algorithms have received comparable verification and have similar data requirements. Mackay's mathematical approach, though highly empirical, has been

adjudged to be the best available at the present time, although the simplicity has been awarded to the ASA, UOT and SAI models, all of which employ Mackay's mathematical approach.

3.3.7 Emulsification

The exact mechanism by which emulsification occurs is not well understood, and as a result, the few formulations developed to model this process contain a high degree of empiricism. Two basic approaches are employed by our selected models. The USC/API emulsification model is based on theoretical considerations, and its complex formulation involves numerous parameters and required extensive input data. Attempts to verify this model (Kolpack et al., 1977) have yielded ambiguous and inconclusive results, and we conclude that it is not suitable for incorporation into SMEAR. The remaining four models employ variations of the empirical approach of Mackay et al. (1980a), in which emulsification is modeled through a simple, first-order equation and is a function of two or three specified constants.

3.3.8 Adsorption/Desorption

This partitioning process, which would be expected to be highly significant in coastal SMEAR situations, is not adequately addressed by any of the models selected. Only the USC/API model contains an expression for the sedimentation of oil, based on the settling velocity models of Gibbs et al. (1971). This model is totally unsuitable for incorporation into SMEAR as it does not consider the turbulence conditions and high-particle loadings encountered in a surf zone. In light of the apparent absence of applicable oil/SPM predictive algorithms, new or emerging models may have to be considered and, if necessary, modified for incorporation into SMEAR. Two such models are briefly discussed in the following paragraphs.

One recently completed study at the Massachusetts Institute of Technology (MIT) examined the effect of several factors on the uptake of crude oil in marine sediments (Wilson, 1985). The MIT study found that both salinity and sediment-particle size are important in determining the amount of oil which might become incorporated into sediments following a spill, consistent with previous results. According to the MIT results, seawater reduces oil uptake by about 50 percent relative to freshwater, and the smaller sediment-size fractions (which are also most susceptible to resuspension and thus would account for a sizeable fraction of the "standing crop" in

a coastal environment) account for the greatest oil uptake. Although any mathematical algorithms and/or constants generated as part of this study are likely to be highly empirical, they may represent the most current data available and should be scrutinized for adaptability to SMEAR (a copy of the final report of this study is presently being solicited for further evaluation).

Another modeling study which is examining the effect of suspended particulate matter on the fate of oil in the water column is presently being undertaken by the SAI corporation under contract to Minerals Management Service. Although still in the development stages, this model is being developed with the express intent of incorporation into SMEAR. Data is currently being generated for use in a series of continuity equations for the oil and particulate species of interest at expected open-ocean conditions. The equations describe the spatial change in the concentration of either a molecular-specific oil species or pseudocomponent in terms of a turbulence dissipation rate and an oil/SPM interaction rate. A submodel designed to calculate either sediment flux from the sea bed or suspended-sediment concentrations resulting from resuspension is also being developed as part of the oil/SPM interaction algorithm. It appears that this model, once completed, could be highly adaptable to the SMEAR model under development. Once model formulation is completed, it should be closely scrutinized to determine exactly how it may be incorporated into SMEAR. In particular, close attention should be paid to how this model (or any other adsorption/desorption algorithm considered) addresses (1) high SPM loadings, (2) agglomeration, and (3) desorption of beached oil.

3.3.9 Photooxidation

Photooxidation is negligible as a weathering/partitioning process over the first few days of a spill from a mass-balance standpoint, but its effects could become noticeable after a week or longer. The primary effect in a coastal SMEAR situation would be removal of the parent oil through the dissolution of products. Photooxidation could also produce changes in viscosity, spreading, and emulsification tendencies of the oil. Because this process is considered to affect less than 1 percent of the total mass, it has been generally disregarded in partitioning models. The USC/API model employs a simple conceptual formulation to calculate a rate of photooxidation, based on the sun angle, cloud cover, and slick thickness. This approach is not entirely satisfactory, as it disregards the complex kinetics of the process and also does not consider the effects of oil composition and other environmental factors.

In a recent review by Payne and Phillips (1985), the mathematical algorithms employed by Zepp and colleagues for the estimation of photooxidation-rate constants and organic-compound half-lives were favorably regarded. Their approach employs solar irradiance of surface and subsurface waters at specific, absorption wave lengths and known molar absorptivities to calculate first-order rate constants (and subsequently half-lives) for individual organic compounds. This empirical approach also has several inherent shortcomings--primarily that it relies on known properties of specific organic compounds and does not take into account real-world environmental factors such as cloud cover and sensitization by naturally occurring, dissolved humic substances. It could, however, be adapted for incorporation into SMEAR by assigning molar absorptivities to pseudocomponent fractions of the spill oil to calculate photolysis-rate constants, which can then be applied in simple, first-order equations to arrive at photo-oxidation rates. But, in conclusion, it is recommended that photooxidation not be included in SMEAR because photooxidation is longer tem than the balance of the other SMEAR components, and the modeling approach to it is uncertain. It could be added later should our knowledge of this process be sufficiently increased.

But, in conclusion, it is recommended that photooxidation not be included in SMEAR because it is longer term than the balance of the other SMEAR components and the modeling approach to it is uncertain. It could be added later should our knowledge of this process be sufficiently increased.

3.3.10 Biodegradation

Biodegradation, like photooxidation, is generally a slow process (although see Gundlach et al., 1983) which only becomes significant once the other partitioning/ weathering processes have been fully manifested. It is generally accepted that there are no adequate rate models for biodegradation of spilled oil, despite the fact that numerous biodegradation studies of organic compounds have been conducted. The USC/API model attempts to describe the growth and decay of microbial populations associated with spilled oil, but not the rate at which biodegradation occurs.

It is possible that in a coastal SMEAR situation, biodegradation could become a significant fate process, depending on the "age" of the spill. The degree of biodegradation, while slow and perhaps relatively negligible when considering waterborne oil, may be significant when oil is left deposited on the shoreline. Extensive field data, obtained by Boehm (1984; and references therein) as part of the Baffin Island

Oil Spill (BIOS) program, indicated that beached oil was affected by biodegradation in a two-week time period and extensively over a 12-month time period. If the SMEAR model is run for long time periods, a simple, first-order equation could be used to model this process given the lack of predictive algorithms. Though highly empirical, this approach is preferred over the similar but slightly more rigorous kinetic models used by Baughman et al. (1980) and Paris et al. (1981), in which biodegradation rates are a function of both bacterial and substrate (in this case, oil) concentrations, for two reasons:

1) The latter would require data on microbial biomass in the oil, which in the present application would prove to be limiting.
2) If rate constants can be extrapolated from data of Lee and Ryan (1983), the proposed approach will address the combined effects of both photooxidation and biodegradation.

One significant limitation of this approach is that the data of Lee and Ryan (1983) are based on degradation rates of specific, polycyclic aromatic hydrocarbons, which disregard both the complexity of petroleum aromatic hydrocarbons and degradation of nonaromatic petroleum hydrocarbons. Alternatively, a more complex approach could be adopted, whereby extrapolated degradation-rate constants could be assigned to specific pseudocomponent fractions corresponding to the spilled oil. The sum of degradation rates for the individual pseudocomponents would represent the overall degradation rate. This approach has some appeal, but would result in the introduction of even more empiricism and uncertainty. Until our understanding of biodegradation is increased, it is recommended that it not be included in the final SMEAR model.

3.3.11 Additional Considerations

In the preceding discussions, predictive algorithms for several of the partitioning processes under consideration were found to be either unavailable or inadequate (e.g., for photooxidation processes). It is probable that this will also be the case when considering algorithms which model weathering processes for beached oil. For example, most of the oil-partitioning models examined in the present evaluation were developed to address the fate of oil in or on water. This modeling approach will likely be inappropriate when considering the fate of oil stranded on a sandy/silt sediment or a hard substrate (rocky coastline). For these spill scenarios, it may become necessary to propose and develop alternate modeling approaches or to extensively modify existing models.

3.4 Summary and Recommendations

Table 3.10 contrasts the evaluation scores awarded to the five models for each of four partitioning processes--spreading, evaporation, emulsification, and dispersion. It is evident from this comparison that the ASA and SAI models have consistently received the highest individual and cumulative scores, and it is therefore recommended that these algorithms be considered for coupling with the top-ranked, sediment-transport models. As the SAI model has been extensively studied by NOAA and MMS and as many investigators are familiar with the SAI model, we recommend that this model be adapted for use in the SMEAR model. With regard to the other four partitioning processes, we recommend the following:

1) Dissolution should not be addressed using a separate series of mathematical algorithms.
2) The adsorption/desorption algorithms contained in either the recently completed MIT study or the ongoing SAI study should be considered for incorporation into the SMEAR model. The SMEAR model will account for gross mixing of oil in sediment with a separate algorithm.
3) Photooxidative processes should be disregarded since they are considered minimal, are longer term that other SMEAR components, and are generally poorly understood.
4) Because the SMEAR model is oriented toward predicting events having less than three months' duration, it will not include an algorithm to account for biodegradation (as outlined in Section 3.10 above).

TABLE 3.10 Summary of evaluation scores for four model processes. Although the ASA model ranks equally with the SAI model, it is recommended that the latter be adapted into SMEAR as the SAI model has been extensively studied by MMS and NOAA and that many investigators are familiar with it.

	Model				
	(1) SAI	(2) USC/API	(3) VKI	(4) ASA	(5) UOT
Spreading	95	66	82	95	95
Evaporation	96	68	87	96	82
Emulsification	92	67	92	92	92
Dispersion	91	72	79	91	91
Average Scores	**93.5**	**68.3**	**85**	**93.5**	**90.0**

4.0 ANALYSIS OF OIL/SHORELINE INTERACTIONS

Section 2 of this report presents an evaluation of the models that are capable of representing the transport of oil in the surf zone while Section 3 evaluates oil-spill chemical partitioning models. The combination of these two models essentially brings the oil adjacent to, but not onshore. The next stage is to bring the oil onto the shoreline and develop a model representing the processes of oil deposition and removal. Presently a model for predicting the distribution and persistence of oil along shoreline environments does not exist (although J. Galt of NOAA is able to add a shoreline absorption factor to the NOAA model; Galt, pers. comm.). For this reason, the following section describes a conceptual approach to model development, primarily based on data derived from actual spill incidences as well as the BIOS (Baffin Island Oil Spill) field-oiling study.

4.1 Conceptual Approach

An oil shoreline model must (1) be generic in application, yet specific enough to be applied to the Bristol Bay region; (2) take into account different shoreline environments; (3) indicate spilled oil persistence and reflotation; and (4) incorporate oil weathering.

The route of model development taken herein is to first describe, in general terms, the interactions of oil within seven particular shoreline types. Following this is an analysis of each important factor needed for input into a shoreline model; these are maximum oil thickness on the beach face and backshore, depth of oil penetration and oil content in the swash and backshore zones, and rate coefficients for oil removal from each shoreline type. Weathering factors, as discussed in the previous section, continue as the oil is deposited onshore. After oil is removed, it will be again exposed to transport and weathering processes, and has the potential for being redeposited onto a shoreline segment.

4.2 Shoreline Classifications

In order to develop a shoreline oil-spill SMEAR model, some basic information concerning the shoreline types to be affected is necessary. Few nationwide, or even regional, coastal classification systems currently exist. The U.S. Fish and Wildlife Service has developed a simple classification scheme as part of their National Wetlands Inventory; however, the areas mapped and the classification scheme utilized are too limited for application to the SMEAR model.

Fortunately, several geomorphic-based classifications are available as a result of oil-spill planning work. Over the past seven years, primarily through the support of MMS and NOAA, a detailed shoreline classification scheme was developed to aid response to oil spills (Gundlach and Hayes, 1981). Currently, the areas mapped now encompass much of the coastal habitats of the United States (Fig. 4.1). This system classifies shorelines into a minimum of ten types (which are then ranked in order of potential oil-spill damage). Other classification schemes [e.g., Woodward-Clyde Consultants (1981) for arctic Alaska, (1982) for northern California, and (1984) for the Chukchi Sea; and ABSORB (1983) for the Beaufort Sea] can also be converted into a format usable for SMEAR. Although the exact shoreline types vary somewhat between the northern Bering Sea and south Florida, the majority of types remain the same from region to region.

For the SMEAR model, limited by budgetary and computer-storage constraints, seven major shoreline types would be utilized. Table 4.1 lists the original shoreline classification used in Bristol Bay and indicates which types would be combined together. The proposed seven shoreline types have broad applicability anywhere in the United States, although oil retention coefficients may vary (e.g., for northern temperate marshes versus Gulf of Mexico mangroves, which would be classified similarly).

TABLE 4.1 Percentage of shoreline by type in Bristol Bay and effects of combining shorelines for the SMEAR model. Original classification is from Michel et al. (1982). These basic shoreline categories are used throughout most of the mapping series indicated in Figure 4.1. Percentage values are rounded to nearest whole number and therefore, in this case, equal over 100 percent. *Not calculated in original report.

Shoreline Types	Percentage		
	Original Classification		SMEAR Classification
1) Exposed rocky	3	>	10
2) Wave-cut platform	7		
3) Fine sand	3	>	16
4) Coarse sand	13		
5) Exposed tidal flat	--*		√
6) Mixed sand/gravel	16	>	21
7) Gravel	5		
7A) Exposed tidal flat	--*		√
8) Sheltered rocky	2		2
8A) Eroding peat scarp	10		10
9) Sheltered tidal flat	--*		√
10) Marshes	42		42
Total	101		101

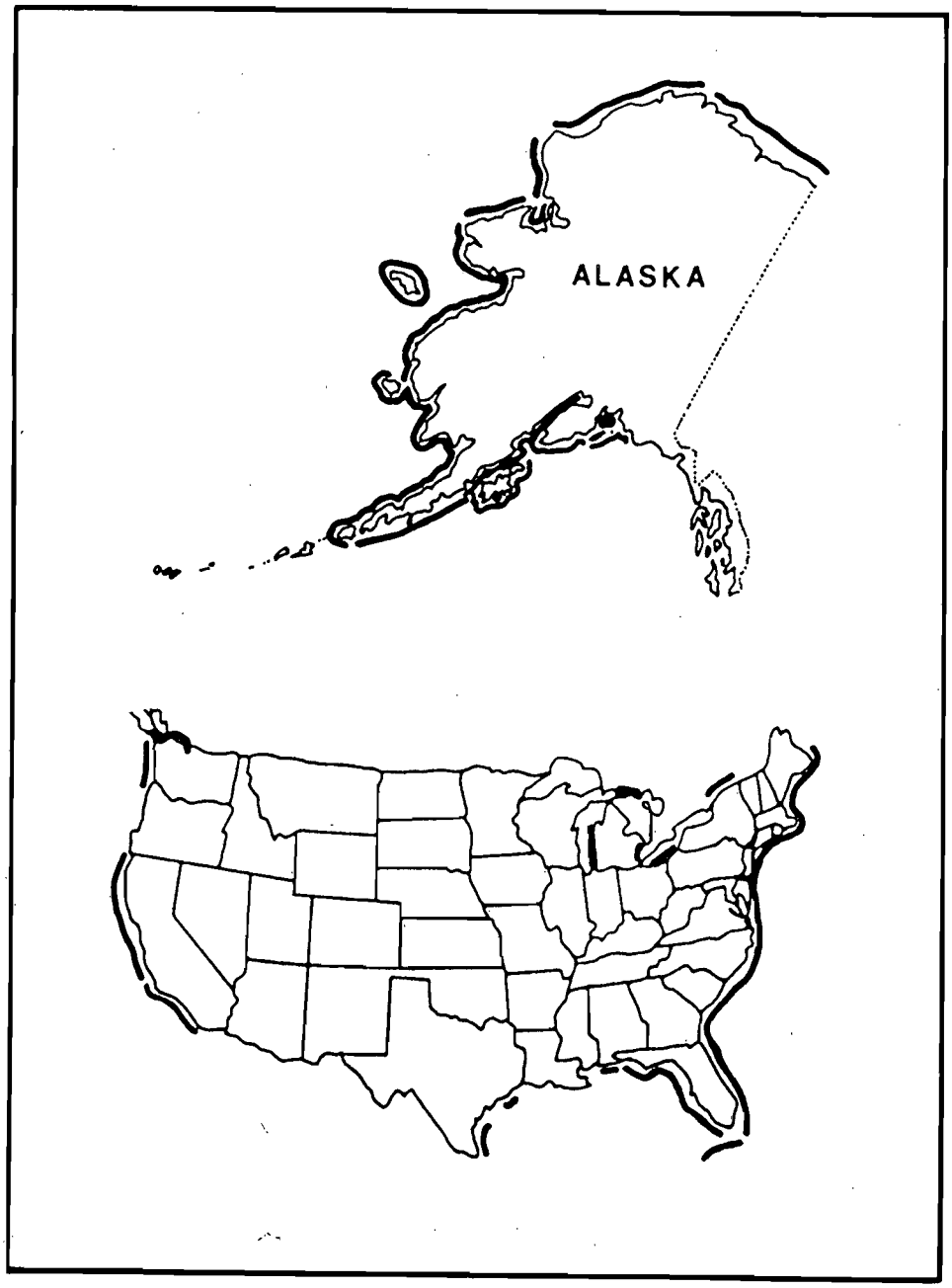

FIGURE 4.1. Locations for which shoreline classifications are presently available (Jan. 1986).

4.3 General Description of Oil Interactions

The following contains a brief description of oil distribution and persistence along each of the seven selected shoreline types: exposed and sheltered rocky shores, sand and gravel beaches (described together), tidal flats, marshes, and eroding peat scarps.

4.3.1 Rocky Shores

The environments included in this category are exposed and sheltered rocky headlands, rock-dominated shorelines, and wave-cut rock platforms.

A diagrammatic representation of oil interactions with a steeply dipping, high-energy rocky shoreline, based on observations of the *Amoco Cadiz* and *Urquiola* oil spills (Gundlach et al., 1981), is presented in Figure 4.2. Depending upon wave energy levels, oil will be held approximately 10-30 m offshore of these coastal types by wave reflection. Therefore, incoming oil will be primarily influenced by alongshore transport and weathering processes. Under very low wave conditions, a minor amount of oil may adhere temporarily to the near vertical slope. The relative amount of oil adherence depends on slope, biological encrustations, and tidal range (area of exposure). The residence time of deposited oil is usually very brief, on the order of only a few tidal cycles depending again on wave energy. After reflotation, oil would reenter the nearshore environment and be exposed to currents. Oil agglomeration onto suspended particles would be represented by the SPM subroutine.

Sheltered rocky areas are very much different in that the persistence of oil can be on the order of months to years, depending on wave and tidal energies. It is also quite common to have a jumbled mixture of bedrock, boulders, and gravel within the same section of shoreline. Oil is particularly likely to remain within the protected areas between the rocks.

4.3.2 Sand and Gravel Beach Types

These environments include fine- to coarse-grained sand beaches, mixed sand and gravel beaches, gravel beaches, and cobble beaches. As referred to in this report sand beaches include fine- and coarse-grained sand beaches; and gravel beaches include those dominated by mixed sand and gravel, gravel, and cobbles. Although coefficients of oil persistence and removal vary with beach type, each of these beaches is basically similar in terms of oil interactions.

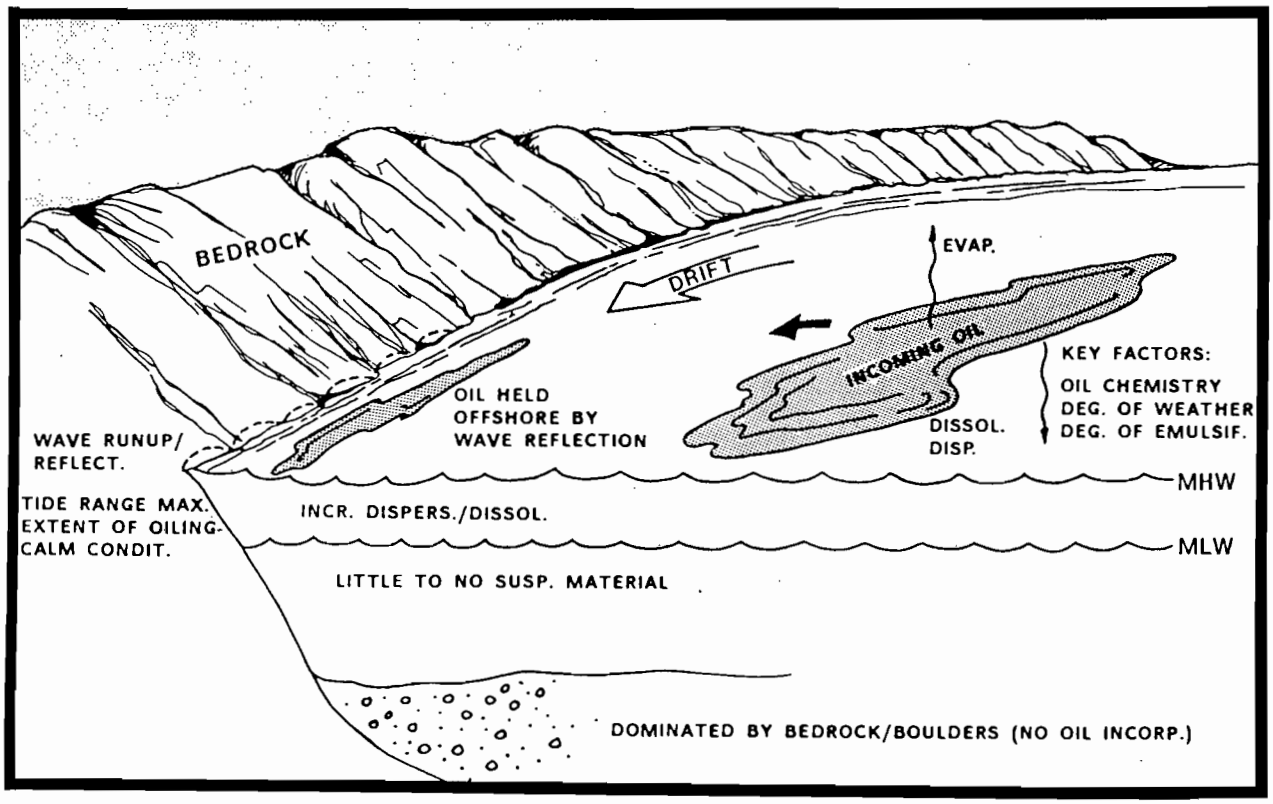

FIGURE 4.2. Representation of oil interactions along a moderate- to high-energy, steeply dipping, rocky shore (from Gundlach et al., 1985). See text for details. REFLECT. = reflection; MAX. = maximum; INCR. DISPERS./DISSOL. = increased dispersion/dissolution; SUSP. = suspended; INCORP. = incorporation; EVAP. = evaporation; DISSOL. = dissolution; DISP.= dispersion; DEG. = degree; WEATHER = weathering; EMULSIF. = emulsification; MHW = mean high water; MLW = mean low water.

A depiction of oil interactions on this beach type is pictured in Figure 4.3. During a spill, oil will be deposited along the upper portions of the beach on an incoming tide. If tidal levels or the area of swash is high, oil can reach the back-berm (or backshore) zone. The lower beach will remain free of oil while the tide is high. As the tide falls, oil may temporarily coat the beach face if oil quantities are great. On the next incoming tide, much of the newly deposited oil will be refloated and be transported toward the backshore or alongshore. As illustrated in Section 4.5, the amount of reflotation varies with beach type (e.g., gravel beaches show less reflotation than water-saturated, fine-sand beaches). In some cases, the incoming oil may mix with sediment and form slightly buoyant masses ("log rollers or stringers") within the shallow, subtidal zone. This oil may be transported along shore, onto shore, or offshore, depending on nearshore processes.

Oil deposited by swashes in the upper intertidal beach face or in the backshore will remain in place until sufficient wave or swash energy reaches this zone to erode the oiled sediment or mechanically disperse the oil through abrasion (grains rubbing against each other). If oil adheres to the sediments, oil and sediment together may be transported to the nearshore zone and be deposited [as at Bay 11 at the BIOS site in northern Canada (Boehm et al., 1985].

As is discussed in the following sections (and in Gundlach et al., 1978; Hayes et al., 1979; Gundlach et al., 1981; among others), a major factor influencing oil longevity and depth of penetration and burial is the grain size (particle-size distribution) of the beach. Gravel- and boulder-dominated beaches naturally offer more spaces for oil to reside, and since substantial wave action is needed to rework these sediments, oil persistence tends to be long. In contrast, very fine-grained sands are easily transported and oil longevity is shorter. Sediment porosity and permeability are major factors influencing the ability of the beach to absorb incoming oil; however, the median grain size is a simpler parameter to measure or estimate (especially during rapid aerial or ground surveys) and yet provides very reasonable accuracy in terms of oil-spill interactions (particularly in estimating interactions along large sections of coastline). [Porosity is defined as the percentage of bulk volume of material that is occupied by interstices, whether isolated or connected. Permeability is the capacity of a material to transmit a fluid.] As information becomes available, it is expected that substrate permeability and penetration, varying with oil viscosity, will be mathematically modeled.

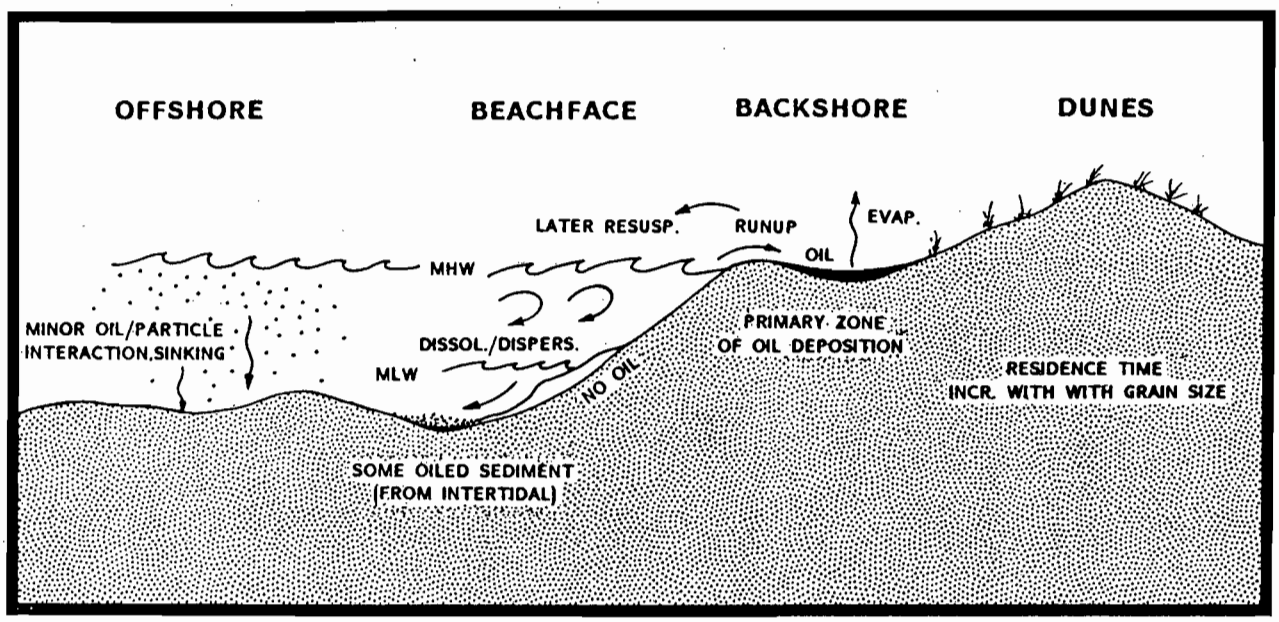

FIGURE 4.3. Oil interaction along a coarse-grained sand beach (from Gundlach et al., 1985). A fine-grained sand beach would be similar but with a gentler beach-face slope, while gravel beaches are commonly steeper and with only minor berm development (backshore). MHW = mean high water; MLW = mean low water; DISSOL./DISPERS. = dissolution/dispersion; EVAP. = evaporation; RESUSP. = resuspension; INCR. = increases.

4.3.3 Tidal Flats

Tidal flats are common features in mesotidal to macrotidal (>2 m tide range) areas. Sediment size can vary from fine-grained muds and silts as in sheltered estuaries, to coarse sand-sized material as in current- or wave-dominated areas. Exposed tidal flats are particularly common in Bristol Bay since the tidal range is so large (>4 m).

Oil deposition onto a tidal flat occurs as the tide drops, exposing the flat to oil previously floating on the water's surface. As the tide rises again, most of the oil is lifted off the flat and transported by local currents. Some oil may bind with the sediments and remain, although this is relatively uncommon especially when the sediments are water-saturated. In muddy tidal flat areas, where a high suspended sediment concentration is likely, oil binding with SPM may cause a portion of the oil to sink.

4.3.4 Marshes

Marsh habitats may occur as a narrow vegetative fringe or may cover a broad expanse. The width or areal extent of the marsh influences the oil-holding capacity of the particular shoreline segment.

Marshes are particularly important in terms of modeling since they:

1) Act as sinks for oil;
2) May have high sedimentation rates which tend to bury oil;
3) Are sheltered, thereby increasing oil persistence;
4) Contain high quantities of suspended matter which increases oil/sediment transport to the bottom; and
5) Commonly have fine-grained offshore sediments, thereby increasing the potential for oil incorporation into bottom sediments.

Areas dominated by marsh vegetation are mostly depositional. Incoming spilled oil, in turn, acts as sediment and will be deposited on the surface of the marsh. On the marsh's surface, oil is prone to evaporation and biochemical weathering. Oil export from the marsh is minimal because mechanical dispersive processes are almost absent.

While in or on the surface of the water column, oil will interact with suspended particles, whereupon it has a likelihood of sinking to the bottom. If the subtidal area adjacent to the marsh is also fine grained, as within the estuaries affected by the *Amoco Cadiz* spill, then substantial amounts of oil can accumulate on the bottom.

Persistence in these sheltered areas will probably be long term. After three years, Marchand et al. (1982) found only an approximate 50 percent hydrocarbon reduction in polluted, subtidal estuarine sediments as compared to over 90 percent in offshore sediments.

An estuarine model, depicted in Figure 4.4, includes oil interaction in the channel, adjacent mud flats, and an upper marsh. The channel contains high concentrations of suspended particulate matter which interacts with the oil causing oil sedimentation and some sinking. The mud-flat portion indicates oil stranding along the upper intertidal zone with leaching into the flat sediments. The marsh illustration indicates oil deposition on the marsh surface with some leaching and penetration into the marsh sediments. Some, although minor, oil export occurs during each successive tidal cycle.

4.3.5 Eroding Peat Scarps

Eroding peat scarps comprise ten percent of Bristol Bay coastal habitat. Within the adjacent Norton Sound, peat scarps dominate in the Yukon/Kuskokwim delta region. In temperate marsh areas, peat scarps may occur within marshes as along cut banks and exposed bays. Figure 4.5 indicates four common types of peat scarps (as observed along the Yukon/Kuskokwim delta). Type (A) represents a straight vertical shore as found along an eroding cut bank of a river channel. Type (B) represents an actively and rapidly eroding area where the adjacent tidal flat and the base of the scarp are completely clear of slump blocks and organic debris. Type (C) contains slump blocks along the flat as well as the base of the scarp. Organic debris is common along the base of the scarp. Type (D) represents an area in which the peat or organic base material is somewhat firmer so that a smaller scarp leading onto a sloping peat base is present. The sloping area (composed of peat) is highly grooved.

Although eroding peat scarps are a relatively common feature along the coastal environments of the Bering Sea, there is no information concerning their actual interaction with spilled oil. For the purpose of the SMEAR model, and until confirmed from field data, the following can be postulated. Basically oil persistence depends on the erosion rates of the area. Most peat scarps, by definition, are located in actively erosional areas so persistence will be minimal providing that the incoming tide again reaches the oiled zone.

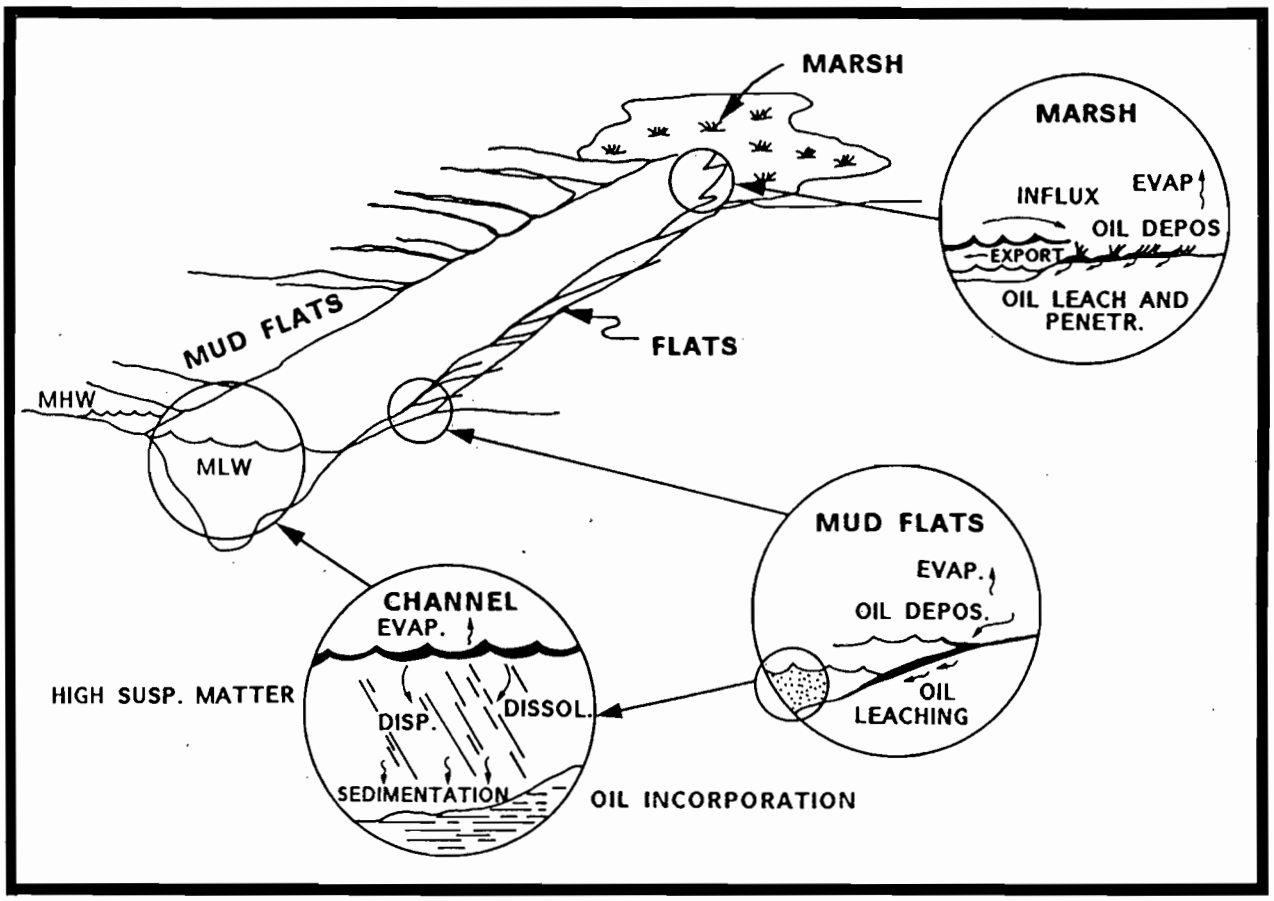

FIGURE 4.4. Depiction of oil interaction within a fine-grained estuary composed of a main channel (with mud-dominated bottom sediments) lined by tidal flats and a marsh (from Gundlach et al., 1985). EVAP. = evaporation; DEPOS. = deposition; OIL LEACH AND PENETR. = oil leaching and penetration; MLW = mean low water; MHW = mean high water; DISP. = dispersion; DISSOL. = dissolution; SUSP. = suspended.

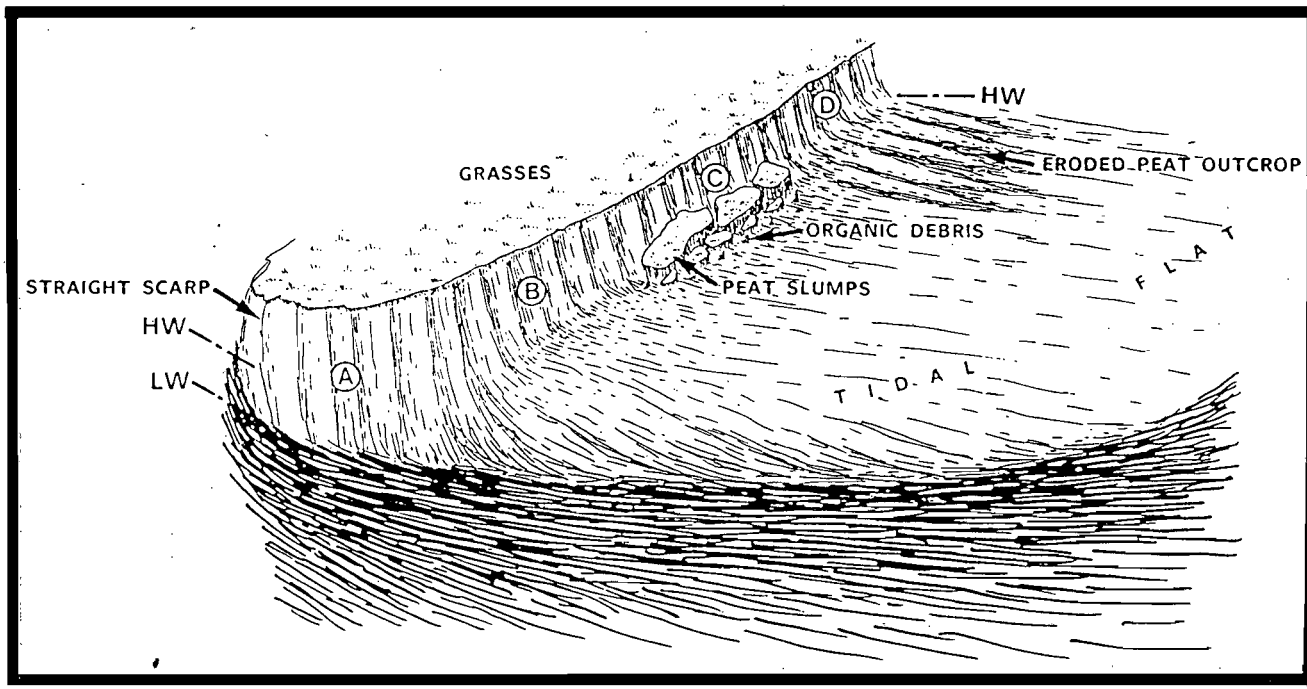

FIGURE 4.5. Typical eroding peat scarps of the Yukon/Kuskokwim delta.
Type (A). Vertical scarp as along cutbanks.
Type (B). Clean scarp leading onto a fine-grained tidal flat.
Type (C). Slump blocks and organic debris at base of scarp.
Type (D). Low-lying peat fronting a smaller scarp.

The capability of the area to accumulate oil will probably depend on which scarp type it is. Type (A) is essentially vertical and will be similar to a vertical rocky shore with minimal oil thicknesses able to accumulate before running off. Type (B) will act similarly but with a concentration of oil remaining at the base of the scarp until washed clean by wave or tidal action. Type (C) is able to accumulate more oil in and around the slump blocks and within the resident organic debris. Type (D) offers a more gentle slope on which oil might temporarily reside.

Within the Bering Sea, peat bluffs in direct contact with the sea during normal tides are basically unfrozen or contain only small ice lenses. However, along the Beaufort Sea, permafrost bluffs with a large ice content are common (Lewellen, 1970; Cannon and Rawlinson, 1981). Because of its similar form and commonly high erosion rate, permafrost bluffs will be considered equal to vertical peat scarps, at least until additional data are evaluated.

4.4 Calculation of an Oil-Holding Capacity

As spillets contact the shoreline, beaching or oil stranding is possible. During onshore winds, it becomes possible to place a large quantity of oil on a given section of shoreline. Based on observed oil spills, the capability of the beach to hold all incoming oil is limited, and once this limit is reached, oil will remain offshore and be exposed to longshore transport processes (see photo in Figure 4.6 from the *Amoco Cadiz* spill).

The maximum amount of oil that can be contained on various beach types is dependent on surface oil thickness, extent of oil incorporated into backbeach sediments, and beach slope. It is important to establish this quantity for a particular site in order to realistically model major spills.

Since temperature and oil type play such a large role in influencing the surface-oil thickness and subsurface-oil penetration, a division of oil types based on viscosity appears to be in order. [Example: as Arabian light crude emulsifies, it can change from a viscosity of 10 to 9,000 centistokes (cst) after 168 hours (CONCAWE, 1981).] A preliminary division of oil types by viscosity follows:

1) Low-viscosity oils: <30 cst (gasoline, kerosene, fresh light crude, and light fuel oils).
2) Mid-viscosity oils: 30-2,000 cst (most crudes plus light bunkers).
3) High-viscosity oils: >2,000 cst (weathered crudes, and heavy plus heavy bunkers).

During the running of SMEAR, viscosities will be calculated.

4.4.1 Surface Oil

Surface oiling of the shoreline can occur throughout the tidal range and into the splash and swash zones. Incoming oil in large quantities tends to "pile up" on the beach (see Fig. 4.7 from Galt, 1978). In the SMEAR model, oil accumulation would occur by the time-step addition of incoming oil (provided the appropriate environmental conditions exist). Gravity, in turn, causes oil to flow downslope and be absorbed into the beach, creating thin surface oil layers.

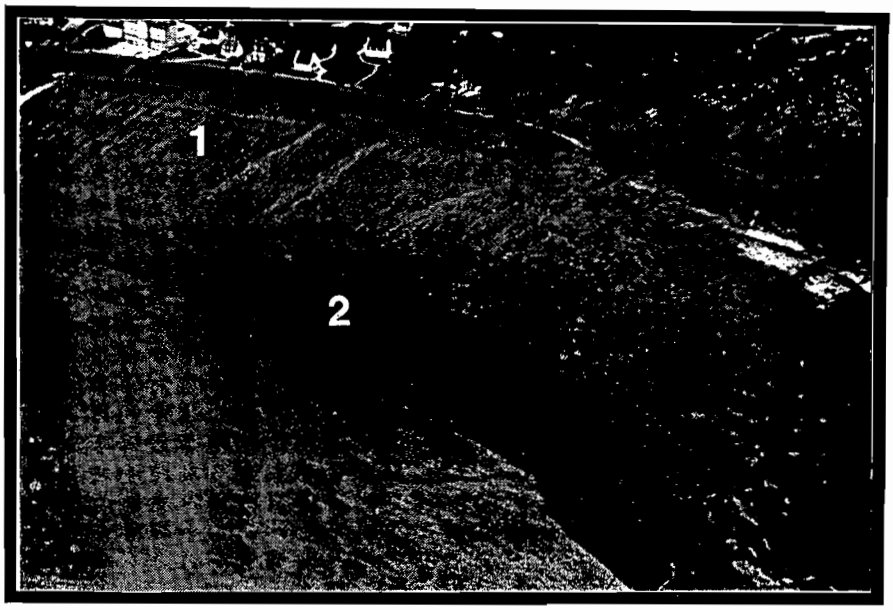

FIGURE 4.6. Aerial photograph from the *Amoco Cadiz* oil spill illustrating the limited capability of a beach to hold spilled oil. The beach face (1) is entirely covered with oil, while oil remaining offshore on the water's surface (2) is exposed to nearshore transport processes.

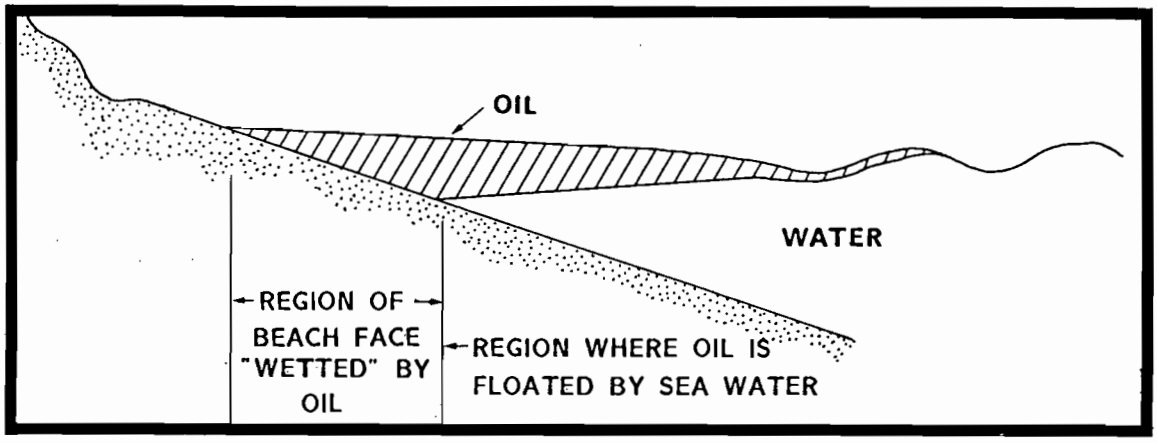

FIGURE 4.7. Suggested cross-section through an oil pool held against the beach face by wind and wave stress (from Galt, 1978).

Data from three major oil spills were researched to determine approximate maximum surface oil thickness on four major beach types. (Data for oil thicknesses on rocky shores and peat scarps are not available.) In each case, data were derived from field measurements such as illustrated in Figure 4.8. Data from the *Amoco Cadiz* are published (Gundlach and Hayes, 1978), while that from *Ixtoc I* and *Urquiola* are derived from field notes and sketches. Only measurements on moderately to heavily oiled beaches were used in this evaluation. Extremely high values, representing scour pits or other minor geomorphic features, were not included. The number of oil observations for each shoreline type vary greatly and indicate a need, if this approach is considered valid, for additional "spill-of-opportunity" data.

Viscosity of the oil varies by oil type and ambient temperature and also influences the thickness of oil measured on a beach. For the *Amoco Cadiz* and *Urquiola*, the oil type was Arabian crude, spilled in a cool (5-15°C) temperate environment. The *Ixtoc I* spill consisted of Campeche crude spilled under tropical (25-35°C) temperatures. Particularly on sand beaches, the Campeche crude formed thinner layers. Observations at a spill of opportunity in Alaska with Alaskan crudes, would enable a better maximum oil-thickness characterization. It should also be noted that (1) as an option, actual values can be used to replace the previously determined thicknesses, and (2) the following information reflects data in the public domain. Default values for other oil types are estimated at the end of this subsection.

Results of the surface crude-oil analysis are presented in Figures 4.9-4.11. For these light-to-medium crude oils (considered as mid-viscosity oils), a summary of mean values and standard deviations (to provide a reference to the degree of data variability) for each shoreline type are presented in Table 4.2. Considering rocky cliffs to have only a thin coating on a near vertical surface, a value of 2 mm was estimated. A slightly higher value of 4 mm was estimated for the eroding peat scarp on the premise that (1) oil could bind to the organic peat material, and (2) lesser slopes were possible particularly with type (D). A value of 5 mm, less than beaches but more than double that of exposed rocky shores, was estimated for sheltered rocky shores since it is composed of sheltered pockets (which tend to concentrate oil) and vertical rock surfaces (from which oil will drain off).

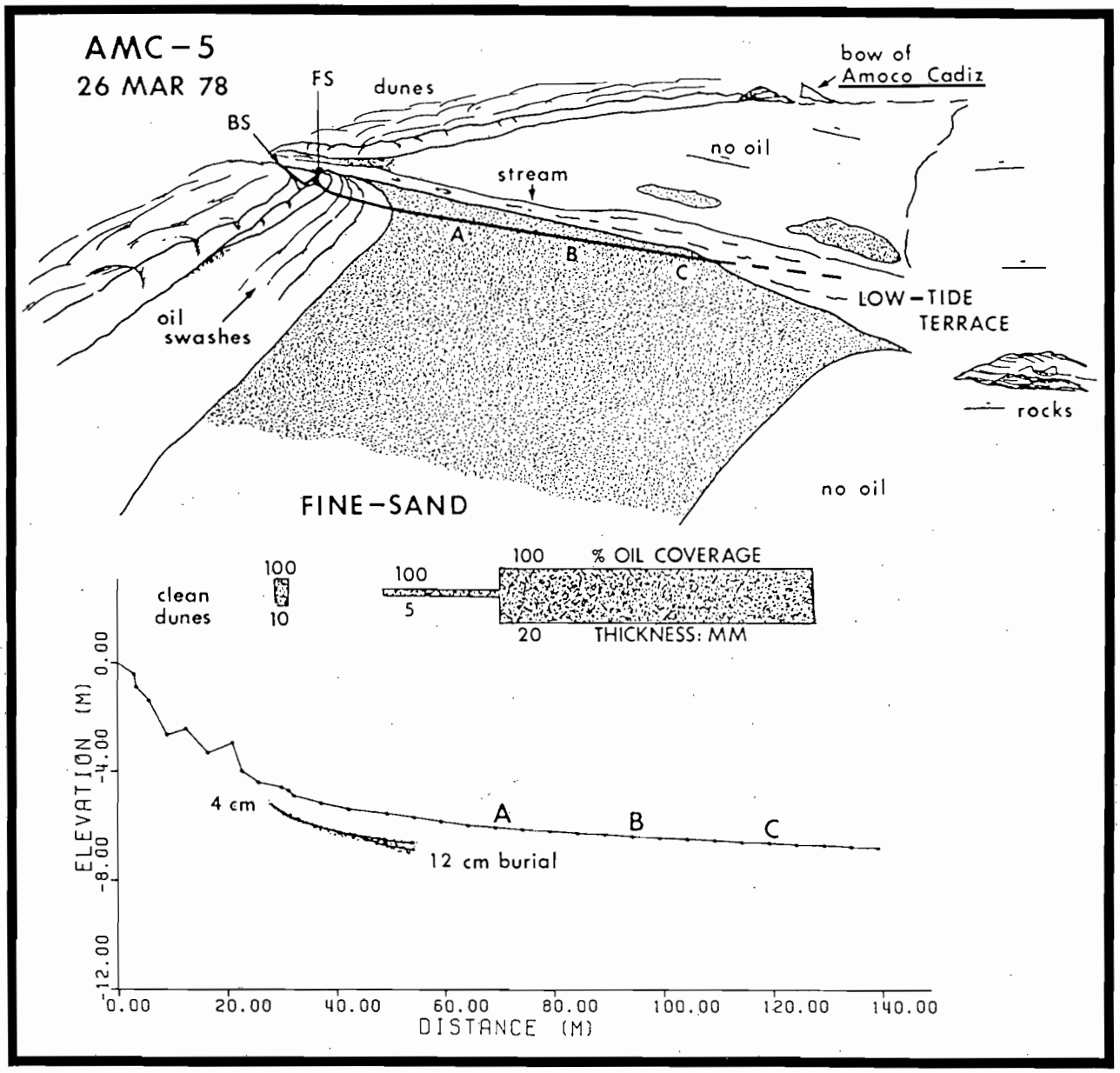

FIGURE 4.8. Example of information used in determining maximum oil thicknesses on beaches (*Amoco Cadiz*; from Gundlach and Hayes, 1978).

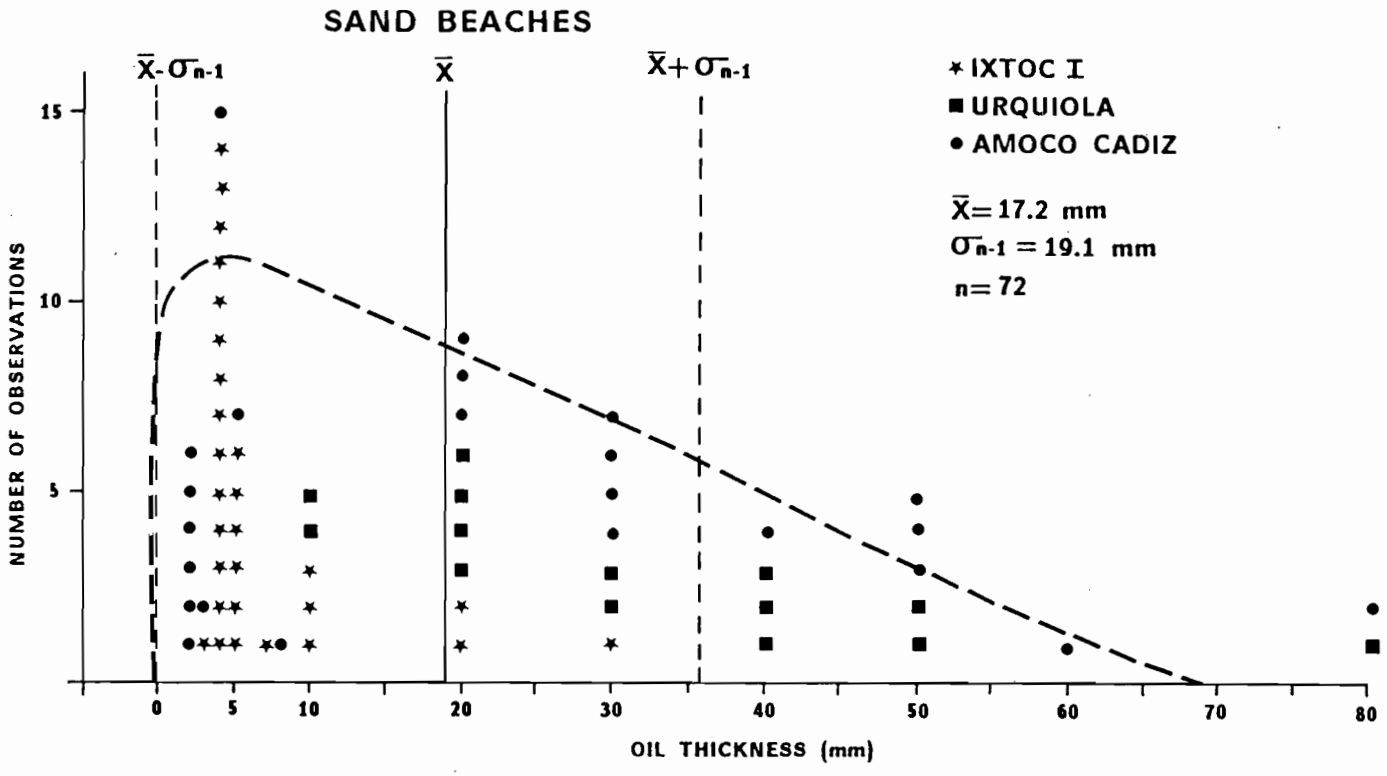

FIGURE 4.9. Measured upper limit of oil thicknesses on heavily oiled sand beaches. Data are from *Ixtoc I, Urquiola,* and *Amoco Cadiz* oil spills. [x = mean, σ_{n-1} = standard deviation, n = number of observations]

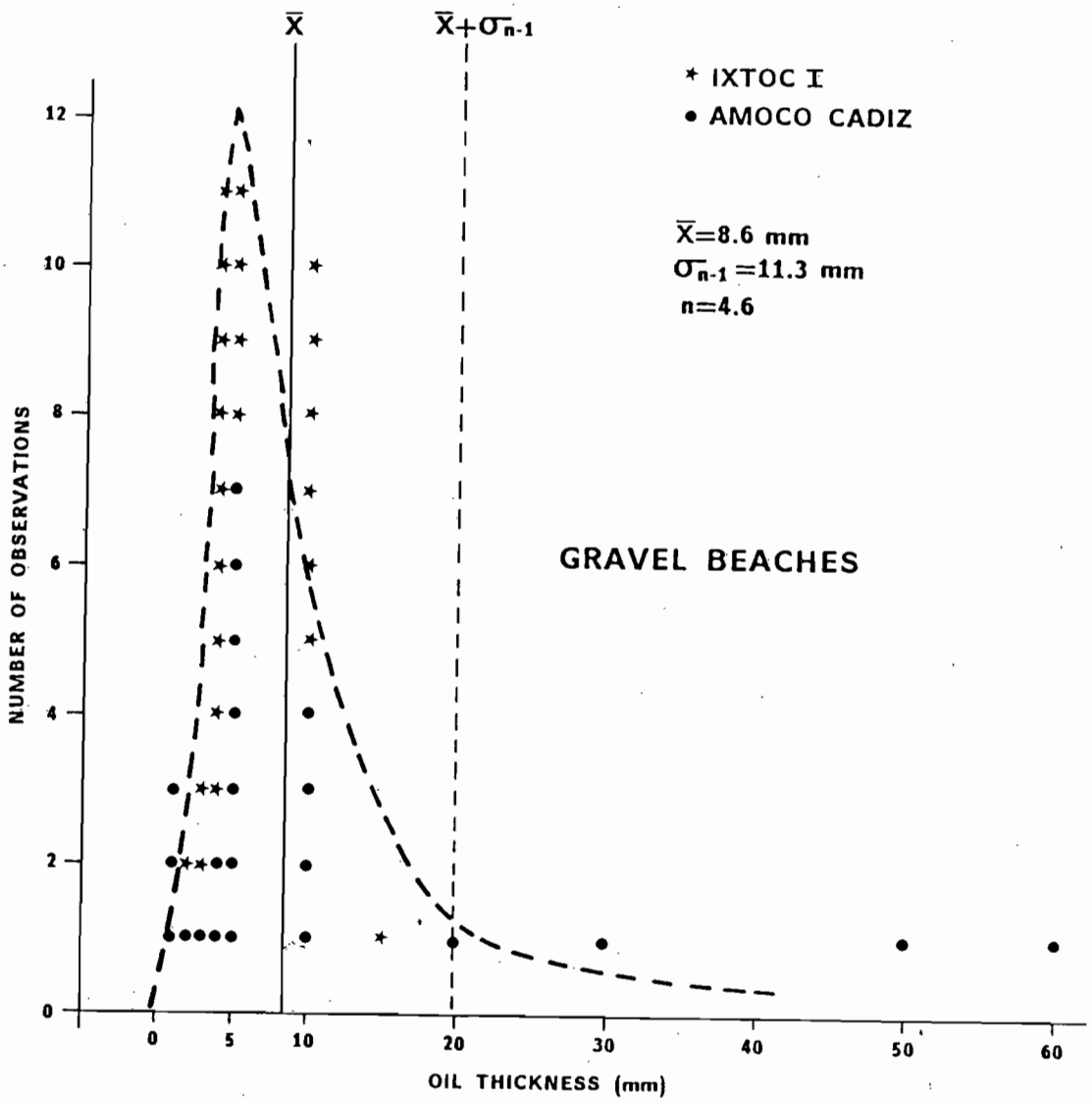

FIGURE 4.10. Measured upper limit of oil thickness on heavily oiled gravel beaches. Data are from *Ixtoc I* and *Amoco Cadiz* oil spills. [x = mean, σ_{n-1} = standard deviation, n = number of observations]

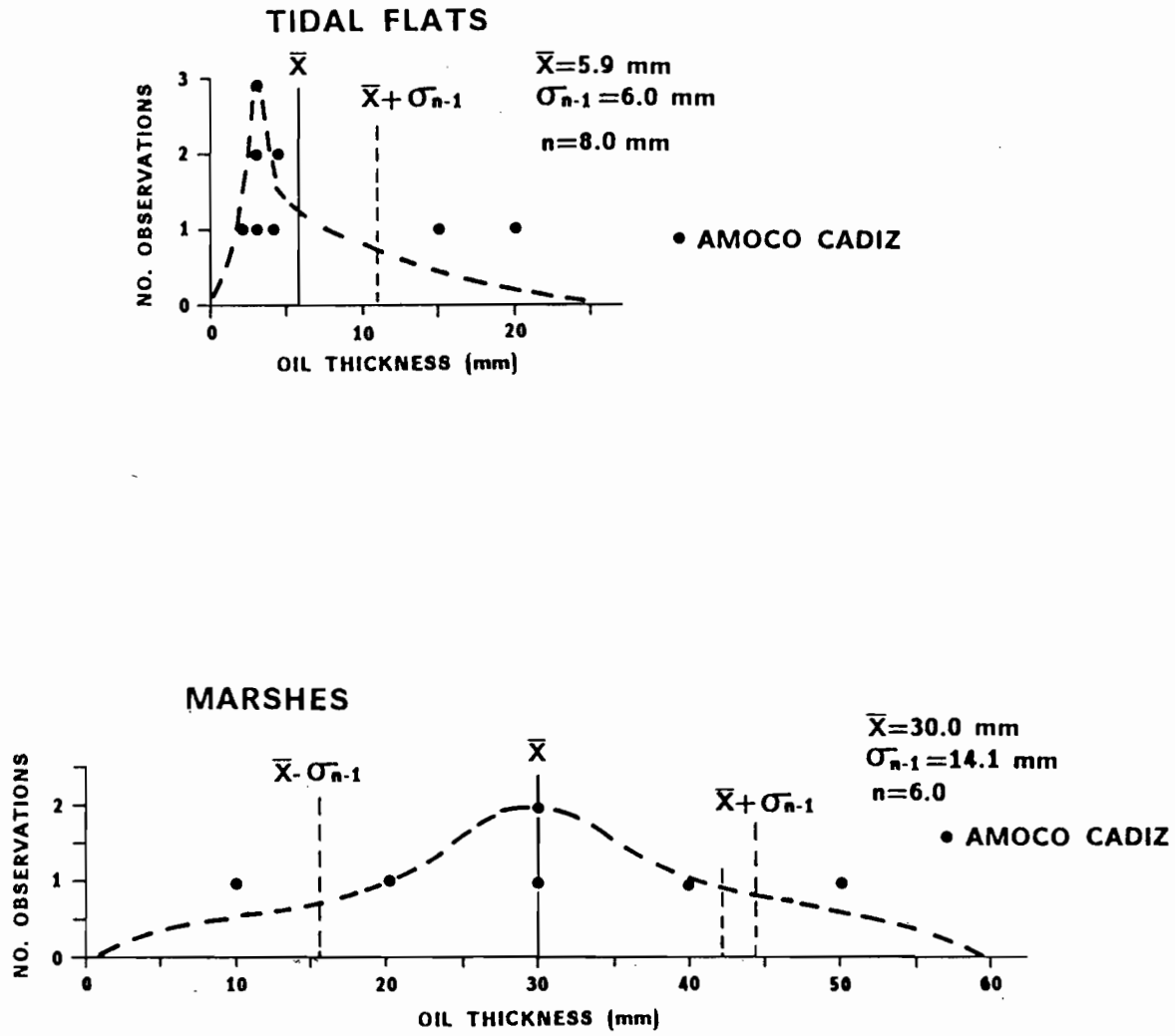

FIGURE 4.11. Measured upper limit of oil thickness on heavily oiled tidal flats and marshes. Data are from the *Amoco Cadiz* oil spill. [x = mean, σ_{n-1} = standard deviation, n = number of observations]

Estimates for probable, maximum oil thickness on each shoreline type for oils other than light to medium crudes are also estimated in Table 4.2, based on the premise that all oils can be concentrated along the shore so thicknesses are greater than on the sea surface. Light oils (diesel, kerosene, jet fuel, No. 2 oil, gasoline, etc.) tend to form very thin layers and are greatly affected by all water movement (whereas crudes and heavy oils can effectively dampen swash motion). Heavy oils (either heavy crude or bunker oils) generally tend to form thicker surface layers on beaches than light- to medium-grade crudes [e.g., as at the *Alvenus* spill (1984) of heavy Venezuelan crude along Galveston Island].

TABLE 4.2 Oil thickness for each shoreline type. For mid-viscosity oils, most values are measured (data sources are indicated in the text). NA indicates data not available because thickness value was not field derived. Values for light- and heavy-viscosity oils are estimated and are meant to be proportionately correct to each other and to light-to-medium viscosity oils for which data are partially available. Typical low-viscosity oils (<30 cst) are kerosene, gasoline, and diesel fuel. Typical heavy-viscosity oils (>2,000 cst) are heavy bunker oils, heavy crudes, and weathered crudes. Typical mid-viscosity oils (30-2,000 cst) are most medium-to-light crude oils and light bunkers.

Shoreline Type	Medium-Viscosity Oils		Light Oil	Heavy Oil
	Thickness (mm)	Standard Deviation (mm)	Thickness (mm)	Thickness (mm)
1) Rocky cliffs (exposed)	2	NA	0.5	2
2) Sand beaches	17	19	4	25
3) Mixed sand and gravel	9	11	2	15
4) Tidal flats	6	6	3	10
5) Rocky shore (sheltered)	5	NA	1	10
6) Marshes	30	14	6	40
7) Eroding peat scarps	4	NA	1	10

4.4.2 Subsurface Oil

Oiling of sand and gravel subsurface sediments, commonly called buried oil, most often occurs in the back-berm areas or along the upper swash zone. Under maximum oiling, there exists the potential for the entire swash zone to absorb oil (as subsurface oil). The total, subsurface oil-holding capacity is, therefore, based on the depth of oil penetration, the oil content of the sediment and the width of the swash zone. Each of these factors is discussed in the following sections.

Along the upper part of sand and gravel beach types, incoming oil has the tendency to percolate or sink into the sediments. The depth of penetration is dependent upon such factors as grain size, sorting, compactness, water content of the beach sediments, level of the water table, and the degree of oil/sediment mixing caused by wave or tidal action. A compacted, clay-dominated tidal flat saturated with water is the most resistant to oil penetration, while a dry, well-sorted, cobble-dominated shoreline has an enormous capability to incorporate oil. While there are no data available for oil on exposed peat scarps, it can be surmised that (1) penetration of oil into the peat is limited because of its compact nature and (2) burial is non-existent since the shoreline type is erosional. Likewise, burial does not occur along a sheltered rocky shore, although oil may percolate into the substrate if it is boulder dominated. However, for the SMEAR model, it is recommended that subsurface oil be neglected along all rocky shores.

For this analysis, original field data from the *Amoco Cadiz* and *Ixtoc I* oil spills and published data from the *Urquiola* spill (Gundlach et al., 1978) were consulted to determine the range and average depths of penetration in sand and mixed sand and gravel beaches. *Amoco Cadiz* data were derived from photographs of trenches cut into oiled beaches. Field sheets were analyzed to obtain the *Ixtoc I* data. Beaches from all three spills were subdivided into categories of fine sand, medium sand, coarse sand (grouped as sand beaches); or mixed sand and gravel, gravel, and cobble (grouped as gravel beaches).

A graphic plot of the results obtained from each spill is presented in Figure 4.12. Average penetration was found to be limited to 5 cm within sand beaches and to 18 cm within gravel beaches. In a laboratory study, Harper et al. (1985) found a similar relationship of increasing penetration with grain size for sandy tidal flats. Although these values are based on observational data, it is expected that the depth of penetration will be computationally determined, based on such factors as hydraulic conductivity, intrinsic permeability, fluid density and viscosity, gravity, water table level, and oil/sediment mixing.

4.4.3 Subsurface Oil Content

The buried-oil zone along the upper beach includes both oil and sediment. To determine the oil content, three spill incidents for which data were available were analyzed:

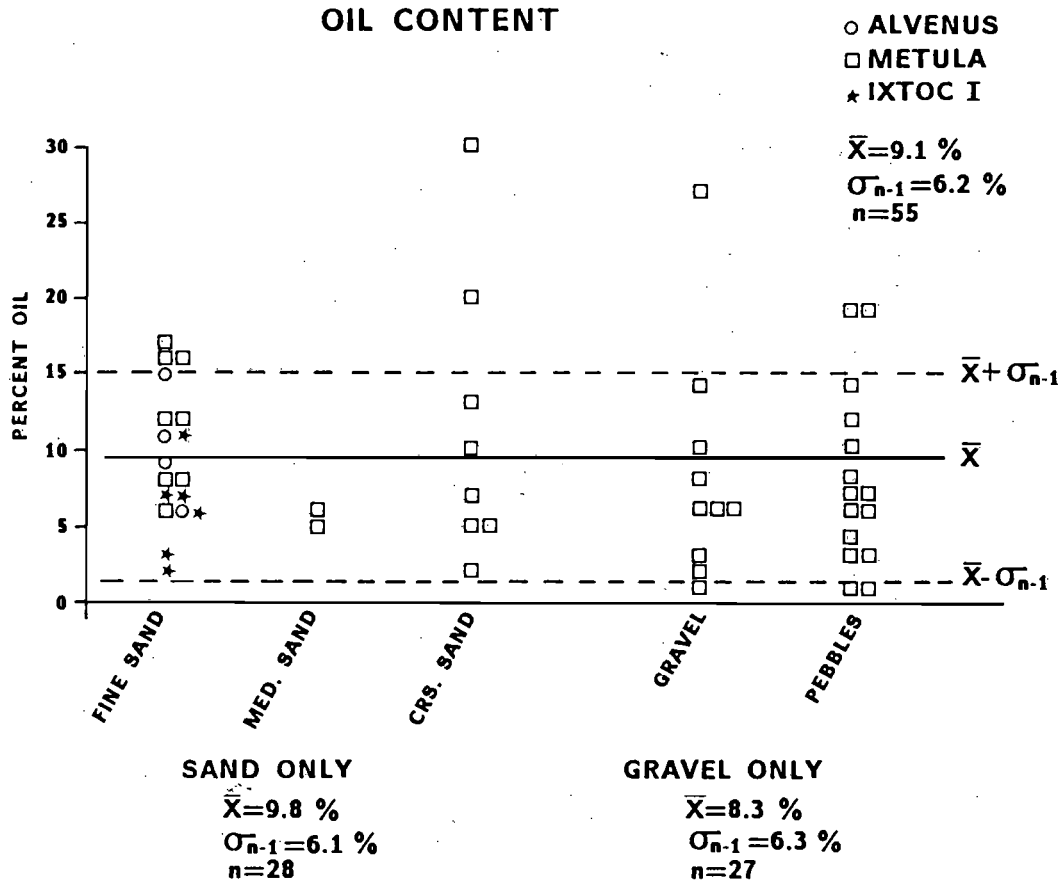

FIGURE 4.12. Measured oil content by volume of oily beach sediments. Data are from the *Metula* (Blount, 1978), *Ixtoc I* (Gundlach et al., 1981), *Alvenus* (unpublished) oil spills. [x = mean, σ_{n-1} = standard deviation, n = number of observations]

1) *Metula.* Blount (1978) measured the oil content of a variety of oiled beach and tidal flat sediments (but analyzed lightly oiled as well as heavily oiled sediments).
2) *Ixtoc I.* Six samples (4 heavily oiled, 2 moderately oiled) were analyzed and reported on by Gundlach and Finkelstein (1981).
3) *Alvenus.* Four heavily oiled samples were analyzed by Conoco Oil Company as part of the U.S. federal spill-response effort (unpublished).

Results of this analysis are presented in Figure 4.13. The average volume percent oil is 9.8 for sand beaches and 8.3 for gravel beaches. Because Blount (1978) analyzed both lightly and heavily oiled gravel beaches, the value for the gravel beaches is artificially low. The combined values for the sand and gravel beaches together is 9 percent (by volume), a value that more appropriately represents beaches in general.

In addition to beaches, oil can also penetrate or become incorporated into marsh and tidal flat sediments. Boehm (1982) reported on a series of core analyses of both marshes and tidal flats after the *Amoco Cadiz* spill. Oil was commonly noted to a depth of 15 cm. The maximum concentration (pyrogenic and *Amoco Cadiz* oil) reached 22,000 μg/g, although more average concentrations were less than 1,000 μg/g or one part per thousand. A recent laboratory study of tidal flat sediments (Harper et al., 1985) also showed relatively low (<1 percent) oil uptake in water-saturated sediments exposed to air for 12 hours or less. Oil incorporation, limited to 3 cm or less, increased to near 5 percent oil as the flat was artificially exposed to air for 15 hours or longer. Because these values are so low relative to the previous assumptions made in the model, it appears best that the model neglect oil incorporation into subsurface tidal flat and marsh sediments. (In contrast, the very slow removal rate and possible thick accumulations make marsh surface oiling extremely important.)

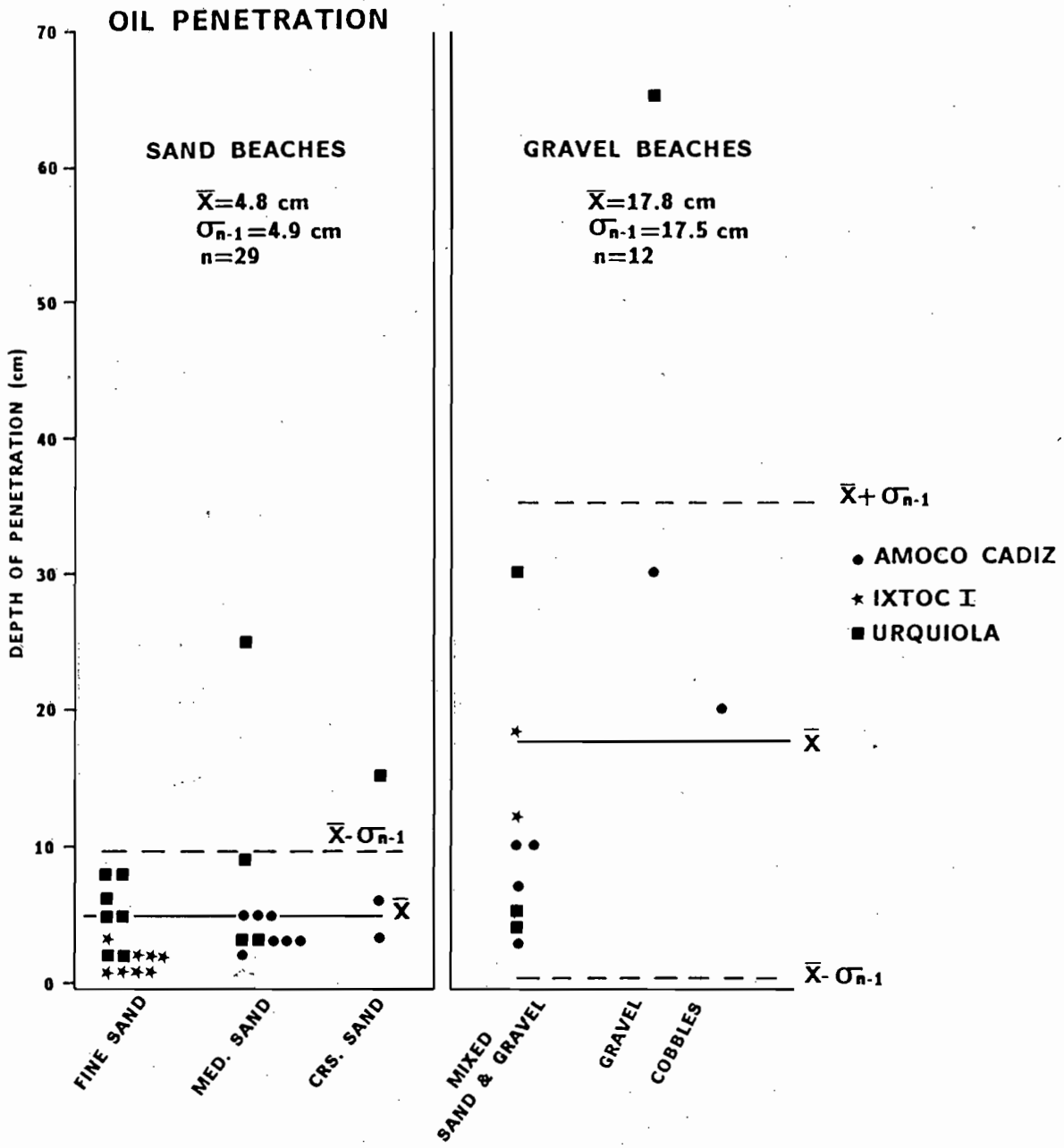

FIGURE 4.13. Measured depth of oil penetration in heavily oiled sand and gravel beaches. Data are from *Amoco Cadiz*, *Ixtoc I*, and *Urquiola* oil spills. [x = mean, σ_{n-1} = standard deviation, n = number of observations]

4.4.4 Sample Calculations

Since the thickness of surface and subsurface oiling has been determined, the maximum oil-holding capacity of each shoreline type is dependent of the slope of the shoreline. For exposed rocky shores a near vertical slope (80°) is postulated, while marshes and tidal flats are assumed to be horizontal (actual values can be input into SMEAR). The slope of sand and gravel beach types can vary considerably depending on grain size, wave length, and wave steepness. For coarse-sand beaches (0.5-1.0 mm), Bascom (1951) found that slopes can vary 8-15 percent. Fortunately, some profile data from Bristol Bay are available and can provide an approximate default value if exact slopes are unknown. Profiles for sand and gravel beach types from Bristol Bay are presented in Figure 4.14. Typical beach-face slopes are 5 percent for sand and 9 percent for gravel. The sand beach type typically has a flatter, back-berm area (2.3 percent slope), while the gravel type does not.

The calculations in Table 4.3 are provided solely as sample methodology to derive the maximum holding capacity. For SMEAR, accumulations onshore will be added in time-step fashion (under appropriate environmental conditions) until the maximum holding capacity is reached. For all beach types, the calculations are based on a 4-m tidal range and a 1-m swash zone height (Δh), with the hypothetical swash extending 0.5 m (Δh) into the flatter backshore of the sand beach type. Since the area of marsh and tidal flat environments that could be potentially oiled is not only related to tidal range or swash height (as in a fringing marsh perched above a narrow tidal flat), arbitrary 10 m and 20 m, respectively, oiled zones were used as examples. The calculations refer only to oil deposition; removal coefficients are discussed in Section 4.5.

From Table 4.3, it is evident that sand beaches can contain the largest quantity of deposited oil (2.16 m^3/m width of beach), primarily because of the wide, gently sloping beach face available for coating. Gravel beach types have steeper slopes, thinner oil coating across the beach face, but greater penetration in the upper swash zone. They are second in average capacity to absorb incoming oil (0.68 m^3/m). The hypothetical fringing marsh (10 m width) is next with an average spilled-oil capacity of 0.30 m^3/m. Rocky shores, with no oil penetration and steep slopes, contain very little oil (0.01 m^3/m) considering the same tidal range and swash factors.

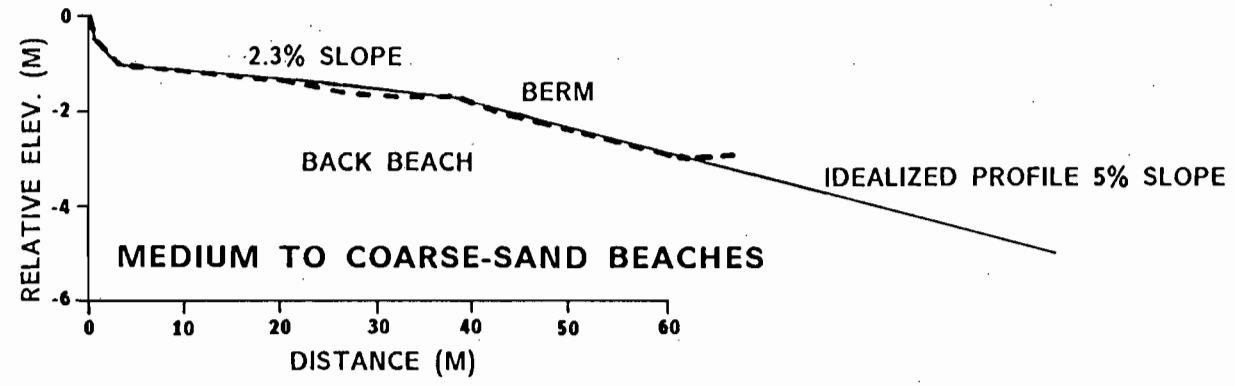

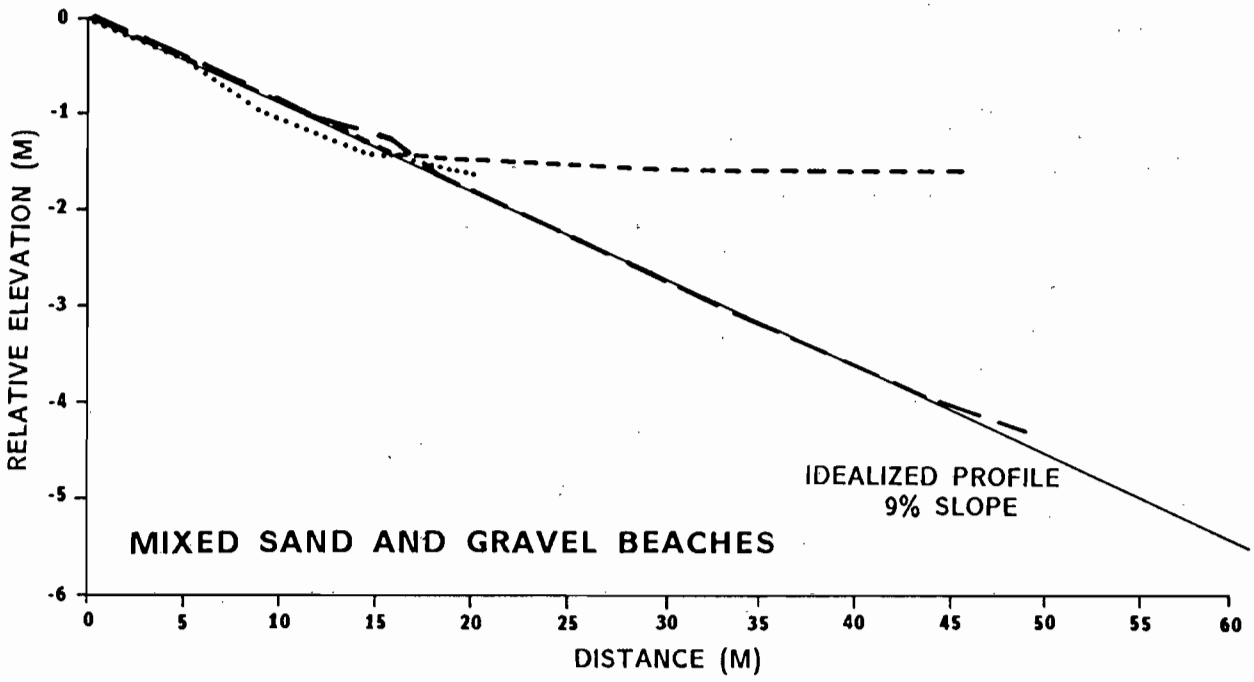

FIGURE 4.14. Measured (dashed, dotted) and idealized (solid) beach profiles from Bristol Bay: (A) sand beach type and (B) gravel beach type.

TABLE 4.3 Examples of a maximum holding capacity for each shoreline type based on a 4-m tide range having a 1-m (Δh) swash. Surface distances are assumed (*) for tidal flats and marshes. The order of filling compartments on the sand and gravel beach types is (1) swash zone buried, (2) beach-face surface, and (3) swash surface. NA = not applicable. Values are given as cubic meters oil per linear meter shorefront.

	Rocky	Sand		Gravel	Tidal Flat	Marsh
		Beach Face	Backshore			
SURFACE OIL						
Beach slope (degrees)	80	2.9	1.3	5.1	0	0
Tidal range + swash (vert., m)	5.0	4.5	0.5	5.0	5.0	5.0
Surface distance (m)	5	90	22	56	20*	10*
Oil thickness, avg. (mm)	2	18	18	9	6	30
Oil thickness, +1 SD	NA	34	34	20	0	16
Oil thickness, -1 SD	NA	2	2	0	12	44
Total Avg. [m^3/m]	0.01	1.62	0.40	0.50	0.12	0.30
Total (+1 SD)	NA	3.06	0.75	1.12	0	0.16
Total (-1 SD)	NA	1.80	0.04	0	0.24	0.44
SUBSURFACE OIL						
Beach slope (degrees)	NA	2.9	1.3	5.1	NA	NA
Swash range (vert., m)	NA	0.5	0.5	1.0	NA	NA
Swash zone distance (m)	NA	10	22	11	NA	NA
Oil penetration, avg. (cm)	NA	4.8	4.8	17.8	NA	NA
Oil penetration, +1 SD	NA	9.7	9.7	35.3	NA	NA
Oil penetration, -1 SD	NA	0	0	0.3	NA	NA
Oil content (%)	NA	9	9	9	NA	NA
Total Avg. [m^3/m]	NA	0.04	0.10	0.18	NA	NA
Total (+1 SD)	NA	0.09	0.19	0.35	NA	NA
Total (-1 SD)	NA	0	0	0	NA	NA

GRAND TOTALS (m^3/m)	Rocky	Sand	Gravel	Tidal Flat	Marsh
Minimum (-1 SD)	0	1.84	0	0	0.16
Average	0.01	2.16	0.68	0.12	0.30
Maximum (+1 SD)	NA	4.09	1.47	0.24	0.44

4.5 Fate of Beached Oil (Estimation of Oil Removal Coefficients)

A method for determining maximum oil-carrying capacity and corresponding estimates for several generic shoreline types has been given in the previous section. This section discusses modeling of oil removal (or the inverse, oil persistence).

During an ebbing tide, oil has the potential for being deposited on the shoreline. During a rising tide, the newly deposited oil most commonly is again refloated, varying with beach type, degree of mixing with sediments (i.e., causing a density change in the oil), and wave action. Although observational evidence of this occurrence is common, few measurements of the amount of oil removed per day or per tidal cycle are available. Diagrams taken from the *Amoco Cadiz* spill are presented in Figures 4.15 and 4.16. Figure 4.15 illustrates oil lifting off of a tidal flat and beach during the first weeks of the spill, but as the oil lost volatility and picked up sediment, less reflotation occurred. Figure 4.16 illustrates oil reflotation occurring on a compacted, well-sorted, and water-saturated, fine-sand beach. Reflotation over muddy tidal flats is illustrated in Figure 4.17 (from Allen et al., 1978).

The greatest extent of reflotation occurs in cases where a thin layer of water (as in water-saturated sands or muds) lies between the oil and sediment and actual oil contact with sediment is minimal. As this contact increases, as when the beach is dry (upper berms) and coarser grained (coarse sand, gravels, and cobbles), the sheet layer of oil (which aids reflotation) is broken, and oil can adhere to or mix into the sediments, thereby greatly reducing reflotation.

Although the general processes of reflotation are fairly well understood, there is only limited data from which to determine the rate at which this occurs. Additional complications may also arise because of unusual climatic conditions, an efficient clean-up operation, minor geomorphic occurrences (e.g., offshore islands causing tombolos where natural oil removal slows markedly), etc. Nevertheless, in order for SMEAR to work, realistic estimates of oil removal rates are necessary.

Based on personal observations of oil removal and affecting processes at several major spills (Gundlach et al., 1978; Gundlach and Hayes, 1978; Gundlach and Finkelstein, 1981; Gundlach et al, 1979; Gundlach et al., 1981; Gundlach et al., 1983) and from the Canadian BIOS study (Woodward-Clyde, 1981), a series of removal coefficients are defined for each of the seven shoreline types that have been previously described. The removal coefficient (K_f) is based on application in a simple, first-order equation that defines the estimated daily rate at which oil will be removed from the shoreline. This equation is as follows:

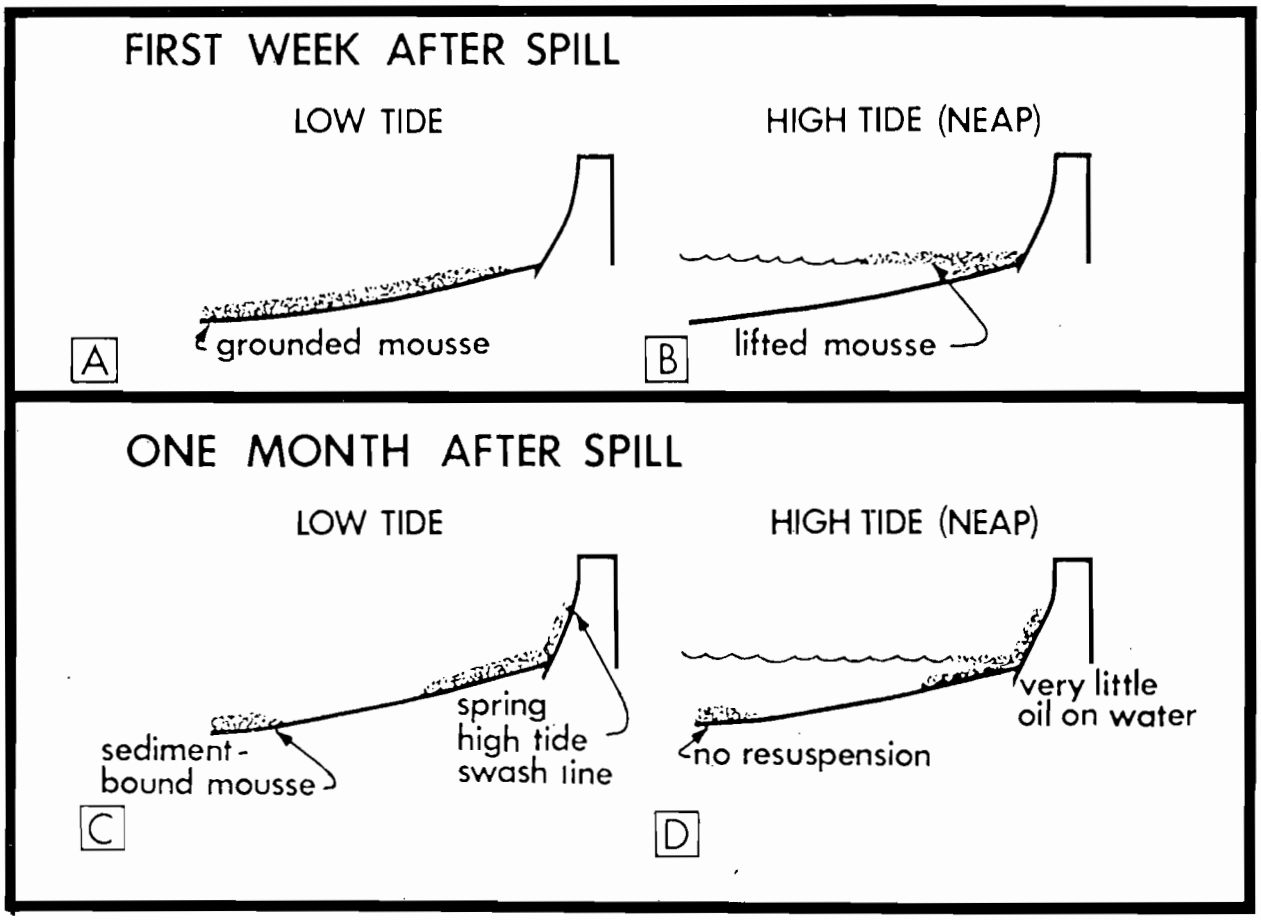

FIGURE 4.15. Examples of oil on a coarse-sand beach and tidal flat during the *Amoco Cadiz* oil spill. During the first few weeks, most of the oil lifted off the flat with each tide. However, after one month some oil remained on the beach and flat as the oil became bound with the sediment. From Gundlach and Hayes (1978).

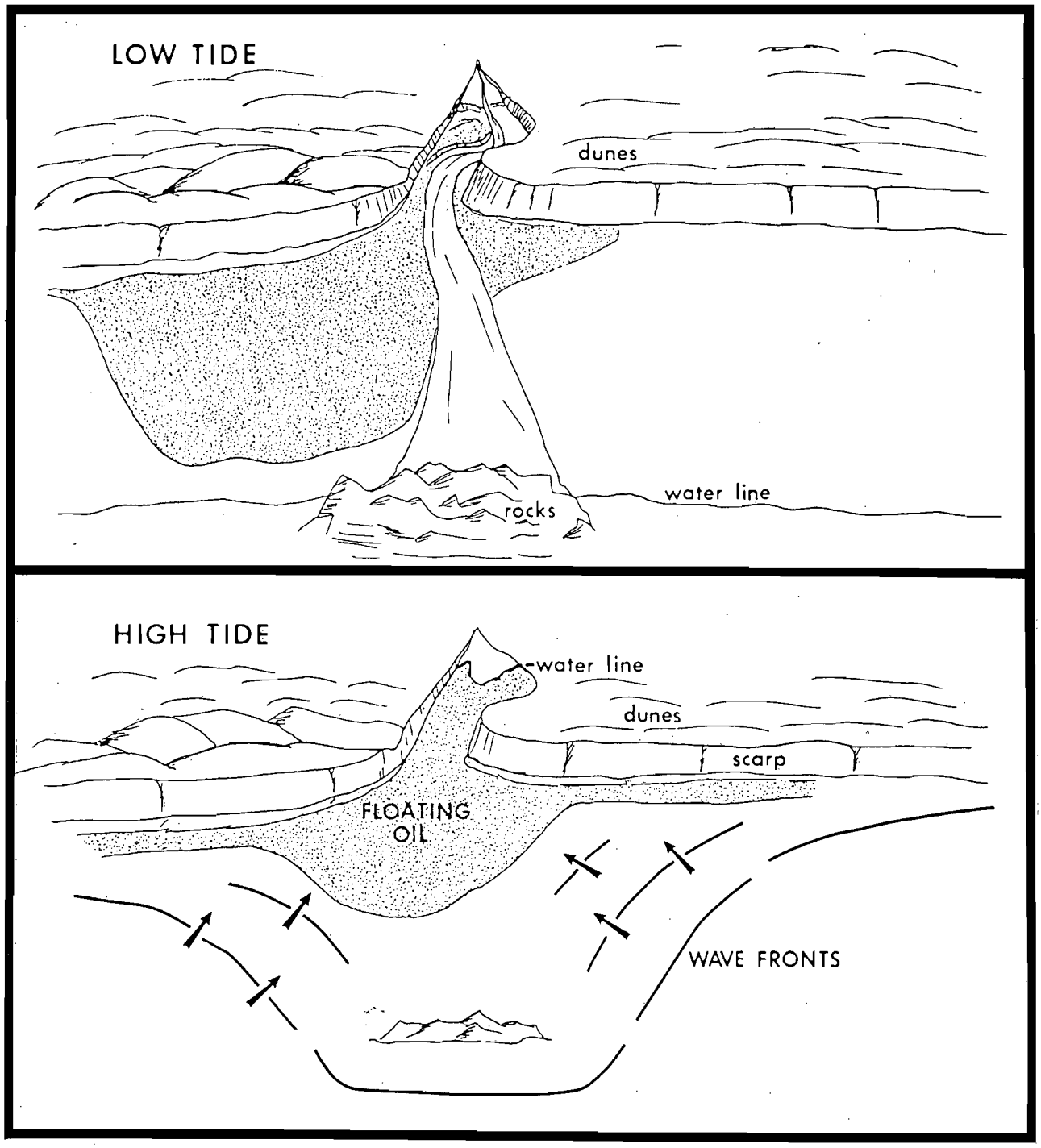

FIGURE 4.16. Example of oil refloating off a fine-sand beach during the *Amoco Cadiz* oil spill. During flood tide, all oil was lifted off the surface of the fine-sand beach and transported back into the marsh channel. As the tide receded, oil was redeposited on the beach face. From Gundlach and Hayes (1978).

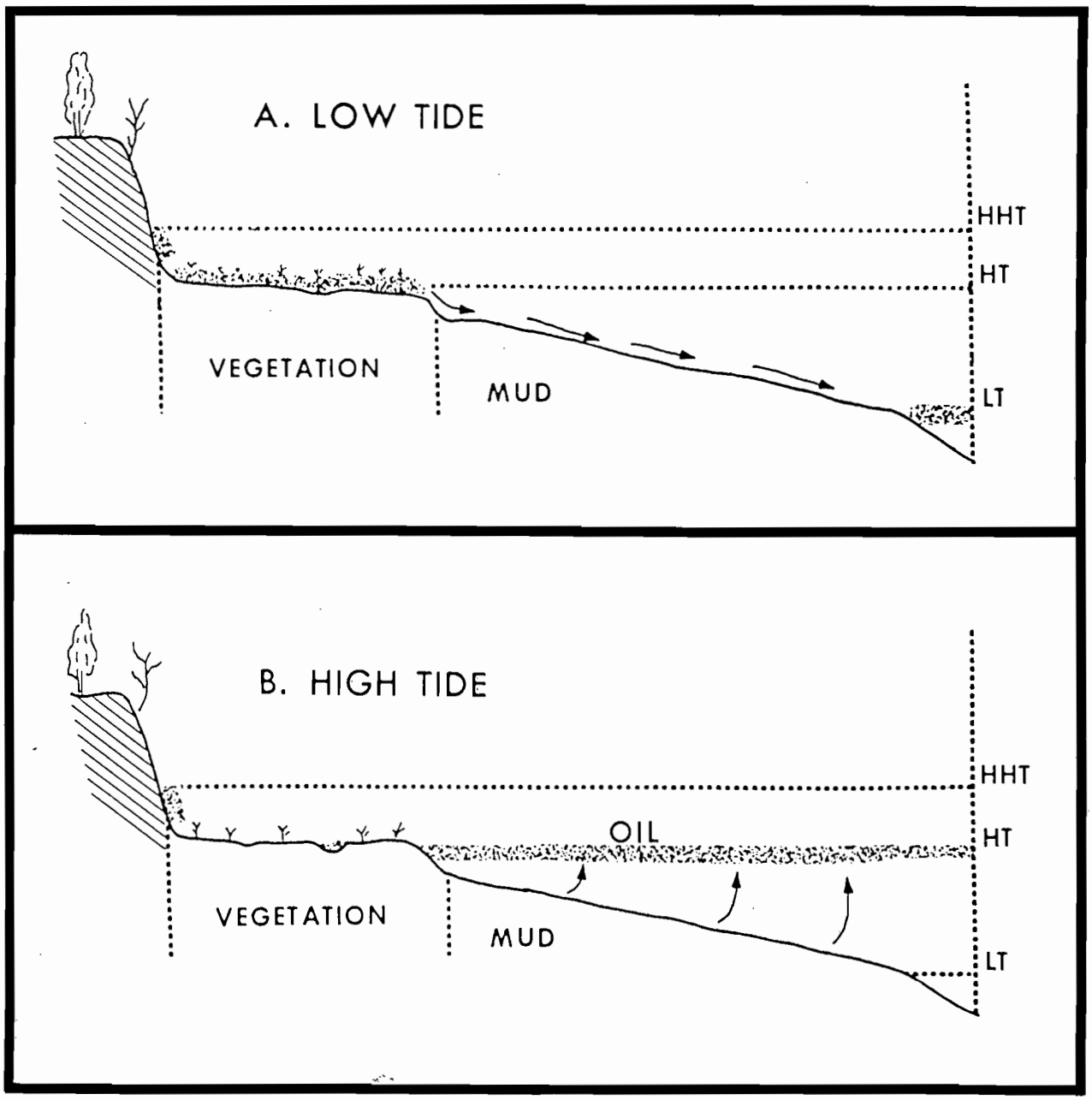

FIGURE 4.17. Cross-section of oil refloating off a mud-dominated tidal flat during the *Amoco Cadiz* oil spill. From Allen et al. (1978). LT = low-tide level; HT = high-tide level; HHT = high high-tide level.

$$M_i = M_{io}\, e^{-K_f t} \qquad (4.1)$$

where M_i = mass of oil in beach segment i.

M_{io} = mass of oil originally deposited on the beach.

K_f = removal rate constant based on exponential decay to characterize oil loss rate for each beach type.

t = time in days since original deposition.

Rate constants for all shoreline types are presented in Table 4.4 and Figure 4.18. In each case, a range of values are given to reflect some of the variability in oil deposition on coasts and yet maintain a specific internal relationship. As indicated, oil on gravel beaches is harder to remove than from sand beaches due to the greater difficulty in moving gravel-sized sediment. Sand and gravel beach types and eroding peat scarps are further divided by wave energy (<1 m or >1 m waves) to indicate that oil removal greatly increases with higher waves (e.g., four times more rapid on sand beaches). Sand and gravel beach types are also differentiated into beach face and backbeach compartments to indicate that removal from the backshore is slower than from the beach face. Marshes, by far, show the slowest oil removal rate while tidal flats and exposed rocky shores show the highest rates.

Of all the beach types indicated in Table 4.4 and Figure 4.18, only eroding peat scarps are without supporting evidence (since no published spill reports include this beach type). It is felt that during oil deposition, oil may bind with the organic peat material, thereby, greatly inhibiting its removal. Under calm or low wave conditions, this oil is likely to remain adsorbed onto the peat so removal rates are relatively low (i.e., equal to those of a gravel beach, but not as low as a marsh). Under higher waves, defined as having wave heights greater than 1 m, oil removal is quite rapid since the entire scarp is likely to experience erosion under these conditions. Therefore, removal was set as greater than for sand beaches, but not as rapid as for tidal flats. Upon field studies during a "spill-of-opportunity," these rates can be better refined.

TABLE 4.4 Preliminary daily oil removal rates as a function of shoreline type and wave energy. K_f values reflect the amount of oil remaining within that particular segment of shoreline via application of Equation 4.1.

Shoreline Type	Characteristics	Percent Removed (1 day)	Percent Removed (5 days)	K_f Value
Rocky Shores				
•Exposed	-Most oil readily lifts off uniform and wetted surface	60-63	99-99.3	0.90-0.99
•Sheltered	-Long-term persistence due to reduced wave energy and rugged substrate	5-10	5-22	0.01-0.05
Eroding Peat Scarps	-Basically erosional but oil may adhere to substrate			
	-Under low wave (<1 m) activity	10-18	49-63	0.10-0.20
	-Under high wave (>1 m) activity	50-55	97-98	0.70-0.80
Sand Beaches	-Mostly surface oiling, but some oil/sand adherence and mixing, particularly with coarse-sand beaches			
	-Generally easy oil removal from beach face, but longer oil persistence along backshore			
	-Under low wave (<1 m) activity:			
	Beach face	18-26	63-78	0.20-0.30
	Backshore	10-18	40-53	0.10-0.15
	-Under high wave (>1 m) activity	40-45	92-95	0.50-0.60
Gravel Beaches	-Mostly surface oil on the beach face, but deep penetration and longer persistence along the backshore			
	-Under low wave (<1 m) activity:			
	Beach face	10-18	40-63	0.10-0.20
	Backshore	5-10	22-40	0.05-0.10
	-Under high wave (>1 m) activity	33-40	86-92	0.40-0.50
Tidal Flats	-Most oil lifts off of wetted tidal flats	60-63	99-99.3	0.90-0.99
Marshes	-Oil tends to adhere to the marsh vegetation and soft, base sediments	0.1-1.0	0.5-5	0.001-0.01

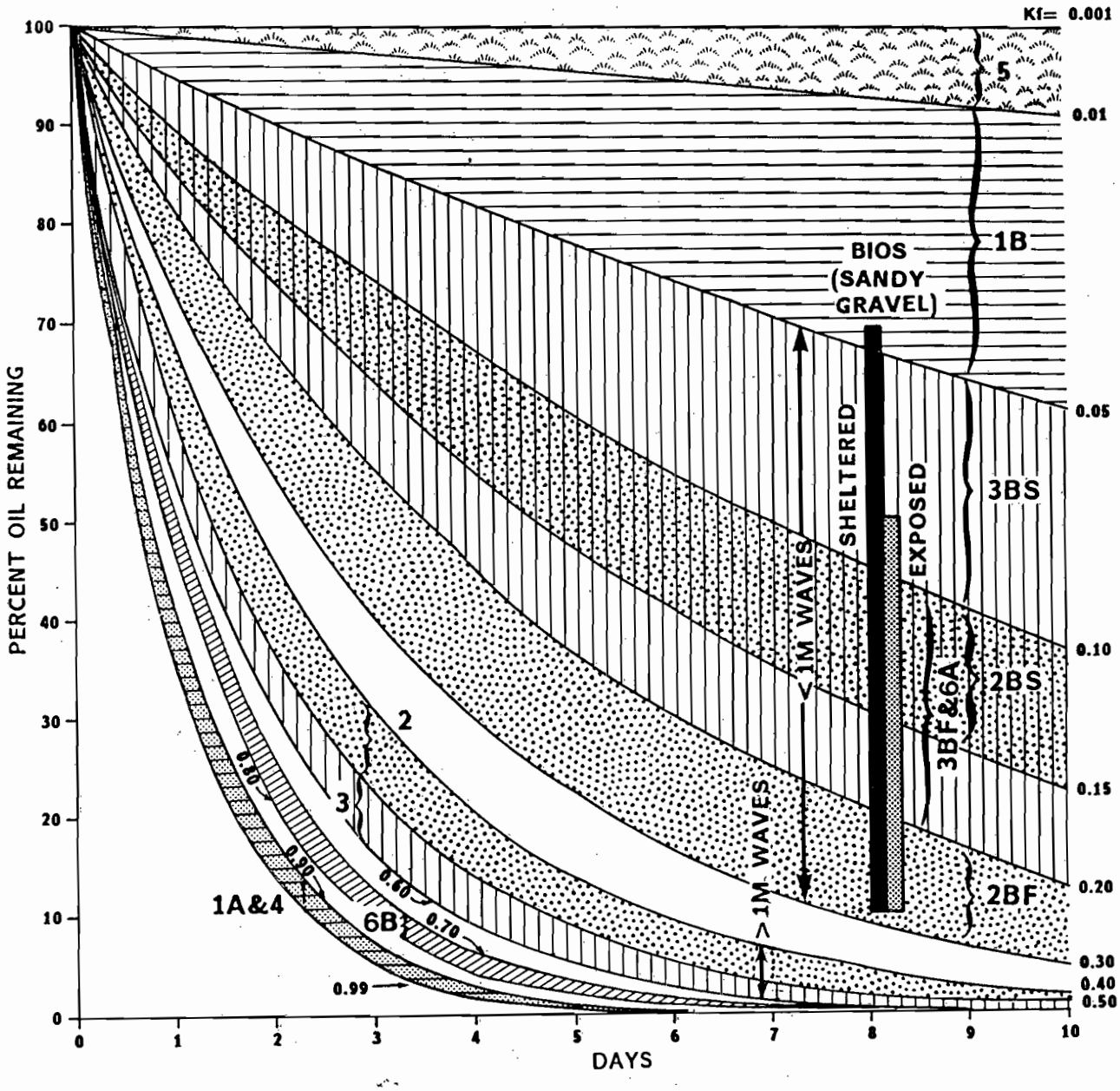

FIGURE 4.18. Predicted oil remaining as a function of K_f (see Equation 4.1) and time for different shoreline types:

1A = Exposed rocky shore
1B = Sheltered rocky shore
2 = Sand beach type
3 = Gravel beach type
4 = Tidal flat
5 = Marsh
6 = Eroding peat scarp
A = <1 m waves
B = >1 m waves
BS = Backshore
BF = Beach face

Oil remaining after 8 days as measured during the BIOS experiments is also plotted (from Woodward and Clyde, 1981).

The BIOS project in the Canadian arctic, which followed a series of test oil plots for several years, provides a test of the rate curves presented in Figure 4.18. In that study, plots were positioned so that approximately 80 percent of the oiled area was below mean high water, 20 percent above. Two adjacent plots along an exposed mixed-sand and gravel coast were rapidly altered by wave-induced erosion, removing most of the oil within two days. In the low wave-energy plots (also mixed sand and gravel), oil was removed comparatively fast by tidal influences alone due to the high groundwater table. A summary of mass balance for the first eight days of the study is presented in Table 4.5. Note that between 29 and 90 percent of the oil was removed within this time period by wave or tidal action, whether along a sheltered or an exposed beach. Figure 4.18 compares the BIOS analysis to the projected rate curves for the model, illustrating a relatively good comparison.

TABLE 4.5 Estimated oil budget for BIOS study plots after eight days (from Woodward and Clyde Consultants, 1981).

	Percent Oil Removal			
	High Energy		Low Energy	
Weathering Process	Aged	Emulsified	Aged	Emulsified
Atmospheric evaporation	<5.0	<5.0	<5.0	<5.0
Wave action	~50.0	~90.0	<1.0	<1.0
Tidal action	?	?	~29.0	~90.0
Microbial decomposition	<1.0	<1.0	<1.0	<1.0
(Residue)	43.0	0.27	64.0	4.8

As an additional test, these coefficients were applied to the *Amoco Cadiz* oil spill. The test is preliminary in nature to indicate if the values can approximate the field data and to serve as a brief method of evaluating which factors inherently account for the greatest percentage. Data from the *Amoco Cadiz* (Finkelstein and Gundlach, 1981) indicate that approximately 62,000 tons of oil were found along the coastline between 19 March and 2 April. Of the total, 7400 tons were located within the Ile Grande marsh. A second survey, undertaken roughly 30 days later between 20-28 April, indicated that the shoreline quantity was reduced 85 percent to 9,200 tons of which 2760 tons remained in Ile Grande marsh.

The shoreline affected by *Amoco Cadiz* consists of exposed and sheltered rocky shores, sand and gravel beach types, various tidal flats, and marshes. The extent of oiling and shoreline composition is presented in Table 4.6 (from D'Ozouville et al., 1981). The Ile Grande marsh was the major vegetated area to be oiled. Since it was subjected to such an extensive cleanup operation, it is not directly considered in this analysis.

TABLE 4.6 Extent of contaminated shoreline, *Amoco Cadiz*, April 1978. [Modified from D'Ozouville et al., 1981.] *Estimated to consist of 60 percent gravel and 40 percent sand beach types for calculation in Table 4.7.

Shoreline Type	Length of Coastline (km)	Percent Coast Without Marshes	Heavy Pollution (km)	Light to Medium Pollution (km)	Clean (km)
HIGH ENERGY ZONE					
Rocky shores and eroding platforms	70	25	50	20	0
Fine-sand, gravel, and cobbles	60	22*	35	25	0
LOW ENERGY ZONE					
Rocky shores and eroding platforms	68	25	34	28	6
Fine sand, gravel, and cobbles	75	27*	37	33	5
Tidal flats and marshes	90	--	20	47	23
TOTAL	**363**	**99**	**176**	**153**	**34**

Additional suppositions are that 20 percent of the incoming oil was deposited on sand and gravel beach types above the normal swash zone (based on the storm surge evidenced in mid-March, and that only swashes (waves <1 m) again reached the area and only for 25 percent of the time (based on the large tidal range, the need for spring tides, and the lack of other storm activity). Oil deposited above the normal high-tide swash primarily represents buried oil.

Table 4.7 contains summary results of this analysis. Basically there is good agreement with the observed data from the spill site. Most of the remaining oil was located within the sheltered, rock-dominated areas particularly adjacent to tidal flats, and along the upper beach (backshore surface and buried). Influences to the variation

between the actual and calculated values are attributable to such factors as the estimated amount and timing of oil along the backbeach, impacts from previously removed oil (over 50,000 tons was naturally removed from the beaches between the two study periods), and to cleanup operations.

TABLE 4.7 Comparison between calculated and observed oil remaining onshore at the *Amoco Cadiz* oil-spill site between 19 March-2 April and 20-28 April (assumed to be 30 days) (Finkelstein and Gundlach, 1981). The backbeach areas are assumed to be exposed to swashes (<1 m waves) for 25 percent of the total time. K_f values relate to Equation 4.1. [*Reduced almost entirely by cleanup operations.]

Shoreline Type •Characteristics	% of Coast	K_f	Days	Initial Tons	Final Tons	
					Minimum	Maximum
Rocky						
•Exposed	25	0.9-0.99	30	13,650	0	0
•Sheltered	25	0.01-0.05	30	13,650	3,046	10,112
Sand						
•Beach face	16	0.20-0.30	30	8,736	1	22
•Backshore	4	0.1-0.2	7	2,184	764	1,085
Gravel						
•Beach Face	24	0.1-0.2	30	13,104	32	652
•Backshore	6	0.05-0.1	7	3,276	1,627	2,308
		SUBTOTAL		54,600	5,470	14,179
Marshes*				7,400	2,760	2,760
		TOTAL		62,000	16,939	8,230
	Final Tons:	•Calculated	8,230-16,939			
		•Observed	9,200			

5.0 COMPARATIVE ANALYSIS OF POSSIBLE SMEAR MODEL COMPONENTS

This section describes the evaluation process for integrating surf-zone (current and sediment transport) models and oil-spill models into a unified SMEAR model. As presented in Sections 2 and 3, two candidate surf-zone and one oil-spill model have been selected for possible linkage to comprise the SMEAR model system. The surf-zone models under consideration are a two-dimensional (2-D), vertically averaged, circulation and sediment-transport model driven by wind, tide, and waves; and a simple (SIMPLE) engineering approximation where the longshore currents and sediment flux are described by bulk longshore fluxes. These two alternatives will be referred to as the 2D/Bijker and 1D/Komar models, respectively. The candidate oil-spill model is the SAI weathering model, which will be used in conjuction with the ASA oil transport model. Thus, there are two possible oil-spill/surf-zone mass-transport model systems to be evaluated. Modifications to the oil spill model will be required to incorporate the sediment/oil interaction algorithms, since these are not currently operational in either model.

5.1 Evaluation Criteria

The strategy for evaluating the alternative SMEAR model systems is based on the assignment of relative weighting factors (WF) to each of the criteria described on the following pages. A WF of 1 specifies a low level of importance, whereas a WF of 10 specifies maximum significance. Each alternative system is then analyzed individually relative to each criterion and assigned a scaling factor (SF) between 1 and 10. The total score for each alternative model system is then the sum of the products SF times WF for all criteria.

Individual assessment criteria are discussed below in terms of rationale for assignment of WFs. These WFs have been developed as a consensus among members of the project team.

Criterion 1: Compatibility of submodels and efficiency of linkages between submodels

It is clear that linkage compatibility and efficiency are closely related. For example, if the linkage to the sediment transport model is the Reynolds-averaged, mean vertical turbulent energy density as a function of distance offshore, but the proposed oil-spill submodel requires a vertical energy-density profile, then some additional

computations will be required. Although an important consideration, many incompatibilities of this sort can be overcome at the cost of some additional theoretical work and computer programming. The weighting factor is 6.

Criterion 2: Ability of the model to be used for different localities

This is clearly important. Wave-climate models which are limited to flat bottoms or waves propagating only normal to the coastline are not acceptable in general. The model should be applicable to rocky coastlines, sand and gravel beaches, eroding peat scarps, and tidal marsh areas. The weighting factor is 8.

Criterion 3: Ability of the model to function effectively with data that are readily and cost-effectively obtainable

Again, this issue is of fundamental importance. A theoretical model system for which parameter values are unobtainable will require the investment of more effort in sensitivity analysis. The weighting factor is 8.

Criterion 4: Accuracy of model predictions of oil tranport

(Estimated probable error with respect to both the distribution in the surf-zone water column and beach materials and longshore transport.) We consider this a key decision criterion from the scientific standpoint, but it is unclear how well estimates of probable errors can be made in the absence of well-focused laboratory or field studies to provide some statistical basis. Although the WF should be maximal, it is uncertain how best to approach scaling under this criterion. The weighting factor is 10.

Criterion 5: Flexibility of the model for interactive use in problem-solving, allowing experimental variation of parameters

Any SMEAR model system, when applied to 100 km of irregular coastline with detailed horizontal and vertical resolution and variable sediment types, beach slopes, wave-approach angles, and oil-densities variable as functions of time and location, will necessarily operate as a batch job on a main-frame computer. Such model systems may be simplified for use in an interactive mode or on a smaller machine. This is usually necessary for verification of the code and for cost-effective sensitivity analysis. An alternate, of course, is to use a much simpler algorithm initially to approximate the process.

For the SMEAR model system, the interactive version will be limited to a user-supplied range of sediment values and specified offshore bathymetry; beach slope, wave height, period, and propagation direction; and initial oil state, amount, and offshore-to-onshore loading (advection) rate. Each of these parameters can be independently specified by the user at the beginning of a run. At this level, the model will be on an IBM PC and can be supplied to MMS on IBM-compatible floppy disks. The weighting factor is 7.

Criterion 6: Cost-effectiveness of simulation, model flexibility, and model application

Except in extreme cases (i.e., very complex versus very simple model system structures), we expect to have some difficulty objectively scaling alternatives under this criterion. On the other hand, model veracity is probably a more important consideration, so a lower weighting factor makes uncertainties in the scaling-factor assignments less critical. The weighting factor is 4.

Criterion 7: Estimated development costs of final programming, testing, sensitivity analyses, and documentation

These costs are expected to be similar for all proposed systems, although sensitivity analysis costs will increase in proportion to the number of model parameters to be evaluated. Even so, the cost variation among alternatives should be relatively small. The weighting factor is 4.

Criterion 8: Compatibility of the model with the outputs of existing MMS circulation and trajectory models, the oil-weathering model developed by Payne et al. (1981), and an offshore suspended particulate model now under development by MMS/SAIC

In brief, the trajectory model supplies the location of an oil-spill centroid as a function of time. The SAI model simulates the weathering processes of evaporation, dispersion, mousse formation, and spreading to estimate the dynamic mass balance and composition of the oil on the water surface as a function of environmental parameters. Although the work by Payne et al. (1981) addresses suspended particulate matter (SPM) interactions with hydrocarbons, the SAI model (Kirstein et al., 1983) appears to neglect this process. Eventual linkage is presently under development. Thus, these three models together will supply the following inputs to the SMEAR model for any specific spill scenario:

1) Advection, loading, or arrival rate of oil at the surf zone as a function of time and location.

2) Weathered state of each arriving increment of oil, depending on its travel history.

The weathered state is reflected in the changing composition of the oil, characterized by pseudocomponents or boiling point/density cuts. This is the same approach as that used in the ASA three-dimensional oil-spill model (Reed et al., 1980; Spaulding et al., 1982a). We thus appreciate the advantages and limitations of this approach and expect this to be the only potential source of compatibility problems under this criterion. Compatibility would appear to be a major issue for MMS program success. The weighting factor is 10.

Oceanographic input data sets of the system include hydrodynamics, wind fields, air and sea temperatures, and sea state. These are assumed to be preprocessed from raw data or other models and stored on magnetic disk for retrieval as needed. Since each oil-spill fates model requires these inputs, they will not be included in our evaluation process.

The oil-spill model will have to include spreading and weathering, and particularly interaction with sediments, as well as surface trajectory capabilities. Minimum quantitative and graphical outputs must include spatial surface and subsurface distributions, weathered state of individual oil slicks, and oil deposited on the beach and backshore areas as a function of time.

5.2 Evaluation of Alternative Model Constructions

The comparative evaluations of alternate SMEAR model systems is based on assessing the total score (weighting factor times scaling factor summed over all the evaluation criterion) for each proposed pair. The ordered pairs to be evaluated include the following:

Model System Name	Score
1) SAI-2D	364
2) SAI-Simple	386

Tables 5.1 and 5.2 show the evaluation of each proposed model system for the four alternatives. In each case, the score for individual criteria is given as well as the total score for the system. Comments are also presented as appropriate to amplify on the scaling factors employed.

Within our ability to differentiate in an analysis of this type, the simple surf-zone model coupled with the SAI oil model outperforms the more complex surf-zone model. A closer look at the analysis shows that while the more complex model

scores higher in applicability and compatibility with ongoing MMS and NOAA program efforts, these factors are not sufficient to overcome its lower scoring in data requirements, potential for interactive use, and development costs.

TABLE 5.1 SMEAR model scoring form SAI-2D/Bijker

Criterion	Weighting Factor	Scaling Factor	Score
1) Internal compatibility	6	4	24
2) Location applicability	8	9	72
3) Data requirements	8	3	24
4) Accuracy	10	9	90
5) Interactive use/microcomputer installation	7	6	42
6) Cost effectiveness	4	5	20
7) Development costs	4	3	12
8) Compatibility with other programs	10	8	80
			364

Comments:
1) Low because we need trajectory and weathering models to run together, oil model and surf model of substantially different complexity.
2) Widely applicable.
3) Severe because of complex surf-zone model.
4) Better than simple surf-zone model.
5) Not possible without substantial simplification of two-dimensional surf-zone model.
6) Moderate, increased because of commonality of approach, decreased due to interfacing of complex surf model to simple oil model.
7) High, complex surf-zone model.
8) Good, same basic approach as in previous MMS studies.

TABLE 5.2 SMEAR model scoring form SAI-1D/Komar.

Criterion	Weighting Factor	Scaling Factor	Score
1) Internal compatibility	6	5	30
2) Location applicability	8	7	56
3) Data requirements	8	8	64
4) Accuracy	10	7	70
5) Interactive use/microcomputer installation	7	8	56
6) Cost effectiveness	4	5	20
7) Development costs	4	5	20
8) Compatibility with other programs	10	8	80
			386

Comments (numbers correspond to above criteria):
1) Low because we need both trajectory and weathering portions to run a simulation.
5) Oil model is interactive only for weathering algorithms.
6) Good, restricted to main-frame applications, and trajectory-weathering models not yet integrated.
7) Easier development than SAI-Simple.
8) Same as SAI-Simple.

6.0 SMEAR Model Development Plan

This section presents an overview of the proposed approach to developing the SMEAR model. Figure 6.1 shows a conceptual model flow chart. At startup, the study area location and physical properties (bathymetry, topography, sediment size, beach slope, and shoreline type) must be defined. The model then enters the time-stepping loop. The first step is to access environmental data describing conditions in the study area at the time of interest. These data include the wind and current fields, air and water temperatures, ice cover and movement, water surface elevation, and suspended particulate matter (SPM) in the water column. When the SMEAR Model is used in conjunction with the offshore circulation model, environmental conditions will be supplied by the offshore model. Otherwise, the user must supply mean current and wind patterns. The nearshore wave environment is then computed, followed by the resulting longshore flow and sediment transport rate inside the surf zone. If marsh, lagoonal, or tidal flat systems are present, we must estimate the flow into these systems, the change in water level, and the area of tidal flats exposed for that stage of the tide. At this point in the time step, we have a description of the circulation and sediment transport pattern in the nearshore zone.

Now spilled oil may enter the area. Oil is introduced into the study area through one of the model boundaries (likely the offshore boundary), either at the surface or subsurface. The oil weathers as appropriate to its location and is either transported at the surface or in the water column by the alongshore currents. Oil in the water column may adsorb to SPM or be deposited to the sea floor, while oil at the surface may be deposited on the foreshore, backshore, in a marsh, on a tidal flat, or be transported alongshore or offshore. (It is considered that oil must pass through the surface boundary to be deposited on the beach.) The "beached" or deposited oil may be resuspended at later times by changes in sea level, either due to the tide or storm surges. The sequence of steps outlined in Figure 6.1 is repeated in time to evolve the spill in space and time. With onshore winds and currents, oil may accumulate onshore until its holding capacity, as discussed in Section 4.4, is reached.

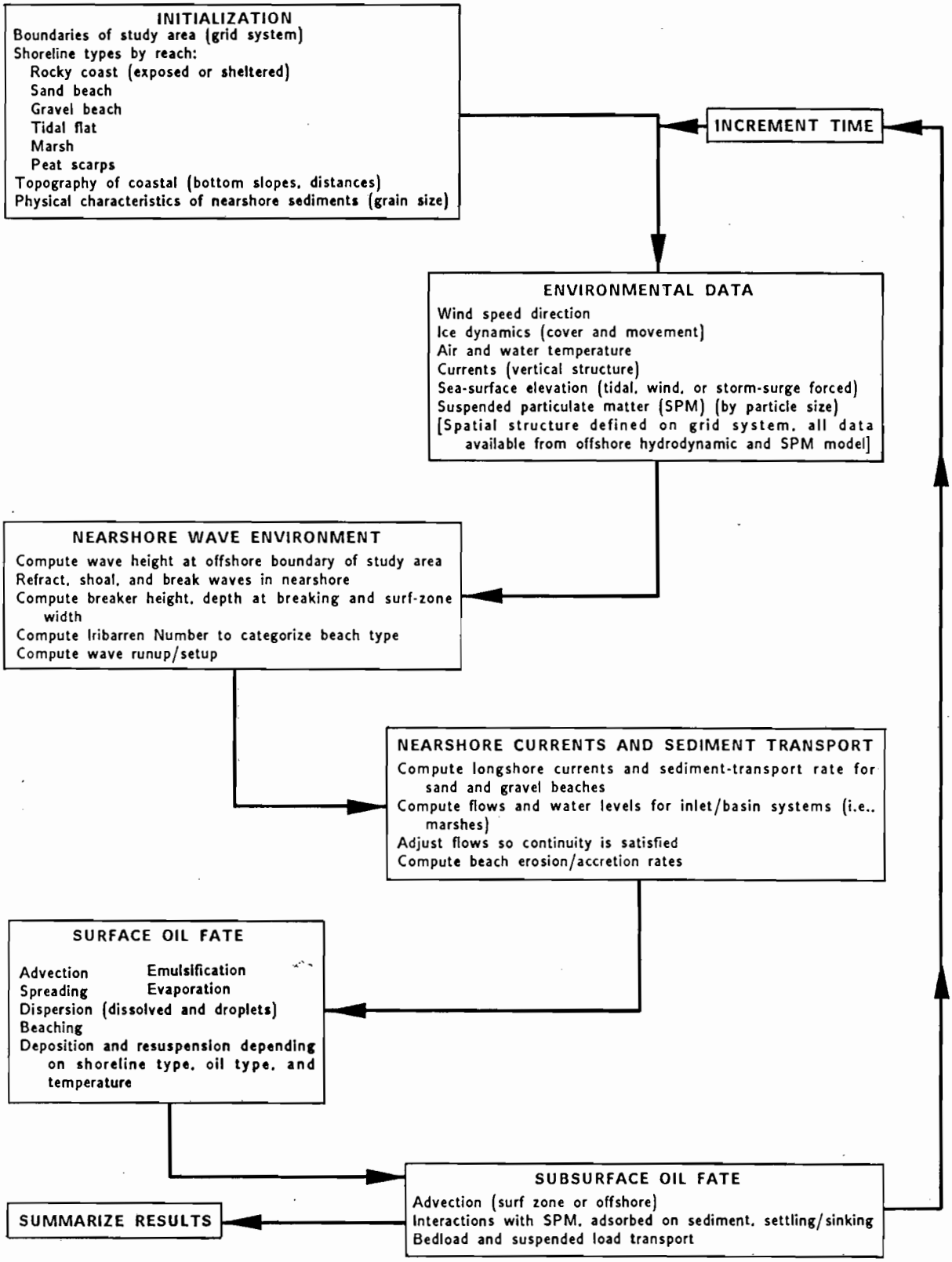

FIGURE 6.1 Conceptual flowchart for the SMEAR model. [*Input data from offshore wind, hydrodynamic, ice, SPM, and oil model system.]

At the end of the simulation, the spatial distribution of the spilled oil is summarized in terms of the mass of oil deposited in the nearshore, on the surface, or in the water column (either in droplet or SPM associated form). These values are also available at selected time steps of the simulation. Pooled results of a series of simulations will give a probabilistic description of oil distribution along a coastline. Twenty to thirty distinct weather scenarios will probably be necessary to adequately reflect interannual variability effects on the stochastic distribution of spilled oil (e.g., Samuels and Lanfear, 1984).

A more detailed presentation of the approach and the particular calculations proposed for each process are presented in the following sections.

6.1 Initialization

As a starting point, we have assumed that our interest in oil spill fate and weathering is focused on the short-term (0-90 days) behavior. This assumption is based on the fact that oil weathering is relatively rapid in the first few days after the spill, and its potential for significant environmental impact decreases as weathering increases. Given this assumption, the study area will typically be on the order of 250-500 km in the alongshore direction and 30-50 km in the offshore direction. The boundaries of the study area will be located such that they follow grid lines of the existing offshore hydrodynamic and planned SPM models (Fig. 6.2). This selection is made in order to simplify interfacing these offshore models with the SMEAR model, and allows us to use the hydrodynamic and SPM models to represent the environmental conditions in the nearshore area.

The model is divided into four zones in the onshore/offshore direction: back beach, beach, surf zone, and nearshore zone, as shown previously in Figure 1.1. Hydrocarbons can enter the nearshore zone (gridded area in Fig. 6.2) either at the surface or in the water column. The processes of dispersion and dissolution control the flux of oil from surface slicks to the water column in both nearshore and surf zones (see Fig. 1.1) Buoyancy of oil droplets in the nearshore zone results in a return flux to the surface slick. The model assumes that vertical turbulence in the surf zone results in continuous mixing, overpowering buoyant effects. The processes of settling and resuspension control the flux of hydrocarbons and SPM between the water column and sediments in both nearshore and surf zones. Oil at the surface in the surf zone can be deposited on the beach or backshore. From there, it is subject to burial (if the beach is in an accretion stage) or reflotation by subsequent tides.

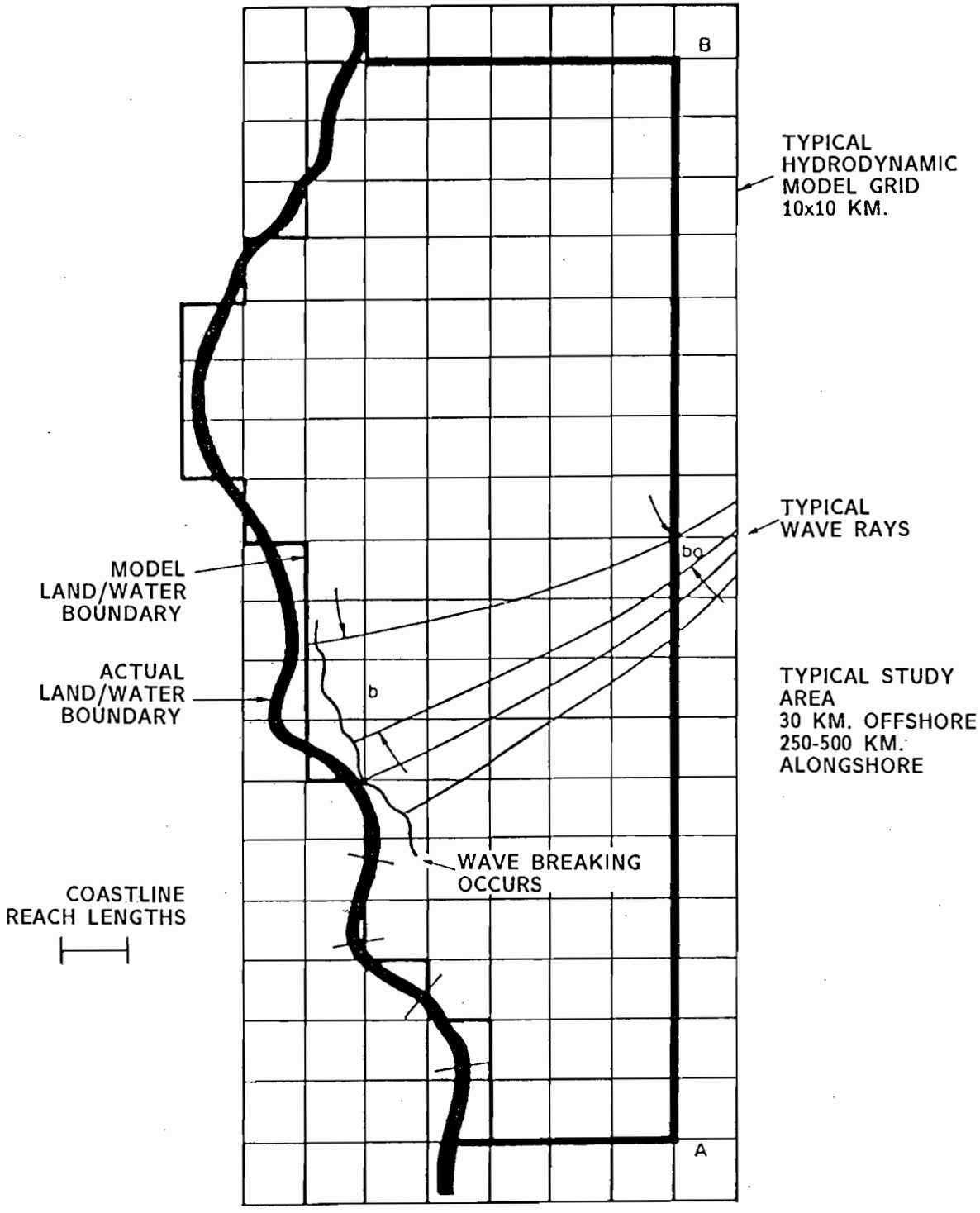

FIGURE 6.2. Specification of study area and its relationship to the hydrodynamic model grid.

The shoreline is divided into seven general classes: rocky shores (sheltered rocky and exposed rocky), sandy beach, gravel beach, peat scarp, tidal flat, and marsh. This classification scheme allows the categorization of most coastlines in Alaska. Coastline types will typically be specified in length or reach increments on the order of 1-10 km. Although one hydrodynamic grid may contain several reach types, no reach may overlay two grids; this simplifies model implementation.

The bathymetry of the study will be derived from the hydrodynamic model grid system for the offshore area. In the nearshore area, detailed local maps and field data (as appropriate) will be used to describe the nearshore topography. To limit the amount of data necessary to describe the nearshore bathymetry, we propose a simple depth/bottom slope system as shown in Figure 6.3. In this approach all shoreline types can be categorized by three angles, three distances, and two depths. In most cases, only a subset of these is needed. The offshore depth, h_o, is obtained from the hydrodynamic model bathymetry; hence, X_o is on the order of the grid size for this model. As an example of the use of the approach, if we wish to represent a medium sand beach with a berm, β_{fs} would be set to about a 5 percent slope, and β_{bs} to 2.5 percent, while X_{fs} and X_l might be 100 m and 40 m, respectively. As another example, if we wish to represent a steep rocky coastline, both β_{fs} and β_{bs} would be set to large values.

For a tidal flat, lagoon, or marsh, one must specify the number of inlets and basins and the interconnections between them along with the cross-sectional areas of the channels and the surface area of the basins. This methodology can also be used to accommodate stream mouths in a shore segment, in which case the above parameters must be specified for the tidally affected portion of the stream or river.

This approach allows enough flexibility to economically represent complex coastal topography. For convenience in the computations, handling of data, and accurate representation of the nearshore features, transects will be described perpendicular to the local shoreline in the approximate center of each hydrodynamic model grid.

To characterize sediment type, a simple grain-size specification is proposed. A mean sediment size will be used to describe the sediment for each shore segment. The value chosen will be selected to best categorize the sediment transport behavior.

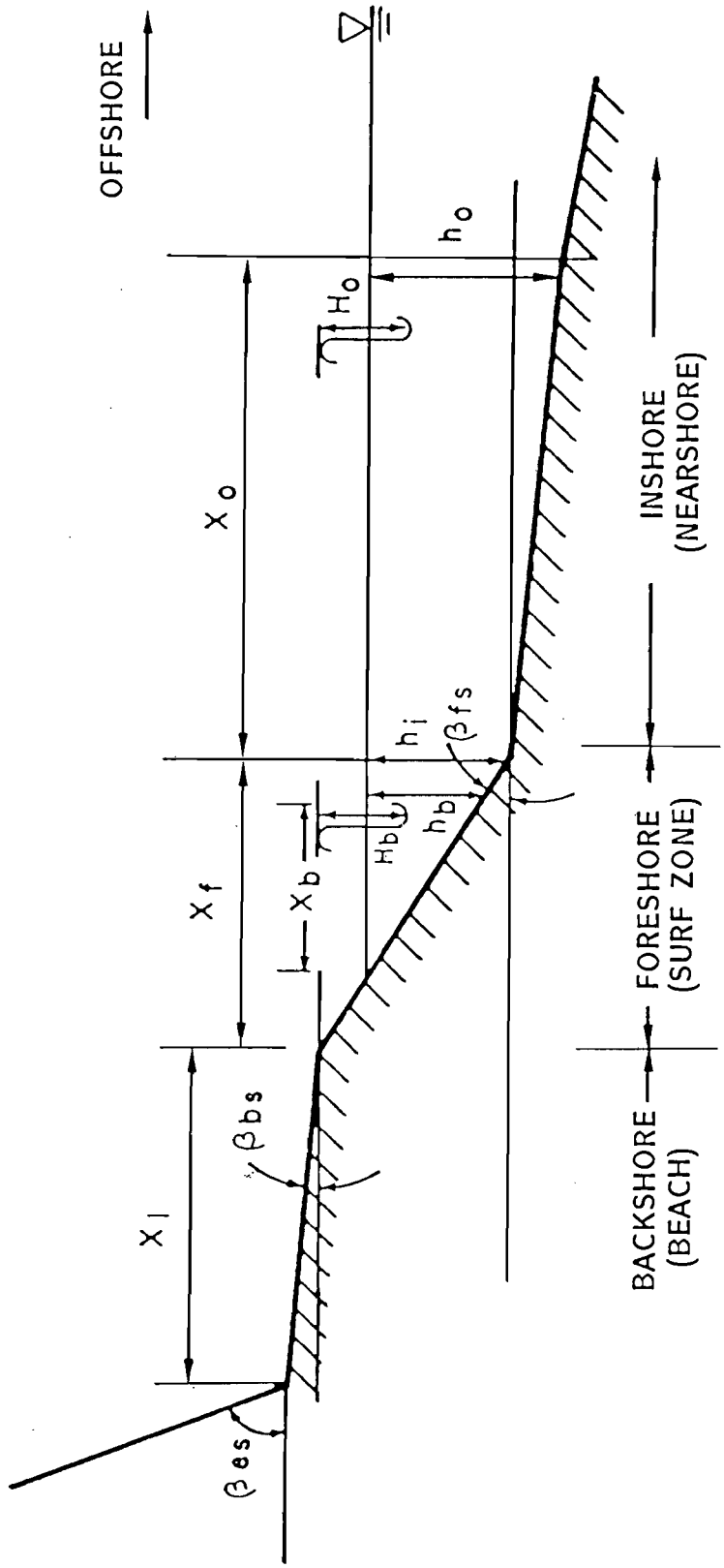

FIGURE 6.3. Description of nearshore bathymetry.

6.2 Environmental Data

Environmental data, including stochastic wind velocities and directions for different localities, ice cover and movement, currents, surface elevation, air and water temperatures, and SPM will be provided by the offshore hydrodynamic model system. These data will be provided as a function of time for each grid point within the study area. Secondary variables, such as vertical and horizontal eddy viscosities, will be averaged over the vertical to parameterize the bulk dispersive behavior. When being run interactively, the model will allow the user to enter necessary environmental information.

6.3 Nearshore Wave Environment

The wave environment is one of the key parameters in determining the nearshore circulation dynamics. As a first step, the wave conditions along the transect AB (Fig. 6.2, i.e., the offshore boundary of the study area) are determined by using the shallow-water, wave-forecasting equations recommended by the U.S. Army Corps of Engineers Shore Protection Manual (CERC, 1984):

$$\frac{gH}{U^2} = 0.283 \tanh\left[0.530\left(\frac{gd}{U^2}\right)^{3/4}\right] \tanh\left\{\frac{0.00565\left(\frac{gF}{U^2}\right)^{1/2}}{\tanh\left[0.530\left(\frac{gd}{U^2}\right)^{3/4}\right]}\right\} \tag{6.1}$$

$$\frac{gT}{U} = 7.54 \tanh\left[0.833\left(\frac{gd}{U^2}\right)^{3/8}\right] \tanh\left\{\frac{0.0379\left(\frac{gF}{U^2}\right)^{1/3}}{\tanh\left[0.833\left(\frac{gd}{U^2}\right)^{3/8}\right]}\right\} \tag{6.2}$$

$$\frac{gt}{U} = 5.37 \times 10^2 \left(\frac{gT}{U}\right)^{7/3} \tag{6.3}$$

where g is gravity, F is the fetch length, d is mean water depth over the fetch, t is the duration, and U is the wind stress factor. U is obtained by estimating the surface wind US in m/s from the offshore weather model, and then setting $U = 0.71\ US^{1.23}$. The position of the pack ice edge, which in some seasons and locations determines the effective fetch length, can be estimated from the ice atlas by La Belle et al. (1983) and will vary stochastically when the model is run.

This approach is designed for use with shallow-water waves (i.e., depth to wave-length ratio less than one-half). For greater depths, the revised deep-water forecasting equations will be used.

Wind information, in terms of speed, direction, and duration, is determined directly from the offshore weather model. Water depth is obtained from the hydrodynamic model bathymetry.

Using a standard refraction/shoaling procedure (CERC, 1984), the wave height, H, at any point can be described in terms of the wave height, H_o, at the study domain boundary by:

$$\frac{H}{H_o} = \left(\frac{Cg_o}{Cg}\ \frac{b_o}{b}\right)^{1/2} \tag{6.4}$$

where b refers to the separation of rays (Fig. 6.2) and Cg is the wave group velocity. The subscript o refers to the reference location, in this case the offshore boundary; an unsubscripted variable refers to any location.

As the wave progresses shoreward, it shoals and refracts as it interacts with the bottom. When the wave height to water depth ratio reaches an approximate value of 0.73, the wave breaks. This is shown schematically in Figure 6.2 for the refractive behavior. Knowing the depth at breaking, h_b, and the local slope of the shore, β_{fs}, we can then compute the width, X_b, and cross-sectional area of the surf zone.

To help quantify the various aspects of waves breaking on a plane beach, such as breaking criterion, breaker type, number of waves in the surf zone, beach type (dissipative versus reflective), etc., the surf similarity parameter, or Iribarren Number (I_r), will be employed:

$$I_r = \frac{\tan\beta}{(H/L_o)^{1/2}} \tag{6.5}$$

where β = beach slope (β_{fs} as noted in Fig. 6.3).
H = wave height.
L_o = deep-water wavelength.

Figure 2.1 shows these and other parameters as a function of I_r. While much of this information is qualitative in nature, it summarizes key descriptors of planar beach systems and will undoubtedly prove useful as the SMEAR model is refined.

6.4 Nearshore Currents and Sediment Transport

We next need to estimate the longshore transport velocity, V, in the surf zone. From the wide variety of formulas available, Sections 2 and 5 determined that the relatively simple, one-dimensional model most adequately fulfills the requirements of the SMEAR system.

This formula, however, is valid only for simple sand/gravel/exposed rocky shores and, hence, must be restricted for use in those areas. For sheltered areas, sheltered rocky shores, tidal flats, and marshes, the flow is assumed to be in the onshore/offshore direction, depending on the stage of the tide.

To represent the flux into and out of coastal lagoons and embayments, three alternatives were considered:

1) A simple parametric approach first developed by Keulegan (1967).
2) A simple inlet/basin model that solves the inlet equations of motion and the basin continuity equation by Runge Kutta numerical technique (Seelig et al., 1977).
3) A hybrid model that uses Seelig's approach for the inlet and a two dimensional vertically averaged finite element hydrodynamic model for the lagoon or basin (Isaji et al.,1985).

While the parametric approach involves only simple calculations, it is restricted to a simple inlet-single basin system, assumes that the free surface elevation throughout the lagoon is in phase, and ignores nonlinear dynamics that may be critical in controlling the flow through the inlet. In contrast, the hybrid model can readily handle multibasin, multi-inlet systems, considers nonlinear dynamics and can address a

wide range of inlet and lagoon responses to various forcing mechanisms. Its critical disadvantage is that the approach is computationally intensive and hence is used only for detailed site specific investigations of inlet/lagoon systems.

The simple inlet basin model represents a compromise between the sophisticated hybrid model and the simple parametric approach. This model requires only several minutes of personal computer time to run and yet can address the flows for complex inlet basin systems. The procedure incorporates all the critical nonlinear inlet flow dynamics and can even address basins where surface area changes as a function of tidal range. This latter feature may be of particular importance in predicting flows into tidal marshes and lagoons. The model is well documented and is used by the U.S. Army Corps of Engineers for studying coastal lagoon circulation (Seelig et al., 1977).

Based on this analysis of the strengths and weaknesses of each approach, the simple, inlet/basin model (Seelig et al., 1977) will be used to estimate the flux into and out of coastal lagoons and embayments. This model uses a time-marching method that simultaneously solves the area-averaged momentum equation for the inlet or breachway and the continuity equation for the bay. At each time step, the geometric and hydraulic factors describing the inlet-bay system are calculated by evaluating flow conditions throughout the inlet and by spatially integrating this information to determine coefficients of the first-order differential equations. As a function of tidal elevation (i.e., tidal flats), this technique can handle any number of interconnected basins and channels as well as embayments with large changes in surface area. Each channel may further be divided into subchannels to better describe the cross-stream structure of flow within the channels.

It is normally assumed in this approach that the pond or marsh surface elevations remain horizontal and that the level simply rises or falls. In the present case, the water levels at the offshore end(s) of the channel(s) are described by the offshore hydrodynamic model. A more detailed presentation of the inlet hydraulics model to include governing equations, assumptions and limitations, comparison to field data for selected inlets, and a user's manual for the computer code are given in Seelig et al. (1977).

Because it is well known that wave runup/setup can transport oil up the beach face and even into the backshore area, a wave runup/setup calculation will be performed. Since runup on natural beaches is too complex to treat theoretically, we will

rely on the numerous laboratory experiments. The graphical procedure outlined in the CERC (1984) manual will be used to make these estimates.

The wave setup, η_{setup} is calculated, based on radiation stress concepts, by the formula:

$$\eta_{setup} = K(h_b - h) + \eta_{setdown} \tag{6.6}$$

where h_b = water depth at breaking.
h = water depth at point of interest in surf zone.
$\eta_{setdown}$ = wave setdown at the breaker location, given as:

$$\eta_{setdown} = \frac{-H_b^2}{8} \quad \frac{k_b}{\sinh 2k_b h_b} \tag{6.7}$$

where k_b = wave number at breaking.
H_b = wave height at breaking
K = a constant, determined by: $K = \frac{1}{1 + (8\Upsilon_b^2/3)}$

where Υ_b is defined by the relation $H=\Upsilon_b (h + \eta_{setup})$ in the surf zone, and is frequently taken to be 0.73, the maximum theoretical value of the ratio between wave height and water depth for a solitary wave. By calculating the surf similarity parameter, we can determine whether setup or runup dominate for a particular section of beach (Fig. 2.1).

For marsh, tidal flats and rocky cliff coastlines, no runup calculations will be performed since it is not of concern in these areas. To account for storm surges in the study area, simulations from the offshore hydrodynamics model or a simplified storm surge estimator (Horikawa, 1978) will be used to predict the free surface elevation along the coast as a function of time. Calculations of the wave environment and oiling of the coast will be made as noted with the exception that the reference water level will be the storm surge level rather than mean sea level (MSL).

6.5 Oil Flux to Study Area

Oil entering the study area will be partitioned into three categories: surface oil and subsurface (water column) oil, free and associated with SPM. The time-dependent oil flux across the study area offshore boundary, including its weathered

state descriptors, will be provided by the offshore hydrodynamic, SPM, and oil models (Fig. 1.1). The surface oil will be described by a series of spillets, each with its own mass, radius, viscosity, density, and weathered state. The subsurface oil will be treated as a number of particles to statistically represent the oil. The particles will be described by a range of sizes to represent the range of oil droplet and oiled SPM sizes and will be distributed to represent the spatial extent of the oil. Given the high turbulence levels inside the surf zone, the subsurface oil will be assumed to be vertically well mixed over the water column. In the nearshore area but seaward of the surf zone, the offshore hydrodynamics model will be used to describe the vertical structure of oil concentration. In the interactive mode, the user must define the stratification profile.

6.6 Shoreline Oil Fate

The surface oil spillets will be advected by the wind and currents (longshore inside the surf zone or nearshore outside the surf zone but inside the study area). In the interactive version of the model the slick advection rate will be calculated as a vector sum of the wind induced drift and the local current field. Spreading, emulsification, and evaporation will follow the Fay (1971)/Mackay et al. (1977; 1980a,b; 1982), Mackay and Leinonen (1977), and Payne et al. (1981) formulations, respectively. Outside the surf zone, dispersion will be calculated according to Mackay's algorithm, while inside the surf zone this basic approach will be modified to reflect the increased dispersion in this highly turbulent area.

For marsh and tidal flat areas, the oil can be transported offshore-onshore into/out of enclosed or semienclosed areas, depending on the stage of the tide and, hence, the currents in the inlet/basin system.

We will calculate the beaching of oil due to a change in tidal height by approximating the differential area of the foreshore/backshore exposed during one cycle. If the tide is outgoing, oil will be deposited according to its thickness, radius, and distance from the shore. If the tide is rising, then some fraction of the oil is resuspended. The amount of oil deposited on or removed from the beach depends on the beach type, oil composition, and temperature.

Beached oil-holding capacities will be computed. The model algorithms may have to be modified after more data become available. Default values (or empirical observations) discussed in Section 4 will be used in conjunction with the model, as

necessary. Under moderate to heavy oiling, the thickness of oil on the beach face averages 18 mm on sand and 9 mm on the gravel beach type. Variability will be reflected by probability density functions fit to the data. To estimate oiling in the backshore, we calculate runup as described above. If the oil reaches the backshore area for a sand beach, we assume that oil penetration of the sediment averages 5 cm in depth. The affected volume per unit shoreline length is then the width of the uprush zone times the penetration depth. Oiled sediment cannot exceed 9 percent of this volume per unit length. This provides a maximum holding capacity for this area. For a gravel beach type, the depth of penetration is 18 cm; the amount oiled remains the same at 9 percent. Oil can be removed from this backshore area during the next high tide, with removal rates depending on estimated K_f values (Table 4.4, Fig. 4.17).

Oil incorporation into a marsh depends on the extent of intertidally exposed marsh since oil is deposited as the tide drops. Based on observations (see Section 4), the average surface oil accumulation in a marsh is approximately 3 cm, and results in an average holding capacity of 30 kg/m^2 surface area. Of the oil that is deposited in a marsh at high tide, 0.1 to 1.0 percent is removed on the ebb.

Oil deposited on tidal flats is assumed not to exceed 6 mm in thickness. Removal rates due to reflotation during the flood tide are assumed to be 90 to 99 percent, given that the oil generally cannot penetrate the hard-packed sediments that comprise most tidal flat areas. As data become available, these values can be appropriately adjusted.

In summary, the loss of oil from the beach is calculated by assuming a simple exponential decay relationship:

$$M_i = M_{io}\, e^{-K_f t} \tag{6.8}$$

where M_i = mass of oil in beach segment i.

M_{io} = mass of oil originally deposited on the beach.

K_f = exponential decay constant to characterize oil loss rate for each beach type.

t = time in days since original deposition.

Based on an analysis of the field observations (Section 4) of oil/beach interaction, proposed K_f values are given in Table 4.4. K_f will be computed by the model as a function of oil viscosity, beach type, and wave energy. The algorithm may require revision as additional information becomes available.

As oil is deposited on the shoreline, weathering due to evaporation continues. Evaporation is also assumed to weather subsurface oil at the same rate. No other weathering processes are active, although biodegradation and photooxidation can be added at a later date.

To handle the numerous deposition/resuspension cycles of oil, we propose to break the surface slick into sublots. As the tide recedes, a sublot of a surface spillet is deposited on the shore. Some portion of this sublot may be resuspended later (i.e., during high tide) or remain deposited on the shore or in the marsh. As the sublots are resuspended, they will be incorporated into existing spillets, using a mass balance weighted by hydrocarbon cut. This procedure should minimize the computational time/storage, but give a relatively accurate representation of the spatial and temporal distribution of the oil.

It is recognized that some fraction of the oil that is resuspended from the beach may not behave as clean oil. This is particularly the case when oil weathering has proceeded to the point where tar balls are formed. Although the literature is extremely sparse in determining the rate of tar ball formation we will attempt to quantify this behavior with the best existing information. Oil that has reached this weathered state will be treated as a separate category throughout the calculations. Mousse rollers or logs, consisting of mousse floating in the water column or along the bottom, is not separately modeled as yet, but is included in the total content of oil in the water column or on the bottom.

6.7 Fate of Oil in the Water Column

Oil in the water column is described by particles that statistically represent oil droplets. There are generally two classes of particles--oiled SPM and free oil particles. Since the quantity of dissolved oil is usually much smaller than that in droplet form, we will lump the dissolved and droplet oils into one category. These particles will be advected according to the local current field (longshore currents if inside the surf zone and hydrodynamic modeled currents outside the surf zone but within the study area) and dispersed by a random walk diffusion procedure (Csanady, 1973). The effective dispersion coefficients will be derived from the hydrodynamic model. Settling of the oiled SPM particles will be performed using a Stokes fall velocity or the results of the SAI oil/sediment interaction study.

The SPM oil interaction will follow the work currently in progress by Payne et al. (personal communication) at SAI under MMS sponsorship. The oil adsorbed onto sediment is calculated by:

$$C_{adsorbed} = K\ S_i\ C_{total} \tag{6.9}$$

where K = dimensionless partition coefficient $\simeq 10^3$.

S_i = suspended particulate matter SPM concentration.

$C_{total} = C_{adsorbed} + C_{dissolved} + C_{droplet}$

Estimates of the concentration of oiled SPM and free droplets of oil can be obtained by dividing the mass of the oiled particles or oil in each grid by the grid volume. This is a relatively coarse estimate, but is probably sufficient for the analysis at hand.

Through this calculation sequence, we can advect and disperse oil droplets and oiled SPM in the nearshore zone. If the fall velocities are sufficiently large, oiled SPM will be deposited on the sea floor and will be either transported as bedload or buried in the bottom sediments.

Outside the surf zone, estimates of the SPM concentration will be obtained from the offshore model. Inside the surf zone, suspended sediment concentration will be computed from field measurements (either published or collected during Phase II of this study).

At this point, we have completed one time step in the SMEAR model simulation. We anticipate a time step on the order of 3-6 hours with total simulation times on the order of 30 days. As time is incremented, the calculation procedure is repeated to describe the spatial and temporal distribution of oil in the nearshore area.

At selected time steps, model output will be provided to describe the spatial distribution of spilled oil:

1) Oil mass, thickness, weathered state, and location (surface, buried) within each coastal segment.
2) Location, mass, weathered state, thickness, and areal extent of each surface spillet.
3) Concentration of oiled SPM, SPM, and droplet oil in the water column. Mass of droplet oil and oiled SPM at the sea bed.

In addition, complete descriptions of the wind, wave, current, and sediment-transport rates are also provided. At the end of the simulation, an alongshore mass balance is provided describing the distribution of oil in the major environmental compartments: land (beach, backbeach; surface, subsurface), water column (oil and oiled SPM), sea bed, atmosphere, and sea surface (as per Fig. 1.1).

The model as presented above is essentially a deterministic calculation in that it follows the fate of a specific spill through a prescribed set of environmental conditions. To run the model in a probabilistic mode, repeated simulations of the deterministic model will be performed. The environmental conditions and the model parameters used to describe the oil spill transport and fate necessary as input to the model will be selected using probability distributions appropriate to each parameter. For instance, the wind speed and direction could be randomly selected from historical records for a particular season. As another example, the oil content by volume of oily beach sediments (Figure 4.12) could be selected by assuming a simple Gaussian distribution of the values.

After multiple simulations have been performed, the results will be aggregated to determine the probability of a given amount of oil in each segment as a function of time since the spill entered the SMEAR model boundaries. Note that this probability distribution is for a given spill event. The exact number of simulations necessary to reliably define the probability distributions is not known at this time but wil be empirically determined once the SMEAR model is in operation. We expect that 20-30 simulations will be required to adequately reflect interannual variability in the results (Samuels and Lanfear, 1983). The user may opt to investigate other oil-spill scenarios by simply repeating the above calculations using the described spill characteristics.

REFERENCES

ABSORB, 1983. Alaska Beaufort Sea coastal region, Alaska clean seas contingency planning manual supplement, Vols. I and II: Alaska Clean Seas, Anchorage, Alaska.

Allen, G., L. D'Ozouville, and J. L'Yavanc, 1978. Etat de la pollution par les hydrocarbures dans l'Aber Benoit: in *Amoco Cadiz*, Premieres Observations de Consequences a Court Terme de la Pollution par Hydrocarbures sur l'Environnement Marin, CNEXO, B.P. 337, Brest, France, pp. 97-114.

Anderson, E.L., 1983. Study of wind and current datasets for *Ixtoc I* oil spill hindcast: in Proc. 1983 Oil Spill Conf., API Publ. No. 4356, American Petroleum Inst., Wash., D.C., pp. 293-299.

Ariathurai, R., R.C. MacArthur, and R.B. Krone, 1977. Mathematical model of estuarine sediment transport: Tech. Rept. D-77-12, U.S. Army Corps of Engineers, Waterways Experiment Station, Vicksburg, Miss.

Atlas, R.M., 1981. Microbial degradation of petroleum hydrocarbons: an environmental perspective: Microbiological Reviews, Vol. 45(1), pp. 180-209.

Atlas, R.M., and R. Bartha, 1972a. Biodegradation of petroleum in seawater at low temperatures: Canadian Journal of Microbiology, Vol. 18(12), pp. 1851-1855.

Atlas, R.M., and R. Bartha, 1972b. Degradation and mineralization of petroleum by two bacteria isolated from coastal waters: Biotechnology and Bioengineering, Vol. 14, pp. 297-308.

Atlas, R.M., and R. Bartha, 1972c. Degradation and mineralization of petroleum in seawater: limitation by nitrogen and phosphorus: Biotechnology and Bioengineering, Vol. 14, pp. 309.

Audunson, T., 1979. Fate of oil spills on the Norwegian continental shelf: in Proc. 1979 Oil Spill Conf., API Publ. No. 4308, American Petroleum Inst., Wash., D.C.

Audunson, T., V. Dalen, J.P. Mathisen, J. Haldorsen, and F. Krogh, 1980. SLIKFORCAST--a simulation program for oil spill emergency tracking and long-term contingency planning: in Proc. Petromar '80, Petroleum and the Marine Environment, Graham & Trotman Ltd., London, UK, pp. 513-542.

Basco, D.R., 1982. Surf zone currents, Vol. I, state of knowledge: Misc. Rept No. 82-7(I), U.S. Army Corps of Engineers, Coastal Engineering Research Center, Ft. Belvoir, Vir.

Bascom, W.N., 1951. The relationship between sand size and beach face slope: Transactions of the American Geophysical Union, Vol. 32(6), pp. 866-874.

Bassin, T.T., and T. Ichiye, 1977. Flocculation behavior of suspended sediments and oil emulsions: Journal of Sedimentary Petrology, Vol. 47(2), pp. 671-677.

Baughman, G.L., D.F. Paris, and W.C. Steen, 1980. Quantitative expression of biotransformation rate: in A.W. Maki, K.L. Dickson, and J. Cairns (Eds.), Biotransformation and Fate of Chemicals in the Aquatic Environment, American Society for Microbiology, Wash., D.C.

Bijker, E.W., 1971. Longshore transport computations: Journal of Waterways, Harbors and Coastal Engineering Division, American Society of Civil Engineers, Vol. 97, No. WW4, pp. 687-701.

Bijker, E.W., 1972. Topics in coastal engineering: Delft University of Technology, Delft, Netherlands.

Blaikley, D.R., G.F.L. Dietzel, A.W. Glass, and P.J. van Kleef, 1977. SILKTRAK--a computer simulation of offshore oil spills, cleanup, effects, and associated costs: in Proc. 1977 Oil Spill Conf., API Publ. No. 4234, American Petroleum Inst., Wash., D.C., pp. 45-52.

Blokker, P.C., 1964. Spreading and evaporation of petroleum products on water: in Proc. 4th Intl. Harbor Conf., Antwerp, Belgium.

Blount, A.E., 1978. Two years after the *Metula* oil spill, Strait of Magellan, Chile; oil interaction with coastal environments: Tech. Rept. No. 16-CRD, Coastal Research Division, Geology Department, University of South Carolina, Columbia, 214 pp.

Bodine, B.R., 1971. Storm surge on the open coast: fundamental and simplified prediction: TM-35, U.S. Army Corps of Engineers, Coastal Engineering Research Center, Ft. Belvoir, Vir.

Boehm, P.D., 1982. The *Amoco Cadiz* analytical chemistry program: in E.R. Gundlach (Ed.), Ecological Study of the *Amoco Cadiz* Oil Spill; Part I, Physical, Chemical and Microbiological Studies After the *Amoco Cadiz* Oil Spill. Report of the NOAA/CNEXO Joint Scientific Commission, U.S. NOAA, Wash., D.C., pp. 35-100.

Boehm, P.D., W. Steinhauer, A. Requejo, D. Cobb, S. Duffy, and J. Brown, 1985. Comparative fate of chemically dispersed and untreated oil in the Arctic - Baffin Island oil spill studies 1980-1983: in Proc. 1985 Oil Spill Conf., API Publ. No. 4385, American Petroleum Inst., Wash., D.C., pp. 561-569.

Bowen, A.J., 1969. The generation of longshore currents on a plane beach: Journal of Marine Research, Vol. 37, pp. 206-215.

Cannon, P.J., and S.E. Rawlinson, 1981. Environmental geology and geomorphology of the barrier island-lagoon system along the Beaufort Sea coastal plain from Prudhoe Bay to the Colville River: in Outer Continental Shelf Environmental Assessment Program, Final Reports of Principal Investigators, Vol. 34, August 1985; U.S. Department of Commerce/ U.S. Department of the Interior.

CERC, 1984. Shore protection manual, Vol. I: U.S. Army Corps of Engineers, Coastal Engineering Research Center, Ft. Belvoir, Vir.

Cochran, R.A., and P.B. Scott, 1971. The growth of oil slicks and their control by surface chemical agents: Journal of Petroleum Technology, pp. 781-787.

Csanady, G.T., 1973. Turbulent diffusion in the environment: D. Reidel Publishing Co., Boston, Mass., 248 pp.

CONCAWE, 1981. A field guide to coastal oil spill control and clean-up techniques: CONCAWE Oil Spill Cleanup Technology Special Task Force No. 1, Den Haag, Holland, 112 pp.

Dean, R.G., 1973. Heuristic models of sand transport in the surf zone: Conference on Engineering Dynamics in the Coastal Zone.

D'Ozouville, L., S. Berne, E.R. Gundlach, and M.O. Hayes, 1981. Evolution de la pollution du littoral Breton par les hydrocarbures de l'*Amoco Cadiz* entre Mars 1978 et Novembre 1979: in *Amoco Cadiz*, Fates and Effects of the Oil Spill, COB-CNEXO, BP 337, 29273 Brest Cedex, France, pp. 55-78.

Fallah, M.H. and R. M. Stark, 1976. Literature review: movement of spilled oil at sea: Marine Technology Society Journal, Vol. 10(1), pp. 3-18.

Fay, J.A., 1971. Physical processes in the spread of oil on a water surface: in Proc. 1971 Oil Spill Conf., American Petroleum Inst., Wash., D.C., pp. 463-467.

Finkelstein, K., and E.R. Gundlach, 1981. Method for estimating spilled oil quantity on the shoreline: Environmental Science & Technology, Vol. 15(5), pp. 545-549.

Galt, J.A., 1978. Chapter 2. Investigations of physical processes: in W.N. Hess (Ed.), The *Amoco Cadiz* Oil Spill, A Preliminary Scientific Report; U.S. NOAA, Wash., D.C., pp. 7-20.

Galvin, C.J., 1972. A gross longshore transport rate formula: in Proc. 13th Coastal Engineering Conf., Vancouver, B.C., Canada, pp. 953-970.

Gibbs, R.J., M.D. Matthews, and D.A. Link, 1971. The relationship between sphere size and settling velocity: Journal of Sedimentary Petrology, Vol. 40(1), pp. 7-18.

Graaff, J.V.D., and J.V. Overeem, 1979. Evaluation of sediment transport formulae in coastal engineering practice: Journal of Coastal Engineering, Delft, Holland, Vol 3(1), pp. 1-31.

Gundlach, E.R., and P.D. Boehm, 1981. Determine the fates of several oil spills in coastal and offshore waters and calculate a mass balance denoting major pathways for dispersion of spilled oil: Final Report (RPI/R/81-30), NOAA Grant No. NA80RAD00060, Research Planning Inst., Columbia, S.C., 28 pp.

Gundlach, E.R., and K.J. Finkelstein, 1981. Transport, distribution, and physical characteristics of the oil: in C.H. Hooper (Ed.), The *Ixtoc I* Oil Spill: The Federal Scientific Response; Part 2, Nearshore Movement and Distribution, U.S. NOAA, Boulder, Colo., pp. 41-74.

Gundlach, E.R., and M.O. Hayes, 1982. The oil spill environmental sensitivity index applied to the Alaskan coast: in Proc. 5th Arctic Marine Oilspill Program (AMOP) Technical Seminar, Environmental Protection Service, Ottawa, Ontario, Canada, pp. 311-323.

Gundlach, E.R., and M.O. Hayes, 1978. Chapter 4. Investigations of beach processes: in W.N. Hess (Ed.), The *Amoco Cadiz* Oil Spill, A Preliminary Scientific Report; U.S. NOAA, Wash., D.C., pp. 85-196.

Gundlach, E.R., D.D. Domeracki, and L.C. Thebeau, 1982. Persistence of *Metula* oil in the Strait of Magellan six and one-half years after the incident: Oil & Petrochemical Pollution, Vol. 1(1), Graham & Trotman Ltd, London, pp. 37-48.

Gundlach, E.R., K.J. Finkelstein, and J.L. Sadd, 1981. Impact and persistence of *Ixtoc I* oil on the south Texas coast: in Proc. 1981 Oil Spill Conf., API Publ. No. 4334, American Petroleum Inst., Wash., D.C., pp. 477-485.

Gundlach, E.R., T.W. Kana, and P.D. Boehm, 1985. Modeling spilled oil partitioning in nearshore and surf zone area: in Proc. 1985 Oil Spill Conf., API Publ. No. 4385, American Petroleum Inst., Wash., D.C., pp. 379-384.

Gundlach, E.R., S. Berne, L. D'Ozouville, and J.A. Topinka, 1981. Shoreline oil two years after *Amoco Cadiz*: new complications from Tanio: in Proc. 1981 Oil Spill Conf., API Publ. No 4334, American Petroleum Inst., Wash., D.C., pp. 525-534.

Gundlach, E.R., C.H. Ruby, M.O. Hayes, and A.E. Blount, 1978. The *Urquiola* oil spill, impact and reaction on beaches and rocky coasts: Environmental Geology, Vol. 2(3), pp. 131-143.

Gundlach, E.R., P.D. Boehm, M. Marchand, R.M. Atlas, D.M. Ward, and D.A. Wolfe, 1983. The fate of the *Amoco Cadiz* oil: Science, Vol. 221, pp. 122-129.

Gundlach, E.R., J. Michel, G.I. Scott, M.O. Hayes, C.D. Getter, and W.P. Davis, 1979. Ecological assessment of the *Peck Slip* (19 December 1979) oil spill in eastern Puerto Rico: in Proc. Ecological Damage Assessment Conf., Society of Petroleum Industry Biologists, pp. 303-317.

Harper, J.R., D.R. Green, D. Hope, and J.H. Vendermeulen, 1985. Experiments on the fate of oil in low energy marine environments: in Proc. 1985 Arctic Marine Oilspill Program (AMOP) Technical Seminar, Environmental Protection Service, Ottawa, Canada; Preprint, 17 pp.

Harrison, W., M.A. Winnik, P.T.Y. Kwong, and D. Mackay, 1975. Disappearance of aromatic and aliphatic components from small sea-surface slick: Environmental Science and Technology, Vol. 9(3), pp. 231-234.

Hartung, R., and G.W. Klinger, 1968. Sedimentation of floating oils: Papers of the Michigan Academy of Science, Arts, and Letters, Vol. LIII, pp. 23-27.

Hayes, M.O., E.R. Gundlach, L. D'Ozouville, 1979. Role of dynamic coastal processes in the impact and dispersal of the *Amoco Cadiz* oil spill (March 1978), Brittany, France: In Proc. 1979 Oil Spill Conf., American Petroleum Inst., Wash., D.C., pp. 193-198.

Hayter, E.J. and A.J. Mehta, 1982. Modeling of estuarial fine sediment transport for tracking pollutant movement: EPA, Atlanta, Ga.

Horikawa, K., 1978. Coastal engineering--an introduction to ocean engineering: University of Tokyo Press, Japan.

Horowitz, A., and R.M. Atlas, 1977. Continuous open flow-through system as a model for oil degradation in the Arctic Ocean: Applied and Environmental Microbiology, Vol. 33(3), pp. 647-753.

Huang, J.C., and F.C. Monastero, 1982. Review of the state-of-the-art of oil spill simulation models: Final Report Submitted to American Petroleum Institute, Wash., D.C., approx. 180 pp.

Ippen, A. (Ed.), 1966. Estuary and coastline hydrodynamics: McGraw Hill, New York, N.Y.

Isaji, T., M. Spaulding, and J. Stace, 1985. Tidal exchange between a coastal lagoon and offshore waters: Estuaries, Vol. 8(2B), pp. 203-216.

JBF, 1976. Physical and chemical behavior of crude ol slicks on the ocean: JBF Scientific Corporation, Report to American Petroleum Inst., Wash, D.C., Publ. No. 4290.

Kana, T.W., 1979. Suspended sediment in breaking waves: Tech. Rept. 18-CRD, Coastal Research Division, Geology Department, University of South Carolina, Columbia, 153 pp.

Keulegan, G.H., 1967. Tidal flow in entrances water-level fluctuations of basins in communication with seas: U.S. Army Corps of Engineers, Tech. Bull. No. 14.

Kirstein, B.E., J.R. Payne, and R.T. Redding, 1983. Oil weathering computer program user's manual for multivariate analysis of petroleum weathering in the marine environment--subarctic: Science Applications Inc., Final Report to NOAA, Contract No. 80RAC000018, Anchorage, Alaska.

Kolpack, R.L., N.B. Plutchak, and R.W. Stearns, 1977. Fate of oil in a water environment--Phase II. A dynamic model of the mass balance for released oil: University of Southern California, API Publ. No. 4313, Report to American Petroleum Inst., Wash., D.C.

Komar, P.D., 1975. Nearshore currents; generation by obliquely incident waves and longshore variations in breaker height: in J. Hails and A. Carr (Ed.), Nearshore Sediment Dynamics and Sedimentation, John Wiley and Sons, N.Y., pp. 17-45.

Komar, P.D., 1976. Beach processes and sedimentation: Prentice Hall, Inc. Englewood Cliffs, N.J.

Komar, P.D., and D.L. Inman, 1970. Longshore sand transport on beaches: Journal of Geophysical Research, Vol. 75(30), pp. 5914-5927.

Kraus, N.C., and T.D. Sasaki, 1979. Effects of wave angles and lateral mixing in the longshore current: Coastal Engineering in Japan, Vol. 22, pp. 59-74.

La Belle, J.C., J.L. Wise, R. Voelker, R. Schulze, and G. Wohl, 1983. Alaska marine ice atlas: Arctic Environmental Information and Data Center, University of Alaska, Anchorage, 302 pp.

Lee, R.F., and C. Ryan, 1983. Microbial and photochemical degradation of polycyclic aromatic hydrocarbons in estuarine waters and sediments: Canadian Journal of Fisheries and Aquatic Science, Vol. 40(2), pp. 86-94.

Lewellen, R., 1970. Permafrost erosion along the Beaufort Sea coast: Arctic Research, Littleton, Colo.

Liu, P.L.F., and R. Dalrymple, 1978. Bottom frictional stresses and longshore currents due to waves with large angles of incidence: Journal of Marine Research, Vol. 36(2), pp. 357-375.

Longuet-Higgins, M.S., 1970. Longshore currents generated by obliquely incident sea waves: Journal of Geophysical Research, Vol. 75(33), pp. 6778-6801.

Longuet-Higgins, M.S., 1972. Recent progress in the study of longshore currents: in R.E. Meyer (Ed.), Waves on Beaches, Academic Press, N.Y., pp. 203-248.

Longuet-Higgins, M.S., and R.W. Stewart, 1964. Radiation stress in water waves, a physical discussion with applications: Deep-Sea Research, Vol II, pp. 529-563.

Mackay, D., and P.J. Leinonen, 1977. Mathematical model of the behavior of oil spills on water with natural and chemical dispersion: Report EPS-3-EC-77-19, Environmental Protection Service, Fisheries and Environment Canada, Ottawa, Ontario, Canada.

Mackay, D., and S. Patterson, 1980. Calculation of the evaporation rate of volatile liquids proceedings: 1980 National Conf. on Control of Hazardous Material Spills, Louisville, Ky.

Mackay, D., S. Patterson, and K. Trudel, 1980a. A mathematical model of oil spill behavior: Report EE-7, Environmental Protection Service, Fisheries and Environment Canada, Ottawa, Ontario, Canada.

Mackay, D., I. Buist, R. Mascarenhas, and S. Paterson, 1980b. Oil spill processes and models: Report EE-8, University of Toronto, Report to Environment Protection Service, Ottawa, Ontario, Canada.

Mackay, D., W.Y. Shiu, K. Hossain, W. Stiver, D. McCurdy, S. Paterson, and P. Tebeau, 1982. Development and calibration of an oil spill behavior model: U.S. Coast Guard Research and Development Center, Contr. No. DTCG-39-81-C-80294, Rept. No. CG-D-27-83.

Marchand, M., G. Bodennec, J.-C. Caprais, and P. Pignet, 1982. The *Amoco Cadiz* oil spill, distribution and evolution of oil pollution in marine sediments: in E.R. Gundlach (Ed.), Ecological Study of the *Amoco Cadiz* Oil Spill; Report of the NOAA/CNEXO Joint Scientific Commission, NOAA/CNEXO Publication, Rockville, Md., pp. 143-158.

McAuliffe, C.D., 1976. Evaporation and solution of C_1-C_{10} hydrocarbons from crude oils on the sea surface: in Proc. NOAA Conf., Fate and Effects of Petroleum Hydrocarbons in Marine Ecosystems and Organisms, Seattle, Wash.

McAuliffe, C.D., G.P. Canevari, T.D. Searl and J.C. Johnson, 1980. The dispersion and weathering of chemically treated crude oils on the sea suface: in Proc. Petromar '80, Petroleum in the Marine Environment, Graham & Trotman, Ltd., London, UK, pp. 593-590.

Meyers, P.A., and T.G. Oas, 1978. Comparison of association of different hydrocarbons with clay particles in simulated seawater: Environmental Science and Technology, Vol. 12, pp. 934-937.

Meyers, P.A., and J.G. Quinn, 1973. Organic matter on clay minerals and marine sediments--effects on adsorption of dissolved copper, phosphate, and lipids from saline solutions: Chemical Geology, Vol. 13, pp. 63-68.

Michel, J., D.D. Domeracki, L.C. Thebeau, C.D. Getter, and M.O. Hayes, 1982. Sensitivity of coastal environments and wildlife to spilled oil of the Bristol Bay area of the Bering Sea, Alaska: Report to U.S. NOAA/OCSEAP, Anchorage, Alaska, 117 pp. + 64 maps.

Moore, S.F., R.L. Dwyer, and A.M. Datz, 1973. A preliminary assessment of the environmental vulnerability of Machias Bay, Maine, to oil supertankers: MIT Sea Grant Report No. 162, MIT, Cambridge, Mass.

Nummedal, D., and R.J. Finley, 1978. Wind-generated longshore currents: in Proc. Coastal Engineering Conf., Hamburg, pp. 1428-1438.

Onishi, Y., and D.S. Trent, 1982. Mathematical simulation of sediment and radionuclide transport in estuaries: Battelle Pacific Northwest Laboratory, Richland, Wash.

Paris, D.F., W.C. Steen, G.L. Baughman, and J.T. Barnett, 1981. Second-order model to predict microbial degradation of organic compounds in natural waters: Applied and Environmental Microbiology, Vol. 41(3), pp. 603-609.

Passman, F.J., T.J. Novitsky, and S.W. Watson, 1979. Surface microlayers of the North Atlantic; microbial populations, heterotrophic and hydrocarbonoclastic activities: in Microbial Degradation of Pollutants in Marine Environments, EPA-600/9-79-012.

Payne, J.R., and C.R. Phillips, 1985. Photochemistry of petroleum in water: Environmental Science and Technology, Vol. 19, pp. 569-579.

Payne, J.R., B.E. Kirstein, R.E. Jordan, et al., 1981. Multivariate analysis of petroleum weathering in the marine environment--subarctic: Annual Report, Res. Unit 597, Science Applications, Inc., La Jolla, Calif., Contr. No. NA80RAC00001.

Payne, J.R., B.E. Kirstein, G.D. McNabb, et al., 1984. Multivariate analysis of petroleum weathering in the marine environment--subarctic: in Environmental Assessment of the Alaskan Continental Shelf, Final Report of Principal Investigators, Vol. 22, U.S. Dept. Commerce, NOAA/NOS/OAD, U.S. Dept. Interior, MMS, Vol. II, Appendices.

Peregrine, D.H. and I.G. Jonsson, 1983. Interaction of waves and currents: Miscellaneous Report, No. 83-6, U.S. Army Corps of Engineers, Coastal Engineering Research Center, Ft. Belvoir, Vir.

Rasmussen, D., 1985. Oil spill modeling - a tool for oil spill cleanup: in Proc. 1985 Oil Spill Conf., API Publ. No. 4385, American Petroleum Inst., Wash., D.C., pp. 243-249.

Reed, M., and M.L. Spaulding, 1979. A fishery oil spill interaction model: in Proc. 1979 Oil Spill Conf., API Publ. No. 4308, American Petroleum Inst., Wash., D.C., pp. 63-73.

Reed, M., M.L. Spaulding, and P.C. Cornillon, 1980. An oil spill-fishery interaction model development and applications: Prepared for U.S. Department of Energy, University of Rhode Island.

Sasaki, T., and K. Horikawa, 1975. Neaashore current system on a gently sloping bottom: Coastal Engineering in Japan, Vol. 18, pp. 123-142.

Sasaki, T., K. Horikawa, and S. Hoffa, 1977. Nearshore current on a gently sloping beach: in Proc. 15th Conf., Coastal Engineering, pp. 624-644.

Samuels, W.B., and K.J. Lanfear, 1983. An oil spill risk analysis for Navarian Basin lease offering (March 1984): U.S. Minerals Management Service.

Schureman, P., 1958. Manual of harmonic analysis and prediction of tides: U.S. Government Printing Office, Wash., D.C.

Siah, S.J., 1985. Sediment transport modeling in gulf estuaries: Report to Research Planning Institute, Inc., for Submittal to U.S. NOAA, Seattle, Wash.; Coastal Science & Engineering, Inc., Columbia, S.C.

Solig, G., and E.M. Bens, 1972. Bacteria which attack petroleum hydrocarbons in a saline medium: Biotechnology and Bioengineering, Vol. 14, p. 319.

Spaulding, M.L., K. Jayko, and E. Anderson, 1982a. Hindcast of the *Argo Merchant* spill using the URI oil spill fates model: Journal of Ocean Engineering, Vol. 9(5), pp. 455-482.

Spaulding, M.L., M. Reed, S.B. Saila, E. Lorda, H. Walker, E. Anderson, T. Isaji, and C. Swanson, 1982b. Oil spill fishery assessment model: sensitivity to spill location and timing: Symposium on Physical Processes Related to Oil Movement in the Marine Environment.

Spaulding, M.L., S.B. Saila, M. Reed, C. Swanson, T. Isaji, E. Anderson, E. Lorda, V. Pigoga, K. Marti, J. Hoenig, H. Walker, F. White, R. Glazman, and K. Jayko, 1982c. Assessing the impact of oil spills on a commercial fishery: Final Report to MMS, Contract No. AA851-CTO-75, NTIS No. PB83-149104.

Spaulding, M.L., M. Reed, S.B. Saila, E. Lorda, and H. Walker, 1982d. Oil spill fishery impact assessment model: application of George Bank: in Proc. NOAA/EDIS/CEAS Workshop in Ecosystems Modeling, pp. 101-130.

Spaulding, M.L., S. Saila, E. Lorda,, H. Walker, E. Anderson, and J.C. Swanson, 1983. Oil spill fishery interaction modeling: application to selected George Bank fish species: Estuarine, Coastal, and Shelf Science, Vol. 16, pp. 511-541.

Spaulding, M.L., M. Reed, E. Anderson, T. Isaji, J.C. Swanson, S. Saila, E. Lorda, and H. Walker, 1985. Oil spill fishery impact assessment model: sensitivity to spill location and timing: Estuarine, Coastal, and Shelf Science, Vol. 20, pp. 41-53.

Thornton, E.B., 1970. Variation of longshore current across the surf zone: in Proc. 12th Conf., Coastal Engineering, pp. 291-308.

URI, 1980. Assessment of treated versus untreated oil spills: Final Report, University of Rhode Island, U.S. Dept. Energy, Contract No. E(11-1) 4047, 700 pp.

Wang, H., and C. Huang, 1979. The effect of turbulence on oil emulsification: in Proc. Workshop on the Physical Behavior of Oil in the Marine Environment, Princeton University.

Wang, H., W.C. Yang, and C.P. Huang 1976. Modeling of oil evaporation in aqueous environment: Ocean Engineering Report No. 7, Department of Civil Engineering, Univ. of Delaware.

Williams, G.N., R. Hann, and W.P. James, 1975. Predicting the fate of oil in the marine environment: in Proc. 1975 Oil Spill Conf., American Petroleum Inst., Wash., D.C.

Winters, J.K., 1978. Fate of petroleum-derived aromatic compounds in seawater held in outdoor tanks: South Texas Outer Continental Shelf Study, Bureau of Land Management, Department of the Interior, Chap. 12, Draft Final Report.

Woodward-Clyde Consultants, 1981. Shoreline countermeasures - 1980 study results: Baffin Island Oil Spill (BIOS) Working Report 80-4, Environmental Protection Service, Environment Canada, Ottawa, Ontario, Canada, 83 pp.

Woodward-Clyde Consultants, 1982. Oil spill vulnerability (risk) assessment of marine and coastal habitats in central and northern California. G.A. Robilliard, E.H. Owens, T.P. Winfield, J.R. Harper, C. Foget, and M. Cramer; Report to the Pacific Outer Continental Shelf Office of Bureau of Land Management, Los Angeles, Calif., Contract No. AA851-CTO-73.

Woodward-Clyde Consultants, 1984. Coastal sensitivity analysis of the northern Chukchi Sea coast of Alaska: Report to NOAA/OCSEAP, Contract No. WASC-83-00112, Anchorage, Alaska.

Wright, L.D., J. Chappell, B.G., Thom, M.P. Bradshaw and P. Cowell, 1979. Morphodynamics of reflective and dissipative beach and nearshore systems: Southeastern Australia, Marine Geology, pp. 105-140.

Zuercher, F., and M. Thuer, 1978. Rapid weathering processes of fuel oil in natural waters: analysis and interpretations: Environmental Science and Technology, Vol. 12(7), pp. 838-843.